

The role of HIG1/MYB51 in the regulation of indolic glucosinolate biosynthesis

Inaugural-Dissertation

zur

Erlangung des Doktorgrades
der Mathematisch-Naturwissenschaftlichen Fakultät
der Universität zu Köln

vorgelegt von

Bettina Berger

aus Heilbronn

Köln 2007

Berichtersteller:

Prof. Dr. U.-I. Flügge
Prof. Dr. M. Hülkamp

Prüfungsvorsitzende:

Prof. Dr. K. Schnetz

Tag der mündlichen Prüfung:

2.Juli 2007

The most exciting phrase to hear in science, the one that heralds new discoveries, is not Eureka! (I found it!), but "That's funny....".

Isaac Asimov

1	Introduction	1
1.1	<i>Glucosinolate biosynthesis</i>	1
1.2	<i>A link between indolic glucosinolate, IAA and camalexin biosynthesis</i>	2
1.3	<i>The biological role of glucosinolates</i>	5
1.4	<i>The regulation of glucosinolate biosynthesis</i>	7
2	Material and Methods	10
2.1	<i>Material</i>	10
2.1.1	Chemicals, enzymes, oligo nucleotides	10
2.1.2	Media, buffers	11
2.1.3	Antibiotics	12
2.1.4	Organisms	12
2.1.4.1	Bacterial strains	12
2.1.4.2	Yeast strains (<i>Saccharomyces cerevisiae</i>)	12
2.1.4.3	Yeast cDNA libraries for yeast-two-hybrid assays	13
2.1.4.4	<i>Arabidopsis thaliana</i>	13
2.1.4.5	<i>Nicotiana benthamiana</i>	13
2.1.5	Vectors	13
2.1.5.1	Bacteria vectors	13
2.1.5.2	Yeast vectors	14
2.2	<i>Methods</i>	14
2.2.1	Methods working with bacteria	14
2.2.1.1	Preparation of chemically competent <i>E. coli</i> cells	14
2.2.1.2	Transformation of chemically competent <i>E. coli</i> cells	15
2.2.1.3	Preparation of electro-competent <i>Agrobacteria</i>	15
2.2.1.4	Transformation of electro-competent <i>Agrobacteria</i>	15
2.2.2	Methods working with yeast	16
2.2.2.1	Yeast transformation on small scales	16
2.2.2.2	Yeast transformation in a multi-well format	16
2.2.2.3	<i>In vivo</i> recombination (“gap repair”)	16
2.2.2.4	Mating of two haplotypes in a multi-well format	16
2.2.3	Plant methods	17
2.2.3.1	Plant growth	17
2.2.3.1.1	Growth on soil	17
2.2.3.1.2	Growth on sterile culture plates	17
2.2.3.1.3	Growth in liquid germination medium	17
2.2.3.2	Stable plant transformation	18
2.2.3.3	Transient transformation	18
2.2.3.3.1	Transformation of <i>A. thaliana</i> suspension culture (Berger et al., 2007)	18

2.2.3.3.2	<i>A. thaliana</i> and <i>N. benthamiana</i> leaf infiltration with <i>Agrobacteria</i>	18
2.2.3.3.3	Transfection of tobacco BY2 protoplasts.....	19
2.2.3.4	Seed surface sterilisation	19
2.2.3.4.1	Wet method	19
2.2.3.4.2	Dry method	19
2.2.3.5	Histochemical GUS analysis, modified after Jefferson et al. (1987).....	19
2.2.3.6	Quantitative GUS activity measurement	20
2.2.3.7	Microscopical documentation	20
2.2.3.8	Hormone treatment of plants.....	20
2.2.3.9	Ethanol induction of transgenic lines.....	21
2.2.3.10	Extraction and measurement of glucosinolates and free auxin	21
2.2.3.11	Dual choice assay with <i>Spodoptera exigua</i> (C. Müller, University Würzburg).....	22
2.2.4	Molecular biology methods	22
2.2.4.1	Small scale plasmid preparation from <i>E. coli</i> cells (miniprep).....	22
2.2.4.2	Large scale plasmid preparation from <i>E. coli</i> cells.....	22
2.2.4.3	Extraction of genomic DNA from plant material (fast prep).....	22
2.2.4.4	Extraction of total RNA from plant material	22
2.2.4.5	DNase I treatment and reverse transcription	23
2.2.4.6	cRNA synthesis and microarray hybridisation.....	24
2.2.4.7	Polymerase Chain Reaction.....	24
2.2.4.8	Yeast Colony PCR.....	24
2.2.4.9	Estimation of quantity and size of DNA fragments.....	25
2.2.4.10	Purification of DNA fragments	25
2.2.4.11	Sequencing of DNA fragments.....	25
2.2.4.12	Classical vector cloning.....	25
2.2.4.13	Gateway® cloning	26
3	Results	27
3.1	<i>Isolation of the HIG1-1D mutant</i>	<i>27</i>
3.2	<i>HIG1 encodes an R2R3 MYB transcription factor</i>	<i>29</i>
3.3	<i>HIG1/MYB51 is nuclear-localised</i>	<i>30</i>
3.4	<i>HIG1/MYB51 is mainly expressed in vegetative organs.....</i>	<i>31</i>
3.5	<i>HIG1/MYB51 overexpression leads to a high glucosinolate profile.....</i>	<i>33</i>
3.6	<i>HIG1/MYB51 overexpression does not alter the growth phenotype.....</i>	<i>35</i>
3.7	<i>HIG1/MYB51 overexpression activates indolic glucosinolate pathway genes</i>	<i>37</i>
3.8	<i>HIG1/MYB51 activates promoters of indolic glucosinolate pathway genes.....</i>	<i>43</i>
3.9	<i>HIG1/MYB51 expression is mechano-sensitive.....</i>	<i>45</i>
3.10	<i>Ethylene activates the HIG1/MYB51 promoter in root tips</i>	<i>46</i>

3.11	<i>Overexpression of HIG1/MYB51 leads to increased resistance against a generalist herbivore</i>	48
3.12	<i>Screening for proteins interacting with HIG1/MYB51</i>	49
3.13	<i>HIG1/MYB51 and ATR2/bHLH05 interact in vivo</i>	55
3.14	<i>ATR2/bHLH05 and HIG1/MYB51 expression overlap</i>	56
3.15	<i>ATR2/bHLH05 represses HIG1/MYB51 activation of indolic glucosinolate promoters</i>	57
4	Discussion	60
4.1	<i>HIG1/MYB51 is a positive regulator of indolic glucosinolate biosynthesis</i>	60
4.2	<i>HIG1/MYB51 is expressed at sites of indolic glucosinolate accumulation</i>	64
4.3	<i>HIG1/MYB51 plays a role in biotic stress response</i>	65
4.4	<i>HIG1/MYB51 has a role distinct from its close homologue ATR1/MYB34</i>	66
4.5	<i>Is HIG1/MYB51 differentially regulated in roots?</i>	68
4.6	<i>Is HIG1/MYB51 part of a complex regulatory network?</i>	68
5	References	72
	Appendix	84
	Abbreviations	104
	Abstract	107
	Kurzzusammenfassung	108
	Danksagung	109
	Erklärung	111
	Lebenslauf	112

1 Introduction

Glucosinolates, also known as mustard oils, are a small but diverse class of sulfur and nitrogen containing secondary metabolites. They can be found in Brassicaceae and related plant families including important crop plants and vegetables, such as oilseed rape or cabbage. Their potential as a plant-defence system, along with recent findings suggesting cancer-protective properties of a glucosinolate-rich diet, led to an increased interest in this class of compounds. Substantial progress has thereby been achieved using the model plant *Arabidopsis thaliana*, which allowed unravelling the core biosynthesis pathway.

1.1 Glucosinolate biosynthesis

The precursors of glucosinolate biosynthesis are a few protein amino acids, mainly methionine, phenylalanine and tryptophan. Depending on the nature of the amino acid residue, the glucosinolates are classified as aliphatic, aromatic and indolic glucosinolates, respectively. The glucosinolate biosynthesis proceeds in three steps: (i) side-chain elongation of amino acids, (ii) formation of the core structure and (iii) secondary side-chain modifications, where step (i) and (iii) give rise to the diversity of these compounds.

The enzymes mediating the biosynthesis of the core structure have been identified in *A. thaliana* (Fig. 1.1), and cytochrome P450 monooxygenases (CYPs) appeared to play a predominant role. CYP79F1 and CYP79F2 convert chain-elongated methionine to the aliphatic aldoxime (Reintanz et al., 2001; Hansen et al., 2001a; Chen et al., 2003; Tantikanjana et al., 2004), CYP79B2 and CYP79B3 mediate the formation of indole-3-acetaldoxime (IAOx) from tryptophan (Mikkelsen et al., 2000; Hull et al., 2000). The subsequent reaction giving rise to an *aci*-nitro-compound is catalysed by CYP83A1 and CYP83B1 in the aliphatic and indolic pathway, respectively (Bak et al., 2001; Naur et al., 2003; Hemm et al., 2003). The formation of the intermediate S-alkyl thiohydroximate might be a spontaneous reaction or dependant on glutathione-S-transferases (GSTs). The C-S lyase and an S-glucosyltransferase (UGT) catalyze the subsequent synthesis of the thiohydroximate and the desulfo-glucosinolate, respectively (Mikkelsen et al., 2004; Grubb et al., 2004). Finally, sulfotransferases mediate the last step of the core pathway resulting in

the synthesis of the parent glucosinolate (Piotrowski et al., 2004; Klein et al., 2006), which can undergo secondary modifications.

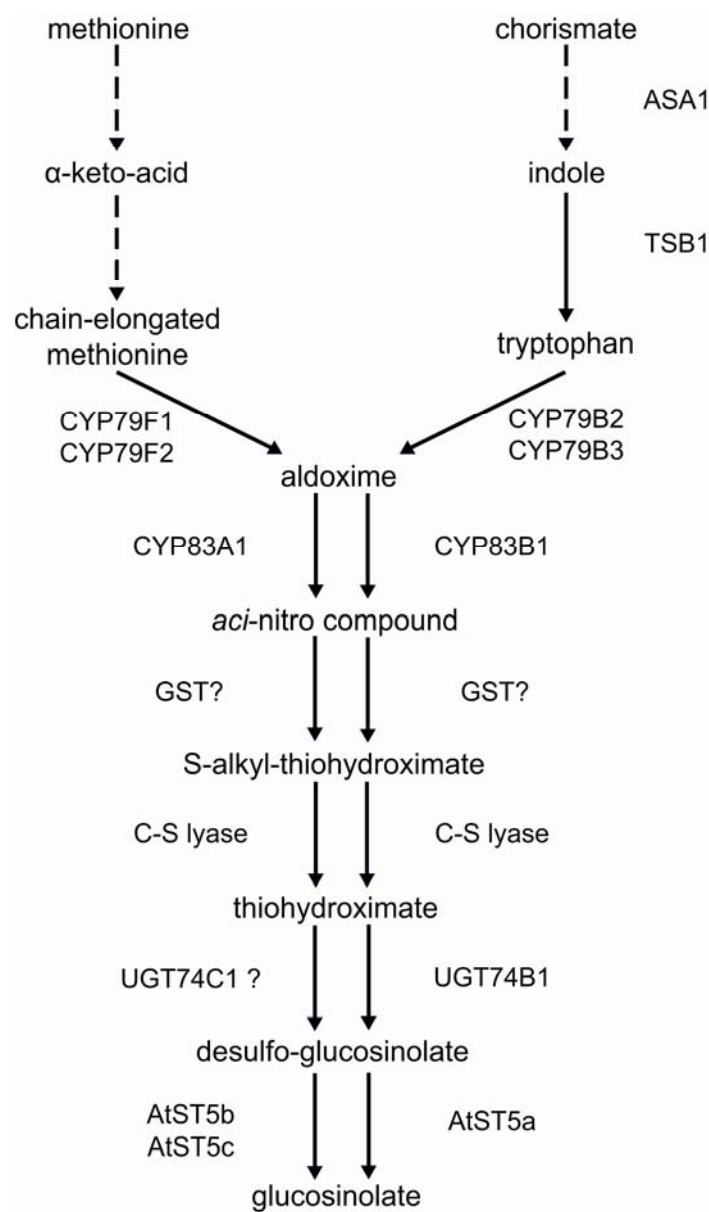


Figure 1.1: Schematic representation of the aliphatic and indolic glucosinolate biosynthesis. ASA1, anthranilate synthase alpha 1; TSB1, tryptophan synthase beta 1; CYP, cytochrome P450 monooxygenase; UGT, S-glycosyltransferase; AtST, *A. thaliana* sulfotransferase.

1.2 A link between indolic glucosinolate, IAA and camalexin biosynthesis

Analyses of mutants defective in the biosynthesis of indolic glucosinolates have revealed a tight link with auxin biosynthesis, since both pathways share the same

precursors (Fig. 1.2). Knock-out plants of *cyp83b1* and the *C-S lyase* were initially described as *superroot* (*sur*) mutants, with respect to their increased number of lateral and adventitious roots (Delarue et al., 1998; Barlier et al., 2000; Mikkelsen et al., 2004). Besides the observed root morphology, *sur* mutants showed elongated hypocotyls and epinastic cotyledons. The observed phenotype thereby resembled that of wild-type seedlings grown on auxin containing media. Indeed, the *sur* mutants contained an elevated indole-3 acetic acid (IAA) level compared to wild-type plants. Moreover, partial or complete blockage of the indolic glucosinolate biosynthesis led to a redirection of IAOx into the IAA biosynthesis pathway, leaving to a high-auxin phenotype (Bak et al., 2001). Further evidence for an increased IAA accumulation in response to an impaired indolic glucosinolate biosynthesis, is provided by studies of an *ugt74b1* mutant line, with stunted, mal formed plants (Grubb et al., 2004).

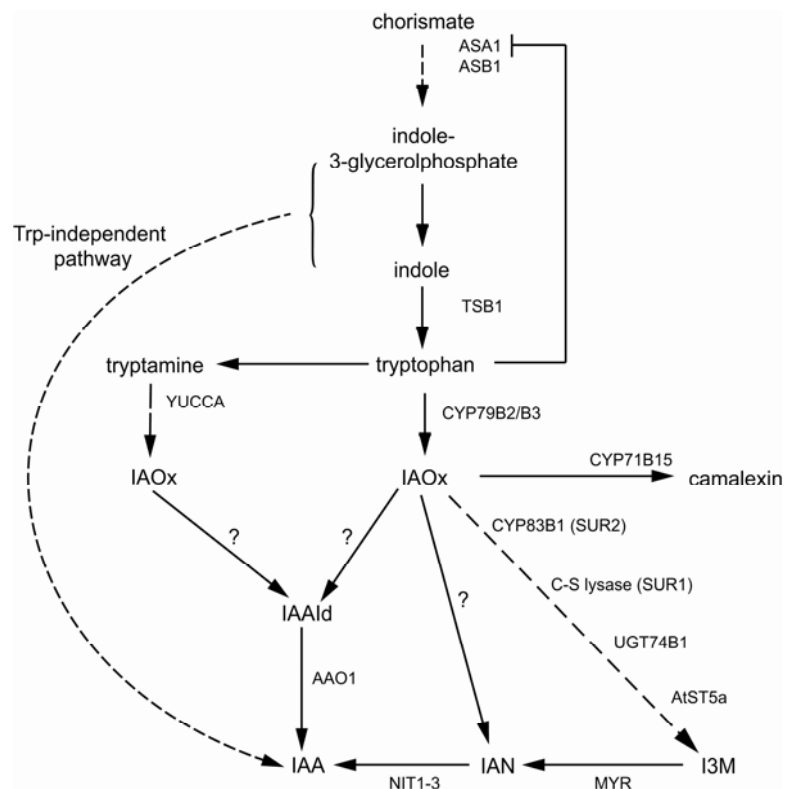


Figure 1.2: Simplified model of the IAA synthesis pathways in *A. thaliana* (modified after Zhao et al., 2002; Woodward and Bartel, 2005; Pollmann et al., 2006). Question marks indicate pathways with unknown enzymes. ASA1, anthranilate synthase alpha 1; ASB1, anthranilate synthase beta 1; TSB1, tryptophan synthase beta 1; CYP, cytochrome P450 monooxygenase; UGT, S-glycosyltransferase; AtST, *A. thaliana* sulfotransferase; NIT, nitrilase; MYR, myrosinase; AAO1, indole-3-acetaldehyde oxidase, YUCCA, flavin monooxygenase-like protein; IAOx, indole-3-acetaldoxime; I3M, indole-3-ylmethyl glucosinolate; IAAld, indole-3-acetaldehyde; IAA, indole-3-acetic acid; IAN; indole-3-acetonitrile.

However, the pleiotropic phenotype of this mutant is caused by both, an accumulation of the thiohydroximate, and an increased auxin level.

An opposite effect was reported for a *cyp79b2/cyp79b3* double knock-out mutant, which contained slightly decreased IAA concentrations (Zhao et al., 2002). Nevertheless, the mutants were still able to produce sufficient amounts of IAA for plant growth and reproduction. A reason for that is the existence of multiple pathways for IAA biosynthesis. One possibility is the tryptophan-independent pathway; another way uses tryptophan as precursor and converts it to IAOx via tryptamine. The key enzyme is the flavin monooxygenase YUCCA. Even though this pathway also produces IAOx and is still functional in *cyp79b2/cyp79b3* knock-out mutants, these plants do not contain any detectable indolic glucosinolates (Zhao et al., 2002). Consequently, IAOx produced by CYP79B2 and CYP79B3 appears to be the sole source for indolic glucosinolate biosynthesis, whereas the IAOx pool derived from the YUCCA pathway is exclusively shuttled into IAA synthesis. Besides IAA and indolic glucosinolate biosynthesis, IAOx also serves as precursor for camalexin (Glawischnig et al., 2004), the main phytoalexin of the model plant *A. thaliana*, and like indolic glucosinolates involved in the biotic stress response. The rate-limiting step in camalexin biosynthesis is catalysed by CYP71B15 (Schuhegger et al., 2006) and the precursor IAOx seems to be solely derived from the CYP79B2/CYP79B3 pool, since the *cyp79b2/cyp79b3* double knock-out contained no detectable amounts of camalexin (Glawischnig et al., 2004). Hence, IAOx constitutes an important branching point of several pathways derived from tryptophan.

A further link between synthesis of the precursor tryptophan and IAA accumulation could be observed in the *cyp83b1* mutant. The increased IAA content was accompanied by an upregulation of *ASA1* (Smolen and Bender, 2002), coding for the feedback-regulated subunit of anthranilate synthase. Along with that, the *cyp83b1* phenotype could be partially rescued by complementation with *asa1* knock-out mutants (Stepanova et al., 2005). This suggests that an increased auxin synthesis is strictly dependent on high *ASA1* transcription. Accordingly, heterologous expression of a feedback-insensitive *ASA1* subunit from rice in *A. thaliana* led to high tryptophan and auxin levels in transgenic plants (Ishihara et al., 2006). Taken together, tryptophan biosynthesis is not only important for providing the amino acid for protein synthesis, but there is a tight connection with the synthesis of indolic glucosinolates, camalexin and auxin that are derived from tryptophan.

1.3 The biological role of glucosinolates

The capacity of plants to synthesise glucosinolates co-occurs with the expression of myrosinases. These are special β -thioglucoside glycohydrolases (also called TGGs), located in idioblasts (myrosin-cells) scattered throughout most tissues that accumulate glucosinolates (Husebye et al., 2002; Barth and Jander, 2006). Upon tissue rupture, the biologically inactive glucosinolates come in contact with myrosinases, which catalyze the hydrolysis of the glucose residue. The unstable aglucone subsequently gives rise to various biologically active breakdown products, including nitriles, thiocyanates and isothiocyanates among others. The nature of the breakdown product thereby depends on the surrounding conditions, such as pH, the presence of ferrous ions or myrosinase interacting proteins (Wittstock and Halkier, 2002; Bones and Rossiter, 2006).

The bipartite glucosinolate-myrosinase system has also implications for human nutrition. The uptake and bioavailability of glucosinolates and their breakdown products not only depend on the respective vegetable consumed, but also on growth conditions, transport, storage and food processing that influence glucosinolate concentration and myrosinase activity (Johnson, 2002). In general, isothiocyanates are believed to contribute predominantly to the anti-carcinogenic properties of *Brassica* vegetables. Case studies showed a negative correlation between cancer development and the uptake and secretion of isothiocyanates due to the consumption of glucosinolate-rich food. This could be shown for cancers of the respiratory and digestive system, but also for hormone-dependent cancers (review by Holst and Williamson, 2004; Keck and Finley, 2004). Interestingly, the protection against cancer may be achieved on two different levels of cancer development. First of all, isothiocyanates are known to stimulate phase II enzymes in the liver that inactivate carcinogens and target them for secretion (Surh, 2003). Second, they have been shown to induce apoptosis in cancer cell lines (Pledge-Tracy et al., 2007). Isothiocyanates might therefore not only inhibit cancer development but also reduce tumor growth and promotion.

Unlike the beneficial effects of moderate glucosinolate intake in human nutrition through *Brassica* vegetables, high ingestion can have adverse effects on animal health when large amounts of *Brassica* crops are used as fodder. Therefore, different methods are employed to reduce the glucosinolate concentration prior to feeding (Tripathi and Mishra, 2007). So far, the detoxification of high-glucosinolate crops

seems to be the most appropriate way of using them as fodder, since breeding of cultivars with lower glucosinolate concentrations might affect the interaction of the plant with pathogens and herbivores.

Indeed, the primary function of the glucosinolate-myrosinase system is thought to be the deterrence of attacking herbivores. A high glucosinolate concentration acts as deterrent against generalist herbivores (Kliebenstein et al., 2002a). However, not only the absolute concentration, but rather the composition of the produced glucosinolates is crucial for plant-herbivore interaction (Mewis et al., 2006; Zhang et al., 2006). Kim and Jander (2007) could show that *A. thaliana* responds to attack by the green peach aphid (*Myzus persicae*) not with an increased glucosinolate biosynthesis but with the conversion of indole-3-ylmethyl glucosinolate (I3M) to 4-methoxyindol-3-ylmethyl glucosinolate (4MOI3M), which is a more potent aphid deterrent than I3M. In contrast to generalist herbivores, specialists have evolved various systems to overcome the glucosinolate-myrosinase system and have learned to take advantage of it. Certain specialist herbivores are able to secrete the glucosinolates and use them for their own defense (Muller et al., 2001), others express enzymes for the detoxification of glucosinolates (Ratzka et al., 2002; Wittstock et al., 2004). The glucosinolate profile can thereby be used by specialists for host-plant recognition and may function as an oviposition or feeding signal (Rask et al., 2000; Ulmer and Dossall, 2006). Altering the glucosinolate profile of crop cultivars in combination with the growth of trap plants might therefore be a potential tool to delimit herbivory by specialists (Cook et al., 2006). A further possibility to reduce the damage by specialists is already present in nature. Volatiles released during herbivore attack can in turn attract natural enemies of the herbivore feeding on the plant (Agrawal, 2000). This offers plants a further possibility for the defence against specialist herbivores that are unaffected by high glucosinolate concentrations.

Besides the role of glucosinolates in the plant-insect interaction, there is emerging evidence that also microbial pathogens are affected by glucosinolates. Treatment with bacterial pathogens or oomycetes triggered an accumulation of indolic glucosinolates in leaves and roots of *A. thaliana*, respectively (Brader et al., 2001; Bednarek et al., 2005) and a role of indolic glucosinolates as defence compounds was demonstrated upon infection with the fungal pathogen *Botrytis cinerea*, which was shown to produce larger lesions on low indolic glucosinolate mutants (Kliebenstein et al., 2005). Moreover, *in vitro* experiments showed adverse effects of

aliphatic isothiocyanates, mainly 4-methylsulphinylbutyl isothiocyanate, on the growth of various plant pathogens, including bacteria and fungi (Tierens et al., 2001). Therefore, it seems that different glucosinolates and their breakdown products have the potential to differentially influence the plant-pathogen interaction. Indeed, an alteration of the glucosinolate profile of *A. thaliana* by introducing new pathway enzymes was proven to enhance the resistance against various pathogens (Brader et al., 2006). Tailor-made glucosinolate compositions might also find application in agronomically important *Brassica* species. Besides the cultivation of *Brassica* vegetables and crops, the use of glucosinolate-containing plants in the so-called biofumigation has gained increasing interest. This describes the use of green manure derived from *Brassica* species to suppress soil-borne pests, ranging from bacteria, fungi and nematodes to insects (Matthiessen and Shackleton, 2005; Matthiessen and Kirkegaard, 2006).

Taken together, the concentration and more important the composition of glucosinolates in *Brassica* species is an important factor when it comes to pest management but also with regard to animal and human nutrition. One way to control the accumulation of glucosinolates would be the manipulation of existing or introduction of novel pathway enzymes (Feldmann 2001; Brader et al., 2006). However, a further possibility would be to alter the expression of multiple enzymes at the same time by manipulating a regulator of the specific pathway (Endt et al., 2002; Broun, 2004).

1.4 The regulation of glucosinolate biosynthesis

The glucosinolate concentration and profile of *A. thaliana* not only differs among different organs and tissues, but also during plant development or in response to environmental stimuli (Petersen et al., 2002; Brown et al., 2003; previous section). Furthermore, indolic glucosinolate and IAA biosynthesis are tightly connected but differ with regard to relative abundance, spatial distribution, developmental control and responsiveness to environmental stimuli. Hence, a complex regulatory network controlling these processes can be expected. However, only few components involved in the regulation of glucosinolate and/or IAA accumulation have been identified to date.

IQD1 is a nuclear-localised calmodulin-binding protein, identified in a screen for mutants with increased glucosinolate accumulation (Levy et al., 2005).

Overexpression of *IQD1* results in increased levels of aliphatic and indolic glucosinolates. However, only genes coding for key enzymes of the indolic pathway were upregulated, the respective structural genes of the aliphatic pathway were downregulated, and the authors speculate about a possible feedback regulation of the two pathways. Nevertheless, the high glucosinolate phenotype was accompanied by an increased resistance against two generalist herbivores and *IQD1* transcription is induced by mechanical stimuli. Therefore, it might play a role in the biotic stress response.

A second putative component of the regulatory network controlling glucosinolate biosynthesis might be *OBP2*. *OBP2* is a member of the DNA-binding-with-one-finger (DOF) transcription factor family and was shown to induce the transcription of at least several genes involved in glucosinolate biosynthesis, mainly *CYP83B1* (Skirycz et al., 2006). Constitutive *OBP2* overexpression lines were characterised by moderately increased levels of short-chain aliphatic and indolic glucosinolates, but also by an elevated IAA concentration and an altered growth phenotype with small, curly leaves. *OBP2* transcription is activated by methyl jasmonate treatment, in response to wounding or herbivore attack. However, the effect on the transcript level was only seen several hours after treatment. Therefore, *OBP2* might not be part of an immediate response to biotic challenge.

Two further regulators of glucosinolate biosynthesis, mainly the indolic pathway, were originally identified as altered tryptophan regulation (*atr*) mutants. *ATR1* codes for an R2R3-type MYB transcription factor (*ATR1/MYB34*; Bender and Fink, 1998; Celenza et al., 2005), *ATR2* is a member of the basic helix-loop-helix (bHLH) proteins (*ATR2/bHLH05*; Smolen et al., 2002). Both, MYB and bHLH proteins, form two of the largest transcription factor families in plants, each with more than 120 members in *A. thaliana* (Stracke et al., 2001; Bailey et al., 2003). The factors, characterised so far, indicate diverse roles in plant development (Schmitz and Theres, 2005; Schellmann et al., 2007), regulation of secondary metabolism and stress response (Winkel-Shirley, 2002; Baudry et al., 2004). Also *ATR1/MYB34* and *ATR2/bHLH05* appear to have a regulatory role in plant secondary metabolism. Both mutant lines (*atr1D* and *atr2D*) are characterised by an increased resistance to the tryptophan analogue 5-methyltryptophan (5MT). 5MT is able to feedback-regulate the anthranilate synthase alpha subunit (Fig. 1.2) but does not substitute for the nutritional role of tryptophan. The *atr1D* and *atr2D* lines overcome this toxic effect by

a constitutive activation of *ASA1* transcription. The dominant mutation in *atr2D* is caused by an amino acid exchange in a conserved domain of ATR2/bHLH05. Interestingly, only overexpression of the mutated form (*atr2D*) but not of the wild-type allele (*ATR2/bHLH05*) leads to a pleiotropic phenotype characterised by the upregulation of multiple stress-related genes (Smolen et al., 2002). Therefore, the authors speculate whether the observed *ASA1* activation might be a secondary stress response rather than a direct effect of ATR2/bHLH05. The activation of several genes in *atr2D* might possibly result from a disturbed protein/protein interaction with other transcription factors. However, an interaction of ATR2/bHLH05 or the mutated protein with ATR1/MYB34 could not be observed in a yeast-two-hybrid assay (Smolen et al., 2002), even though the formation of regulatory bHLH/MYB heterodimers has been reported in other cases previously (Zimmermann et al., 2004a; Feller et al., 2006). The *atr1D* line carries a mutation upstream the *ATR1/MYB34* ORF, leading to a constitutively high expression level (Bender and Fink, 1998). The mutation results in an increased accumulation of indolic glucosinolates and IAA, caused by an activation of pathway genes (Celenza et al., 2005). The gene-to-trait relation was confirmed by ectopic overexpression of *ATR1/MYB34* and in a loss-of-function mutant. Interestingly, the *atr1-1* knock-out line could complement the high auxin phenotype of the *cyp83b1* mutant, indicating an important role of ATR1/MYB34 in the homeostasis of indolic glucosinolate and IAA biosynthesis.

Even though several players of a regulatory network controlling indolic glucosinolate biosynthesis and accumulation have been identified to date, they do not solely account for the complex regulation observed. Aim of the presented study was the identification of further components, accounting for the coordinate regulation of indolic glucosinolate biosynthesis and the characterisation of such regulators with respect to their role *in planta* and possible interactions with known regulators. To this end, multiple strategies were applied to characterise an activation-tagging line with an altered glucosinolate accumulation. Biochemical analyses were used to study the mutant chemotype in detail, and molecular biology approaches were employed to identify the underlying genotype and further investigate the influence of the altered expression profile *in planta*.

2 Material and Methods

2.1 Material

2.1.1 Chemicals, enzymes, oligo nucleotides

Unless otherwise stated, all chemicals were of analytical purity. Chemicals, laboratory equipment and enzymes were purchased from the following companies:

Amersham Pharmacia Biotech UK Ltd (Buckinghamshire, GB); Biorad (München, D); Roche (Mannheim, D); Difco (Hamburg, D); Duchefa (Haarlem, NL); DuPont Company (Wilmigton, GB); Fermentas GmbH (St. Leon-Rot, D); Fluka AG (CH); GibcoBRL (Karlsruhe, D); Heraeus (Düsseldorf, D); Intas (Göttingen, D); Merck (Darmstadt, D); Invitrogen Life Technologies (Karlsruhe, D); Molecular Dynamics (Krefeld, D); New England Biolabs (Schwalbach, D); Promega (Mannheim, D); Qiagen GmbH (Hilden, D); Roche (Mannheim, D); Roth (Karlsruhe, D); Sarstedt (Nümbrecht, D); Schleicher & Schuell (Dassel, D); Serva (Heidelberg, D); Sigma-Aldrich (Taufkirchen, D); Stratagene Europe (Amsterdam, NL).

The following kits were used according to the manufacturer's instructions:

QIAquick Gel Extraction Kit (Qiagen GmbH, Hilden, D)

QIAquick PCR Purification Kit (Qiagen GmbH, Hilden, D)

Quantum Prep Plasmid Miniprep Kit (BioRad, München, D)

Qiagen Plasmid Midi Kit (Qiagen GmbH, Hilden, D)

pENTR/D-TOPO[®] cloning Kit (Invitrogen Life Technologies, Karlsruhe, D)

Gateway[®] LR clonase[™] Enzyme Mix (Invitrogen Life Technologies, Karlsruhe, D)

Gateway[®] BP clonase[™] Enzyme Mix (Invitrogen Life Technologies, Karlsruhe, D)

Big Dye Terminator v3.1 Cycle Sequencing Kit (Applied Biosystems, Foster City, USA)

Agilent Low RNA Input Fluorescent Linear Amplification Kit (Agilent Technologies, Böblingen, D)

BCA[™] Protein Assay Kit (Pierce, Rockford, USA)

Oligo nucleotides were purchased from Metabion (Martinsried, D) and are listed in the appendix.

2.1.2 Media, buffers

All media and buffers were prepared with deionised water purified with a Milli-Q Plus PF system (Millipore, Schwalbach, D). Media were sterilised by autoclaving, heat-sensitive substances were filter sterilised. Unless otherwise stated solid media were prepared with 1% (w/v) agar. Plates used for the vertical growth of plant seedlings were prepared with 0.7% (w/v) gelrite.

Frequently used media and buffers:

TAE	40 mM Tris-Acetate, pH 7.5, 1 mM EDTA
TE	10 mM Tris-HCl, pH 8, 1 mM EDTA
LB	1% (w/v) bacto tryptone, 0.5% (w/v) yeast extract, 1% (w/v) NaCl
SOC	2% (w/v) bacto tryptone, 0.5% (w/v) yeast extract, 10 mM NaCl, 2.5 mM KCl, 10 mM MgCl ₂ , 10 mM MgSO ₄ ·7H ₂ O, 20 mM glucose
YEB	0.5% (w/v) bacto peptone, 0.5% (w/v) beef extract, 0.1% (w/v) yeast extract, 0.5% (w/v) sucrose, 0.05% (w/v) MgSO ₄ ·7H ₂ O
MGL	0.5% (w/v) bacto tryptone, 0.25% (w/v) yeast extract, 0.5% (w/v) NaCl, 0.5% (w/v) mannitol, 0.116% (w/v) sodium glutamate, 0.025% (w/v) KH ₂ PO ₄ , 0.01% (w/v) MgSO ₄ , 1 mg/L biotin
YPAD	2% (w/v) bacto peptone, 1% (w/v) yeast extract, 100 mg/L adenine, pH 5.8; After autoclaving 40% (w/v) filter sterilised glucose was added to a final concentration of 2% (w/v).
SD-medium (yeast selection medium)	6.7 g/L yeast nitrogen base w/o amino acids (Difco), 0.6 g/L DO Supplement -Ade/-His/-Leu/-Trp (BD Biosciences Clontech, Palo Alto, USA), pH 5.8; The amino acids used for negative selection were not added to the medium, the others at the given concentrations: Adenine (100 mg/L), Histidine (20 mg/L), Leucine (100 mg/L), Tryptophan (50 mg/L); After autoclaving 40% (w/v) filter sterilised glucose was added to a final concentration of 2% (w/v); For SD -His medium, 1M filter sterilised 3-amino-1,2,4-triazole(3-AT) was added to a final concentration of 5 mM.
Germination medium	2.2 g/L MS (245, Duchefa, Haarlem, NL), 1% (w/v) sucrose, pH 5.6;

2.1.3 Antibiotics

Antibiotics and their concentration used for the selection of positive transformed *E. coli* and *A. tumefaciens*:

Kanamycin	50 µg/mL
Ampicillin	50 µg/mL
Carbenicillin	50 µg/mL (<i>E. coli</i>); 100 µg/mL (<i>A. tumefaciens</i>)
Hygromycin	50 µg/mL
Chloramphenicol	10 µg/mL (<i>E. coli</i>); 75 µg/mL (<i>A. tumefaciens</i>)
Rifampicin	150 µg/mL (<i>A. tumefaciens</i> strain GV3101); 20 µg/mL (<i>A. tumefaciens</i> strain LB A4404.pBBR1MCS <i>virGN54D</i>)
Gentamycin	10 µg/mL (<i>E. coli</i>); 25 µg/mL (<i>A. tumefaciens</i>)

2.1.4 Organisms

2.1.4.1 Bacterial strains

Strain / Purpose	Genotype (Reference)
<i>Escherichia coli</i>	
DH5 α / Plasmid amplification	F ⁻ Φ 80d <i>lacZ</i> Δ M15 Δ (<i>lacZYA-argF</i>)U169 <i>deoR recA1 endA1 hsdR17</i> (r _K ⁻ m _K ⁺) <i>phoA supE44</i> λ ⁻ <i>thi-1 gyrA96 relA1</i> ; (Hanaha, 1983)
TOP10/ Plasmid amplification	F ⁻ <i>mcrA</i> Δ (<i>mrr-hsdRMS-mcrBC</i>) Φ 80d <i>lacZ</i> Δ M15 Δ <i>lacX74 recA1 araD139</i> Δ (<i>ara-leu</i>)7697 <i>galU galK rpsL</i> (Str ^R) <i>endA1 nupG</i> ; (Invitrogen)
DB3.1/ Propagation of <i>ccdB</i> containing plasmid	F ⁻ <i>gyrA462 endA1</i> Δ (<i>sr1-recA</i>) <i>mcrB mrr hsdS20</i> (r _B ⁻ , m _B ⁻) <i>supE44 ara-14 galK2 lacY1 proA2 rpsL20</i> (Sm ^R) <i>xyI-5</i> λ - <i>leu mtI1</i> ; (Invitrogen)
<i>Agrobacterium tumefaciens</i>	
GV3101/ Stable plant transformation	Rif ^R , Gent ^R ;; (Koncz and Schell,1986)
LB A4404.pBBR1MCS <i>virGN54D</i> / Leaf infiltration and cell culture transformation	Rif ^R , Chlor ^R ; (van der Fits et al., 2000)

2.1.4.2 Yeast strains (*Saccharomyces cerevisiae*)

Strain	Genotype (Reference)
Y187	MAT α , <i>ura3-52, his3-200, ade2-101, trp1-901, leu2-3, 112, gal4</i> Δ , <i>met-</i> , <i>gal80</i> Δ , URA3::GAL1UAS-Gal1TATA- <i>lacZ</i> , MEL1; (Harper et al., 1993)

AH109	MATa, trp1-901, leu2-3, 112, ura3-52, his3-200, gal4 Δ , gal80 Δ , Lys2::GAL1UASGAL1TATA-HIS3, MEL1, GAL2UAS-GAL2TATA-ADE2, URA3::MEL1UAS-MEL1TATA-lacZ; (James et al., 1996)
-------	--

2.1.4.3 Yeast cDNA libraries for yeast-two-hybrid assays

Library	Source
Ara 446	<i>A. thaliana</i> suspension culture grown in darkness; K.Salchert, AG C. Koncz, MPIZ Cologne
Ara-1101	Clontech Matchmaker cDNA Library; green leaf material from <i>A. thaliana</i> ; 3-week-old plants, ecotype Columbia; (Clontech)
HS-Ara1	polyT-cDNA from whole plants of <i>A. thaliana</i> , ecotype Columbia; Hans Sommer, MPIZ Cologne

The yeast-two-hybrid screens with these libraries were performed by the AG Uhrig, University of Cologne.

2.1.4.4 *Arabidopsis thaliana*

All plants and suspension cell cultures used or generated were in the background of *Arabidopsis thaliana* L.Heyn cv. Columbia (NASC-Nr. N1093).

Public available transgenic lines used in this study were:

Line 19.4, TAMARA activation tagging population (Schneider et al., 2005),

Line 228B12, GABI-Kat collection (Rosso et al., 2003).

2.1.4.5 *Nicotiana benthamiana*

Wild type plants (cv. Samsun) were used for leaf infiltration with *Agrobacteria*. The Bright Yellow cell culture (BY2) was used for subcellular localisation of fluorescent fusion proteins.

2.1.5 Vectors

2.1.5.1 Bacteria vectors

Vector	Source	Cloning purpose
pENTR/D-TOPO	Invitrogen	Creating a Gateway compatible entry clone
pDONR207	Invitrogen	Creating a Gateway compatible entry clone
pGWB1	T. Nakagawa, Shimane University	Gateway compatible binary destination vector, no promoter, no tag
pGWB2	T. Nakagawa, Shimane University	<i>In planta</i> overexpression under control of the CaMV 35S promoter

pGWB3	T. Nakagawa, Shimane University	<i>In planta</i> expression of the <i>uidA</i> reporter gene driven by the cloned promoter
pGWB3i	T. Nakagawa, Shimane University, modified (Berger et al., 2007)	<i>In vivo</i> expression of the <i>uidA</i> reporter gene containing an intron to prevent expression in <i>Agrobacteria</i>
pGWB5	T. Nakagawa, Shimane University	Expression of translational GFP fusion proteins for subcellular localisation
pSPYN	Klaus Harter, University of Tuebingen	Bimolecular fluorescence assay, “split-YFP”, translational fusion with the YFP N-terminus
pSPYC	Klaus Harter, University of Tuebingen	Bimolecular fluorescence assay, “split-YFP”, translational fusion with the YFP C-terminus
pUC Δ <i>alcAN</i>	Caddick et al., 1998	Ethanol inducible expression system
pBin Δ <i>alc-R</i>	Caddich et al., 1998	Ethanol inducible expression system

2.1.5.2 Yeast vectors

Vector	Source	Cloning purpose
pCD2-attR	Joachim Uhrig, University of Cologne	Gateway compatible yeast expression vector for construction of yeast-two-hybrid bait constructs; Trp1 ⁺
pC-ACT2-attR	Joachim Uhrig, University of Cologne	Gateway compatible yeast expression vector for construction of yeast-two-hybrid prey vectors / libraries; Leu2 ⁺
pACT	Joachim Uhrig, University of Cologne	Classical yeast expression vector used as empty control and for “gap repair”
pAS-SNF1	Joachim Uhrig, University of Cologne	Bait vector interacting with SNF4, used as positive control
pACT-SNF4	Joachim Uhrig, University of Cologne	Prey vector interacting with SNF1, used as positive control

2.2 Methods

2.2.1 Methods working with bacteria

2.2.1.1 Preparation of chemically competent *E. coli* cells

The protocol was adapted from Inoue et al. (1990) and slightly modified.

Several *E. coli* colonies were inoculated in 250 mL LB (supplemented with 50 mM MgCl₂) and grown at 18°C until an OD₆₀₀ of 0.6. The suspension was chilled on ice for 10 min, distributed to 50 mL tubes and centrifuged at 4500 g in a cooled centrifuge. The pellets were resuspended in 80 mL ice-cold TB buffer (10 mM Pipes,

55 mM MnCl₂, 15 mM CaCl₂, 250 mM KCl) and incubated on ice for another 10 min. The cells were harvested by centrifugation and resuspended in 20 mL ice cold TB buffer. DMSO was slowly added to a final concentration of 7% (v/v). The cell suspension was incubated on ice for 10 min. Aliquots of 100 µL were frozen in liquid nitrogen and kept at -80°C until use.

2.2.1.2 Transformation of chemically competent *E. coli* cells

An aliquot of chemical competent *E. coli* cells was thawed on ice and about 200 ng of vector DNA were added. After 30 min on ice, the cells were heat-shocked by incubation for 30-60 sec at 42°C and cooled immediately on ice for about one minute. The cells were recovered in 900 µL LB or SOC medium and incubated at 37°C for one hour with gentle shaking. For selection of positive transformands, an aliquot of the cells was plated on solid LB medium containing the respective antibiotics and incubated overnight at 37°C.

2.2.1.3 Preparation of electro-competent *Agrobacteria*

A preculture of *Agrobacteria* was diluted in 100 mL MGL medium (OD₆₀₀ of 0.04-0.08) and grown for about 4 h to an OD₆₀₀ of 0.5. Subsequently, all steps were performed on ice and a cooled centrifuge was used. The cells were harvested by centrifugation and resuspended in 40 mL 1 mM HEPES, pH 7. After that, three further washing steps followed. Each time, the cells were centrifuged and resuspended in 1 mM HEPES, pH 7, 10% (v/v) glycerol, decreasing the volume from 40 mL to 2 mL and 1mL, respectively. 50 µL aliquots of the final cell suspension were snap frozen in liquid nitrogen and stored at -80°C until use.

2.2.1.4 Transformation of electro-competent *Agrobacteria*

Electro competent *Agrobacteria* were thawed on ice and about 50-200 ng vector DNA were added. The cells were transferred to a chilled electroporation chamber (2 mm gap) and subjected to electroporation (25 µF, 400 Ω, 2.5 kV pulse for about 2 sec). Immediately, 1 mL YEB medium at RT was added and the cells were allowed to recover for 2 hours at 28°C with gentle shaking. Positive transformands were selected by plating an aliquot on solid YEB medium containing the respective antibiotics and incubation for 2 days at 28°C.

2.2.2 Methods working with yeast

2.2.2.1 Yeast transformation on small scales

Small scale preparation of competent cells and yeast transformation was performed according to the LiAc method described by Gietz et al. (1995). About 200-500 ng plasmid DNA were used per transformation. If multiple transformations were done in parallel, the DNA was distributed to Eppendorf tubes and the competent yeast cells were then added.

2.2.2.2 Yeast transformation in a multi-well format

For 100 transformations, 5 mL of an overnight yeast culture were inoculated in 150 mL YPAD and grown at 30°C for about 4 hours. The cells were harvested by centrifugation and washed once in 25 mL H₂O. The cells were again centrifuged, the supernatant discarded and the pellet resuspended in the remaining liquid. The following reagents were added in the given order: 7 mL PEG 3350 (50% w/v); 1.06 mL 1 M LiAc, pH 7.5; 735 µL single stranded DNA (2 mg/mL); 1.3 mL H₂O. The cells were resuspended by pipetting and 100 µL competent yeast cells were added to each well, already containing the vector DNA. The cells were mixed with the DNA and the plates were incubated for 30 min at 30°C, then for 20 min at 42°C. The cells were sedimented by centrifugation, the supernatant removed and the pellet mixed with 100 µL selection medium. A second plate with a 1:100 dilution in selection medium was prepared and both plates were kept at 30°C. After 2-3 days the positive transformands were transferred to solid medium plates using a multi-well replicator.

2.2.2.3 *In vivo* recombination (“gap repair”)

Yeast offers the advantage of high frequency homologous recombination. It allows therefore the high throughput cloning of PCR fragments into linearised plasmids (“gap repair”), given the PCR fragments and plasmid have homologous sequences. For this purpose, PCR fragments and a linearised, dephosphorylated plasmid are introduced into yeast by co-transformation in a multi-well format (2.2.2.3).

2.2.2.4 Mating of two haplotypes in a multi-well format

Introducing two separate plasmids into yeast can be achieved by co-transformation of both plasmids into a single yeast strain, or by introducing each construct into yeast strains of opposite mating types and subsequent mating of these strains. This allows

handling the transformants separate from each other and allows the generation of larger numbers of double positive transformants than achieved with the co-transformation method.

As well as “gap repair” and yeast transformation, mating can be performed in a multi-well format. Therefore, colonies of both mating partners were resuspended each in 50 μL YPAD (PEG 3350 10% (w/v)) and mixed together in a multi-well plate (100 μL final volume). The plates were incubated for at least 3 hours at 30°C before the cells were transferred to solid selection media with a multi-well replicator.

2.2.3 Plant methods

2.2.3.1 Plant growth

To break the seed dormancy, freshly sown seeds on either soil or culture plates were stratified for 2-4 days in the dark at 4°C.

2.2.3.1.1 Growth on soil

Seeds were sown on humid, freshly prepared *A. thaliana* or tobacco culture soil and covered with a transparent plastic lid for the first days to maintain high humidity. Plants were either grown in the greenhouse with a 16 h/8 h light/dark regime and an average photon flux density of 150-200 $\mu\text{mol}\cdot\text{m}^{-2}\cdot\text{s}^{-1}$, or in a growth cabinet with an 8 h/16 h light dark cycle and an average photon flux density of 70 $\mu\text{mol}\cdot\text{m}^{-2}\cdot\text{s}^{-1}$. The temperature was kept at 22°C during the light and 18°C during the dark period. Relative humidity was approximately 40%.

2.2.3.1.2 Growth on sterile culture plates

Surface sterilised Arabidopsis seeds were plated on solid germination medium and incubated in growth cabinets with a 12 h /12 h light dark or a 8 h /16 h light/dark regime, and an average photon flux density of 70 $\mu\text{mol}\cdot\text{m}^{-2}\cdot\text{s}^{-1}$. For the selection of T_1 transformants the seeds were mixed with 0.1% (w/v) agarose and evenly distributed on germination medium supplemented with 50 $\mu\text{g}/\text{mL}$ kanamycin. The resistance of seedling to 5-methyl-tryptophan (5MT) was tested by growth on germination medium containing 15 μM 5MT.

2.2.3.1.3 Growth in liquid germination medium

15 - 25 surface sterilised Arabidopsis seeds were added to 100 mL liquid germination medium in a 250 mL Erlenmeyer flask and grown for 7 days under constant light and

constant shaking (140 rpm). The concentrations of substances were as indicated for growth on solid medium, unless otherwise stated.

2.2.3.2 Stable plant transformation

Flowering *Arabidopsis* plants were transformed by the floral dip method, adapted from Clough and Bent (1998). In brief, the respective *Agrobacterium* strain was grown in 300 mL LB medium until OD₆₀₀ of 0.8-1.0. The cells were harvested by centrifugation (2500 g for 15 min at RT) and resuspended in infiltration medium (5% (w/v) sucrose, pH 5.7, 0.03% (v/v) Silwet L-77; in tap water) to an OD₆₀₀ of 0.8. The inflorescence of the *Arabidopsis* plants was submerged in this suspension for 20 sec and the plants were afterwards kept horizontally in the dark for one day, prior to transfer to the greenhouse.

2.2.3.3 Transient transformation

2.2.3.3.1 Transformation of *A. thaliana* suspension culture (Berger et al., 2007)

A. thaliana cells were grown in the dark at 22°C with gentle shaking at 160 rpm. The cells were inoculated weekly at a 1:5 dilution into fresh medium (4.3 g/L MS basal salts (Duchefa, NL), 4 mL/L Gamborg's vitamin solution (Sigma, Munich, D), 1 mg/L 2,4-dichlorophenoxyacetic acid (2,4-D), 30 g/L sucrose, pH 5.8).

The *Agrobacteria* strains used were the hypervirulent strain LBA4404.pBBR1MCS *virGN54D* (van der Fits et al., 2000) for the effector and reporter vectors and the antisilencing strain 19K (Voinnet et al., 2003). *Agrobacteria* from fresh plates were grown overnight in YEB medium with the respective antibiotics. Cells were harvested by centrifugation, washed once in the plant cell culture medium and resuspended in 25 % of the initial culture volume. 25 µL of the 19K strain and 25 µL of the reporter and/or effector strains were added to 3 mL of 1:5 diluted plant cell culture in 6 well sterile culture plates (Corning Inc., USA). After 3-4 days of co-culture (dark, 22°C, 160 rpm), 1 mL of each sample was centrifuged and the pellet was stored at -80°C until GUS analysis. The remaining cells were treated with 500 µL X-Gluc staining solution (50 mM NaH₂PO₄, pH 7, 1 mM X-Gluc) for one hour to overnight at 37°C in the dark (without shaking).

2.2.3.3.2 *A. thaliana* and *N. benthamiana* leaf infiltration with *Agrobacteria*

For the transient expression in leaves, *A. thaliana* and *N. benthamiana* plants were grown in the greenhouse for about 4-6 weeks (vegetative growth phase).

The Agrobacteria (LB A4404.pBBR1MCS *vir*GN54D) carrying the desired constructs and the anti-silencing strain 19K were grown overnight in 3-5 mL YEB medium with the respective antibiotics. The cells were harvested by centrifugation (15 min, 4000 rpm) and the supernatant discarded. The Agrobacteria were resuspended in AS medium (10 mM MgCl₂, 10 mM MES, pH 5.6, 150 µM acetosyringon) and the OD₆₀₀ adjusted to 0.7-0.8. The cells were left at RT for about 4 hours. Prior to leaf infiltration, the Agrobacteria were mixed in an equimolar ratio and injected into the abaxial air space of the leaves using a syringe. The plants were kept in the dark overnight and then transferred to the greenhouse. Leaves were analysed about 3-4 days after infiltration.

2.2.3.3.3 Transfection of tobacco BY2 protoplasts

The transfection of BY2 protoplast was performed as described by Sheen (2001), based on the PEG mediated transfection with 30 µg of total DNA.

2.2.3.4 Seed surface sterilisation

2.2.3.4.1 Wet method

Arabidopsis seeds were surface sterilized in 3.6% (v/v) sodium hypochlorite, 0.02% (v/v) Triton X-100, for 15 min followed by several washes with sterile deionised water.

2.2.3.4.2 Dry method

Arabidopsis seeds were distributed into Eppendorf tubes and placed in a glass desiccator next to a beaker with 100 mL 12% (v/v) sodium hypochlorite. Three mL 37% (v/v) hydrochloric acid were added carefully to the sodium hypochlorite and the desiccator was closed tightly. The seeds were surface sterilized for at least 4 hours up to overnight incubation. The chlorine gas was allowed to evaporate from the Eppendorf tubes for 2-3 hours under the cleanbench.

2.2.3.5 Histochemical GUS analysis, modified after Jefferson et al. (1987)

Histochemical detection of GUS activity was performed using 5-bromo-4-chloro-3-indolyl-β-D-glucuronid acid (X-Gluc) as substrate. The plant material was initially fixed for about 30 min in Fixans (0.3% (v/v) formaldehyde, 10 mM MES, pH 5.6, 0.3 M mannitol) and then rinsed in washing buffer (50 mM Na₂HPO₄, pH 7) for the same time. The fixed material was infiltrated with staining solution (50 mM Na₂HPO₄, pH 7, 1 mM X-Gluc) and stained overnight at 37°C in the dark. If plant material with a

hydrophobic surface was stained (leaf, stem), Triton X-100 was added as surfactant to a final concentration of 0.1% (v/v). Chlorophyll of stained sample was removed by incubation in 70% (v/v) ethanol until the plant material was clear. The destaining process could be accelerated by microwaving the samples in 70% (v/v) ethanol.

2.2.3.6 Quantitative GUS activity measurement

Proteins were extracted from leaf of cell pellets in 200-800 μ L protein extraction buffer (50 mM Na_2HPO_4 , pH 7, 1 mM EDTA, 0.1% (v/v) Triton X-100). The homogenate was centrifuged (15 min, 13000 rpm, 4°C) and the clear supernatant was used for protein quantification (BCA kit, Pierce, Rockford, USA) with BSA as a standard. The GUS activity was determined using 4-methylumbelliferyl- β -D-glucuronide (MUG) as substrate. The amount of 4-methylumbelliferone (4MU) formed, was recorded fluorometrically (Ex 340 nm; Em 465 nm). For this, 200 μ L substrate buffer (protein extraction buffer with 1 mM MUG) and 25 μ L protein extract were mixed, incubated at 37°C in the dark and measured every 10-30 min on a Tecan multi-well plate reader (Crailsheim, D).

2.2.3.7 Microscopical documentation

Fluorescence fusion proteins were analysed with a Nikon Eclipse E800 using a GFP specific filter (GFP-BD; EX 460-500; DM 505; BA 510-560).

GUS stained plant material was either analysed with a Nikon Eclipse E800 (microscope) or a Nikon SMZ-U (stereoscope).

Pictures were taken with a 1-CCD colour video camera (KY-F1030; JVC, Singapore) operated by the DISKUS software (Technisches Büro Hilger, Königswinter, D).

2.2.3.8 Hormone treatment of plants

Arabidopsis plants were treated with hormones either by direct spraying or growth on hormone supplemented media. The hormones were used at the given concentrations:

Hormone	Concentration used for spraying (in 0.1% (v/v) ethanol, 0.05% (v/v) Tween)	Concentration added to growth media (0.01% (v/v) ethanol final concentration)
1-Aminocyclopropane-1-carboxylic acid (ACC)	10 μ M	10 μ M
Salicylic acid (SA)	0.5 mM	10 μ M
Methyl jasmonate (MeJ)	0.45 mM	10 μ M

For spraying experiments, 6-week-old wild type plants (grown under short day conditions, vegetative growth phase) were used. The rosettes were sprayed with the respective hormone solution to cover each leaf and the plants were kept under a transparent lid to maintain vapour and avoid cross contamination with other hormones. Samples for RNA extraction were taken after 0, 0.5, 2 and 4 hours.

For growth on hormone supplemented media, transgenic *Arabidopsis* plants carrying a GUS reporter construct were used. Liquid culture experiments were performed with 7-day-old seedlings by adding the hormones to the medium yielding the respective final concentration. Samples for histochemical GUS staining were taken 0, 4, 24 and 48 hours after hormone induction. Hormone treatment on solid media was achieved by growing seedlings vertically, allowing the roots to grow on top of a sterile filter paper, laid on the surface of the medium. For hormone induction, the filter paper was soaked with 2 mL of the respective hormone solution and samples were taken at the same time points as for liquid culture experiments.

2.2.3.9 Ethanol induction of transgenic lines

Six-week-old transgenic *Arabidopsis* plants (short day conditions, vegetative growth phase) carrying an ethanol inducible construct and control plants were induced by watering with 0.1% (v/v) ethanol. The plants were covered with a transparent lid to maintain the ethanol vapour. Rosette leaves for RNA extraction were taken 0, 6, 12 and 24 hours after induction.

2.2.3.10 Extraction and measurement of glucosinolates and free auxin

The original identification of I3M in the transgenic *HIG1-1D* line is described in Schneider et al. (2005) and Gigolashvili et al. (2007).

For a detailed analysis of the chemotype, glucosinolates were extracted from rosette leaves and analysed as described by Gigolashvili et al. (2007). In brief, glucosinolates were isolated from methanolic extracts of lyophilised rosette leaves. The extracts were loaded to an anion exchange column (DEAE Sephadex A25) for purification. After an overnight digestion with sulfatase (E.C. 3.1.6.1; designated 'type H-1, from *Helix pomatia*, Sigma, D) the deslufo-glucosinolates were eluted from the column, vacuum dried and resuspended in a small volume of HPLC grade water for subsequent HPLC analysis (performed by C. Müller, University Würzburg).

Extraction and quantification of free auxin was performed as described by Muller and Weiler (2000; quantification was performed by AG Weiler, University Bochum).

2.2.3.11 Dual choice assay with *Spodoptera exigua* (C. Müller, University Würzburg)

Dual-choice assays were performed to study the consumptional preference of the generalist lepidopteran herbivore, *Spodoptera exigua* (Lepidoptera:Noctuidae). Eggs of *S. exigua* were provided by Bayer CropScience (Monheim, D) and larvae were kept on artificial diet. Fourth-instar larvae were used in dual-choice assays. Larvae were tested individually in Petri dishes (5.5 cm in diameter) offering them two leaves of equivalent age of different *Arabidopsis* lines on moistened filter paper for 8 h at 25°C. Leaves were weighed and scanned before and after feeding. Leaf area was analyzed using Winfolia (Regent Instruments Inc.). Three different pair combinations of leaves were provided to each 20 larvae: *HIG1-1D* and wild-type (Col-0), *HIG1-1D* and *hig1-1*, and Col-0 and *hig1-1*. The consumed fresh weight was calculated by [(weight begin*area end)/area begin].

2.2.4 Molecular biology methods

2.2.4.1 Small scale plasmid preparation from *E. coli* cells (miniprep)

Small scale plasmid preparations (Miniprep) from *E. coli* cells were performed with the Biorad Quantum Prep[®] Plasmid Miniprep Kit according to the protocol provided by the manufacturer.

2.2.4.2 Large scale plasmid preparation from *E. coli* cells

Large quantities of plasmid DNA were prepared using the QIAGEN Plasmid Midi Kit following the manufacturer's instructions.

2.2.4.3 Extraction of genomic DNA from plant material (fast prep)

About 50 mg rosette leaves from *Arabidopsis* were collected in an Eppendorf tube and homogenised in 400 µL extraction buffer (200 mM Tris-HCl, pH 7.5, 250 mM NaCl, 25 mM EDTA, 0.5% (w/v) SDS) and mixed on a vortex. The cell debris were removed by centrifugation (13000 rpm, 5 min) and the supernatant was mixed with 350 µL isopropanol. The samples were incubated for 10 min at RT before the DNA was pelleted by centrifugation (13000 rpm, 15 min). The pellet was washed once with 70% (v/v) ethanol, air dried and resuspended in 50 µL TE.

2.2.4.4 Extraction of total RNA from plant material

Total RNA used for RT-PCR analysis was extracted from plant tissue using TRIzol[®] reagent (Invitrogen, Karlsruhe) according to the protocol provided by the

manufacturer. Total RNA used for microarray hybridisation was isolated according to a modified protocol from Chomczynski and Sacchi (1987). The RNA extraction solution was prepared as follows. First, a pre-solution was prepared (50% (w/v) guanidinium thiocyanate, 0.5% (w/v) sodium laurylsarcosil, 2.5 mM sodium acetate, pH 7), which was autoclaved and stored stable for several months. Prior to use the pre-solution was mixed 1:1 with phenol (DNA grade, water saturated) and β -mercaptoethanol was added to 0.35% (v/v) final concentration. The plant material (0.3 g) was homogenized with liquid nitrogen in a mortar and the powder was resuspended in 2 mL RNA extraction solution. The homogenate was evenly distributed to two 2 mL reaction tubes and briefly incubated at RT. Subsequently, 500 μ L of chloroform-isoamyl alcohol (24:1) was added to each tube. The mixture was shaken vigorously and left on ice for 30 min, prior to centrifugation (10 min, 12000 g, 4°C). The upper, aqueous phase was transferred to new tubes and mixed with 1 N acetic acid and ethanol at final concentrations of 0.05% (v/v) and 0.7% (v/v), respectively. The samples were incubated for 30-60 min on ice and the RNA was sedimented by centrifugation (10 min, 14000 g, 4°C). The pellet was resuspended in 800 μ L 3M sodium acetate, pH 5.2, centrifuged (10 min, 14000 g, 4°C) and washed twice with 1 mL 80% (v/v) ethanol. The supernatant was removed carefully and the pellet was dried under the fume hood for about 15-20 min. The total RNA was carefully resuspended in 50 μ L DEPC treated water.

Quantity and quality of the isolated RNA were tested spectrophotometrically at 260 nm and 280 nm in 50 mM Na₂HPO₄, pH 7. A ratio of OD₂₆₀:OD₂₈₀ between 1.8-2.1 was considered as pure enough for subsequent cDNA or cRNA synthesis for microarray hybridisation.

2.2.4.5 DNase I treatment and reverse transcription

To remove any contaminating genomic DNA from isolated total RNA the samples were treated with RNase-free DNase I (Roche, Mannheim, D) according to the manufacturer's instructions. About 1-4 μ g DNase I treated total RNA were then used for reverse transcription, taking on account never exceeding one fourth of the total reaction volume. Synthesis of cDNA was performed using SuperScript® II Reverse Transcriptase (Invitrogen Life Technologies, Karlsruhe, D) as described in the provided protocol and using oligo dT primers (Metabion, Martinsried, D).

2.2.4.6 cRNA synthesis and microarray hybridisation

The Agilent Low RNA Input Fluorescent Linear Amplification Kit was used according to the protocol provided for cRNA synthesis and labelling. Hybridisation of the Agilent Arabidopsis2 22K microarray v4.1 and processing were performed according to the Agilent 60-mer oligo microarray processing protocol.

2.2.4.7 Polymerase Chain Reaction

Standard PCR conditions were as follows:

	25 μ L final volume	50 μ L final volume
10x buffer (Qiagen, Stratagene, Biorad)	2.5 μ L	5 μ L
50 mM MgCl ₂	0-1 μ L	0-2 μ L
10 mM dNTPs	0.5 μ L	1 μ L
10 pmol/ μ L primer A and B	0.5 μ L each	0.5 μ L each
Taq (Qiagen, Stratagene, Biorad)	1 unit	1-2 units
template DNA	0.5-2 μ L or a single bacteria colony	0.5-2 μ L
HPLC grade water	to 25 μ L	to 50 μ L

All PCRs were performed on a MJ Research thermocycler (München, D).

Standard cycling conditions were:

cycle number	temperature	time
1	94°C	2.5-3 min
23-32	94°C	30 sec
	$\sim 5^\circ\text{C} < T_m$	30 sec
	72°C	1 min/kb
1	72°C	10 min

(T_m indicates the annealing temperature of the primers used)

2.2.4.8 Yeast Colony PCR

A single colony was picked and mixed with 25 μ L freshly prepared 0.02 N NaOH. The cells were lysed for 5 min at RT and 2 μ L of the lysate was added to the prepared PCR mixture (0.1 mM dNTPs, 10 pmol of primer AD_5N and BD_3N, 1x PCR buffer, 2.5 mM MgCl₂, 1.25 U Taq) with a final volume of 50 μ L. The cycling conditions were as follows: 94°C (2 min); followed by 40 cycles of 94°C (45 sec) – 50°C (45 sec) – 72°C (2 min) and a final extension at 72°C (5 min).

2.2.4.9 Estimation of quantity and size of DNA fragments

DNA fragments were separated electrophoretically on 1% (w/v) agarose gels in 1x TAE buffer. Size and quantity of DNA fragments was estimated by comparison to the 1 Kb DNA ladder (Invitrogen Life Technologies, Karlsruhe, D).

2.2.4.10 Purification of DNA fragments

DNA fragments were either purified after PCR (QIAquick PCR Purification Kit, Qiagen GmbH, Hilden, D) or excised from agarose gels and purified with the QIAquick Gel Extraction Kit (Qiagen GmbH, Hilden, D).

2.2.4.11 Sequencing of DNA fragments

The sequencing reactions were performed with the Big Dye Terminator v3.1 Cycle Sequencing Kit (Applied Biosystems, Foster City, USA) using the following reaction conditions:

DNA	10-100 ng
5x buffer	1 μ L
Big Dye v3.1	2 μ L
Primer (10pmol/ μ L)	1 μ L
HPLC grade water	to 10 μ L

The cycling program was as follows:

cycle number	temperature	time
1	96°C	20 sec
35	96°C	10 sec
	55°C	10 sec
	60°C	4 min

After termination of the reaction, 10 μ L HPLC grade water were added to reach a final volume of 20 μ L and the samples were processed in the Institute of Genetics, University of Cologne on a ABI 3730 Genetic Analyser (PE Applied Biosystems GmbH). The chromatogram files were analysed using the Chromas lite v2.0 software.

2.2.4.12 Classical vector cloning

Unless otherwise stated, all classical cloning procedures were performed as described by Ausubel et al. (1997).

2.2.4.13 Gateway[®] cloning

The Gateway[®] technology is extensively described on the Invitrogen homepage (<http://www.invitrogen.com/content.cfm?pageid=4072>). Furthermore, all kits and enzymes used for Gateway[®] cloning were used according to the manuals provided with modifications regarding reaction volume and time. All reactions were performed in one fifth of the recommended volume to reduce costs, and the reaction time was 30 min to 2 h for TOPO reactions and 3 h to overnight incubation for BP and LR reactions.

3 Results

3.1 Isolation of the *HIG1-1D* mutant

Sequencing of the Arabidopsis genome has revealed that many genes form part of gene families. Examples are transcriptional regulators that, unlike in animals, belong to large families in *A. thaliana*. Studying the function of these genes by classical knock-out screenings is often limited due to a high functional redundancy. One way to overcome this problem is the use of dominant mutants, such as activation-tagging populations. An artificial transcriptional enhancer (activation-tag) is integrated randomly into the genome as transfer DNA (T-DNA). Integration of the activation-tag in close proximity of a gene can result in the transcriptional upregulation, thereby generating a dominant overexpression line. Several activation-tagging populations have been described, and they have been used successfully to assign functions to so far uncharacterised genes (Weigel et al., 2000; Borevitz et al., 2000). One of these populations is the TAMARA collection, which was employed in a high-through put HPLC screen to identify mutants with an altered secondary metabolite profile (Schneider et al., 2005). Rosette leaves of T₁ generation plants grown in the greenhouse were used for the preparation of methanolic extracts and analysis by HPLC according to Reichelt et al. (2002). One of these lines, line 19.4, showed a significant upregulation of a single compound (Fig. 3.1), eluted at 13.8 minutes retention time under the chosen conditions (Schneider et al., 2005). Preparative

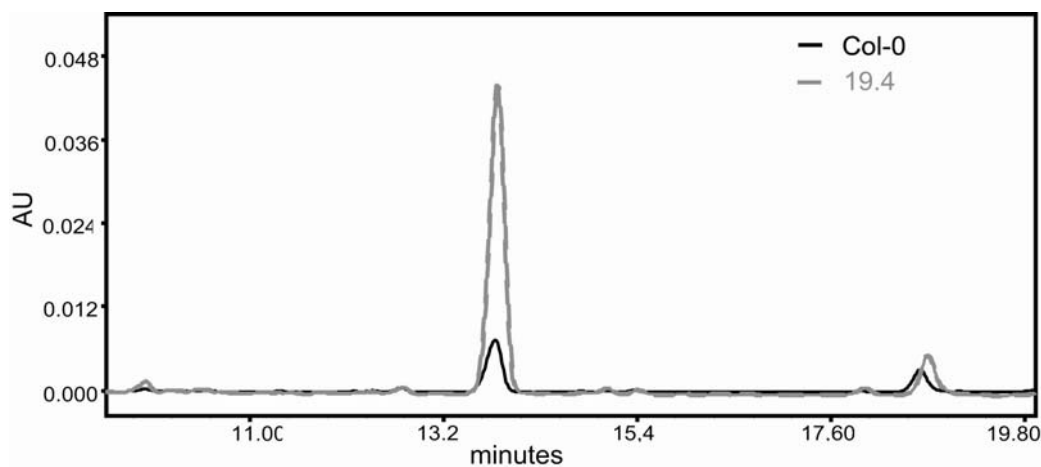


Figure 3.1: HPLC profile of rosette leaf extracts taken from wild-type (Col-0) and the activation-tagging line 19.4. The peak at 13.8 minutes retention time is clearly increased in the activation-tagging line and was identified as indol-3-ylmethyl glucosinolate.

HPLC analysis in combination with mass spectrometry allowed the identification of the compound as indol-3-ylmethyl glucosinolate (I3M; all biochemical analysis were performed by H.-P. Mock, Gatersleben).

The observed accumulation of I3M was stable over four generations and the mutation was shown to be dominant by backcrossing with wild-type. The mutant was therefore called *HIG1-1D* for *High Indolic Glucosinolate 1 – 1 Dominant* and was chosen for subsequent detailed analysis.

Since the mutation was generated by T-DNA integration, the site of integration could be identified by TAIL-PCR (performed by T.Gigolashvili, University of Cologne; Schneider et al., 2005) and was localised on chromosome 1, about 1.4 kb upstream of the At1g18570 locus. To confirm the gene-to-trait relation between the presence of the activation-tagging element and the accumulation of I3M, a segregating F₂ population generated by backcrossing to wild-type, was analysed. The genotype of the F₂ individuals was verified by PCR and HPLC analyses were performed to quantify the amount of I3M (Fig. 3.2). Plants carrying the activation-tagging element showed an up to 4-fold accumulation of I3M when compared to wild-type plants. Plants heterozygous for the activation-tag showed slightly less accumulation than homozygous *HIG1-1D* plants, indicating that the I3M accumulation might be dosage dependent.

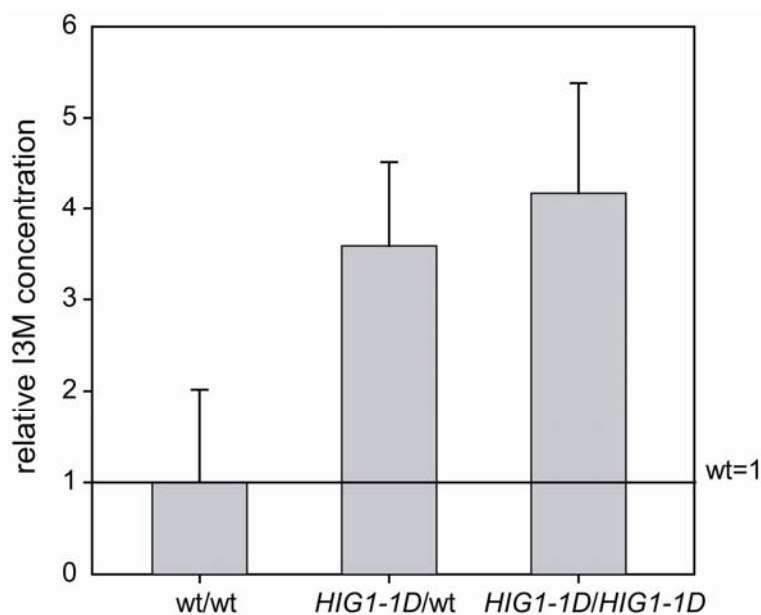


Figure 3.2: Relative I3M concentration of a segregating F₂ population. Plants heterozygous and homozygous for *HIG1-1D* showed up to 4-fold increase in I3M accumulation compared to wild-type plants (mean ±SD; n=10).

3.2 **HIG1 encodes an R2R3 MYB transcription factor**

To identify the cause of high I3M accumulation in the *HIG1-1D* mutant, the candidate genes, surrounding the activation-tag insertion were analysed, since overexpressed genes are often found adjacent to the inserted enhancer (Weigel et al., 2000). The transcript profiles of two genes upstream and three genes downstream of the insertion were analysed by semi-quantitative RT-PCR (T.Gigolashvili, University of Cologne). Only the transcript of At1g18570 was significantly upregulated in the *HIG1-1D* mutant, compared to the wild-type control (Fig. 3.3). The transcript of At1g18550 (kinesin motor protein-related) was unchanged, transcription of At1g18560 (transposase-related protein) could not be detected, neither in *HIG1-1D* nor in wild-type plants. The expression level of At1g18580 (putative galacturonosyl transferase; Sterling et al., 2006) and At1g18590 (sulfotransferase AtST5c; Piotrowski et al., 2004; Klein et al., 2006) were comparable in the wild-type and the mutant line. Therefore, the overexpression of At1g18570 appeared to be the cause for I3M accumulation in the *HIG1-1D* mutant.

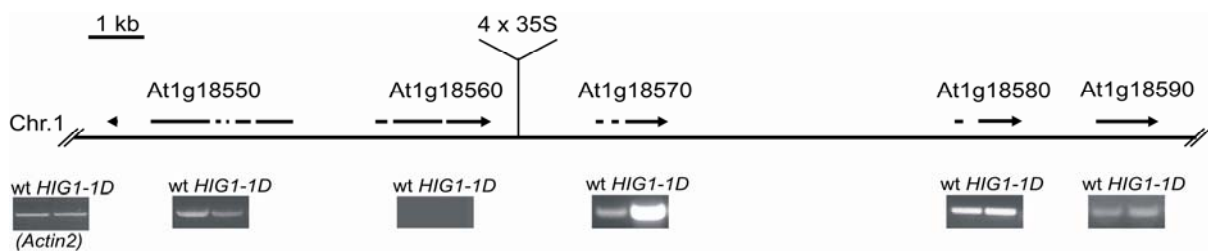


Figure 3.3: Schematic representation of the T-DNA integration site of *HIG1-1D* on chromosome I. The transcript of the indicated loci were analysed by RT-PCR. Only the transcript of At1g18570 was altered in comparison to the wild-type level. *Actin2* was used as control.

At1g18570 encodes for an R2R3-type MYB transcriptional regulator, classified as MYB51 (Stracke et al., 2001). MYB51 is a member of the subgroup 12 of R2R3 MYB factors that share the common motif [L/F]NK[K/R]VA in the carboxy-terminal region (Fig. 3.4). There are five additional members in subgroup 12, with MYB122 being the closest homologue. ATR1/MYB34 has been previously characterised as a regulator of tryptophan biosynthesis (Bender and Fink, 1998) and was shown to play a role in the auxin-glucosinolate homeostasis (Celenza et al., 2005). The other members are currently under investigation.

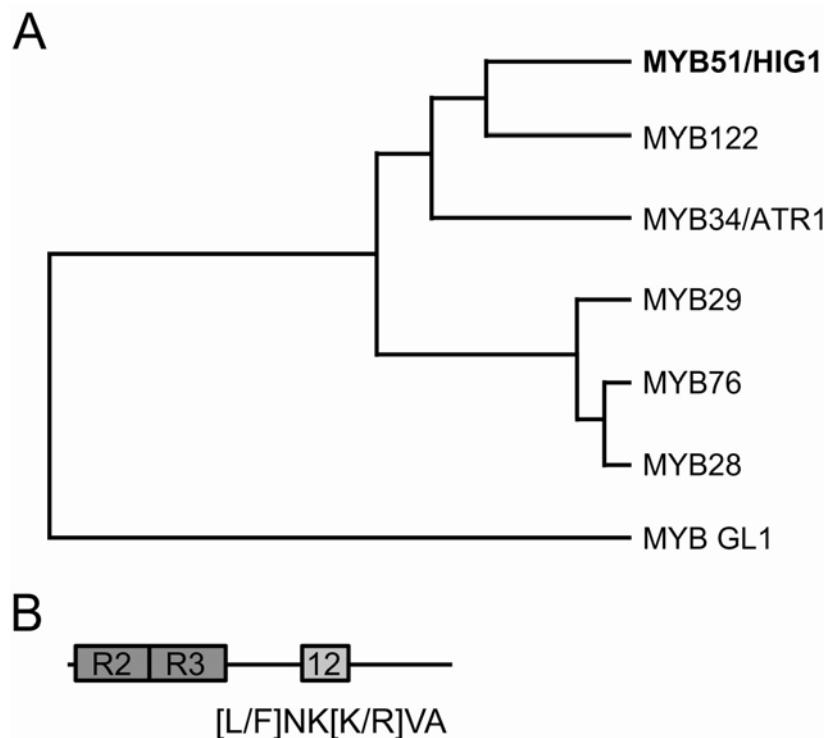


Figure 3.4: (A) Phylogenetic tree of subgroup 12 R2R3 MYB transcription factors in relation to MYB GL1. (B) Schematic representation of the protein structure. R2 and R3 indicate the two MYB domains at the amino-terminal end. 12 indicates the common motif [L/F]NK[K/R]VA with unknown function.

The gene structure of *HIG1/MYB51* consists of 3 exons and two introns, encoding a protein of 352 amino acids (aa) with a calculated mass of 39 kDa and an isoelectric point (pI) of 5.6. The two MYB domains are located at the amino-terminal region of the protein (R2:aa 9-62; R3: aa 63-113), while the motif specific for subgroup 12 is located in the middle of the sequence (aa 174-179).

3.3 *HIG1/MYB51* is nuclear-localised

Several programs that predict the subcellular localisation of proteins are available online. Examples are the servers of WoLF PSORT (<http://wolfpsort.org/>; Horton et al., 2006) or LOCTree (<http://cubic.bioc.columbia.edu/services/loctree/>; Nair and Rost, 2005). Both software systems predict *HIG1/MYB51* to be nuclear-localised, consistent with the idea of a transcriptional regulator. To confirm the *in silico* prediction, the subcellular localisation was tested *in vivo*. The full-length coding sequence of *HIG1/MYB51* was cloned into pGWB5 for translational fusion with the green fluorescent protein (GFP) under control of the *CaMV* 35S promoter. Whereas transfection of tobacco BY2 protoplasts with the empty pGWB5 vector resulted in a

disperse GFP staining, the *HIG1/MYB51*-GFP fusion protein was clearly detectable in nuclei of transfected cells (Fig. 3.5), confirming the sequence based prediction. The DNA specific DAPI staining was used as a nuclear staining control.

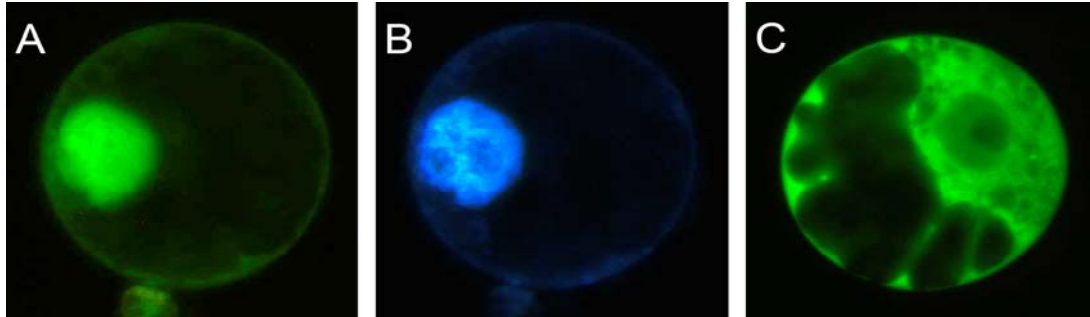


Figure 3.5: Subcellular localisation of the *HIG1/MYB51*-GFP fusion protein in tobacco BY2 protoplasts. (A) *HIG1/MYB51*-GFP signal; (B) DNA specific DAPI staining; (C) empty vector control.

3.4 *HIG1/MYB51* is mainly expressed in vegetative organs

To get a general idea about the expression pattern of *HIG1/MYB51*, samples from different organs of *A. thaliana* wild-type plants in the reproductive growth phase were taken for RT-PCR analysis. Transcription of *HIG1/MYB51* could be detected in the roots and rosette leaves of 6-week-old plants (Fig. 3.6). Furthermore, *HIG1/MYB51* could be amplified from cDNA synthesised from stem samples. However, *HIG1/MYB51* transcription was not detectable in mature siliques or flowers. Therefore, the expression of *HIG1/MYB51* is restricted to vegetative organs of *A. thaliana*, and is not found in reproductive organs.

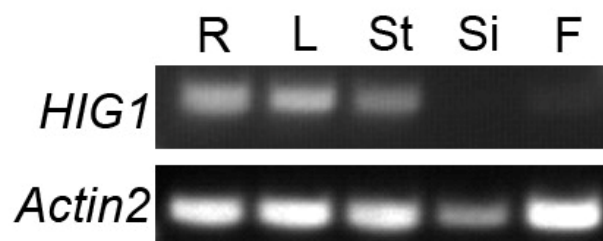


Figure 3.6: RT-PCR analysis from different organs of 6-week-old *A. thaliana* wild-type plants. R=roots, L=rosette leaves, St=stem, Si=mature silique, F=mature flowers. Gene specific primers were used for *HIG1/MYB51* and *Actin2*, as positive control.

In order to study in more detail the expression of the gene, the promoter activity of *HIG1/MYB51* was analysed using the GUS reporter system. A 2 kb fragment, including 1.6 kb upstream the start codon, as well as the first exon, first intron and

part of the second exon (-1676 to +342 bp) was amplified from genomic DNA and cloned into pGWB3 for translational fusion with the GUS reporter protein. More than twenty independent transgenic *A. thaliana* lines carrying the Pro_{HIG1/MYB51}-GUS construct were analysed. Twelve lines showing a qualitatively similar expression pattern were chosen for more detailed histochemical studies (Fig. 3.7). Reporter gene activity could be observed in the hypocotyl of 3-day-old seedlings (Fig. 3.7A). GUS expression was undetectable in the cotyledons at this stage, but appeared in the cotyledons of 7-day-old seedlings (Fig. 3.7B). New emerging rosette leaves did not show activity of the *HIG1/MYB51* promoter (Fig. 3.7C,D). However, expanding rosette leaves showed blue GUS staining around the mid vein and in the trichome pavement cells (Fig. 3.7D,E). Trichomes themselves also expressed the GUS reporter. In fully expanded rosette leaves, blue GUS staining was additionally detectable in the mesophyll, indicating *HIG1/MYB51* expression in the complete rosette leaf at the fully expanded stage (Fig. 3.7F). Furthermore, as indicated by the RT-PCR analysis, *HIG1/MYB51* promoter activity was detectable in roots, mainly in the differentiation zone close to the root tip, but

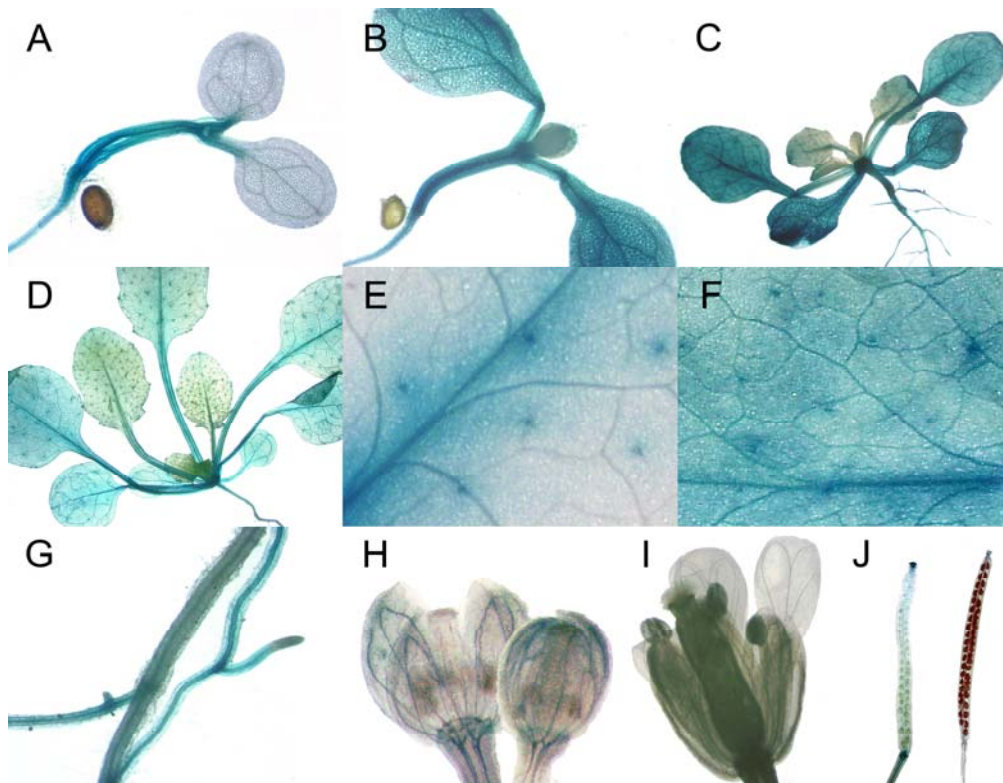


Figure 3.7: Histochemical GUS staining of Pro_{HIG1/MYB51}-GUS plants. (A) 3-day and (B) 7-day old seedling; (C) young and (D) mature rosette; (E) young rosette leaf; (F) fully expanded rosette leaf; (G) main and lateral root; (H) young and (I) mature flower; (J) young and mature silique.

also to a lesser extent in the vasculature of mature roots (Fig. 3.7G). Reproductive organs like flowers and siliques showed GUS activity only at an early stage of development. Young flowers showed faint expression in the vasculature of sepals (Fig. 3.7H). GUS expression was absent in mature flowers (Fig. 3.7I), coherent with the results obtained by RT-PCR. In young siliques, reporter gene activity was detectable at the stigma and the abscission zone. Mature siliques did not show any GUS activity (Fig. 3.7J). Summarising, expression of *HIG1/MYB51* was mainly detected in vegetative organs, while in reproductive organs it was observed only at an early stage of development. These results are in agreement with additional gene expression data available at Genevestigator (www.genevestigator.ethz.ch; Zimmermann et al., 2004b).

3.5 *HIG1/MYB51* overexpression leads to a high glucosinolate profile

The initial HPLC analysis showed an increased I3M content in the *HIG1-1D* mutant line. I3M is the main indolic glucosinolate present in *A. thaliana* and it was interesting to find out, whether other glucosinolates were also affected by *HIG1/MYB51* misexpression. Therefore, *HIG1/MYB51* overexpression lines and a knock-out line, together with *HIG1-1D* were analysed in more detail in collaboration with C. Müller (University Würzburg). The knock-out line was isolated from the GABI-Kat collection. The line 228B12 carries a T-DNA insertion in the second exon of *HIG1/MYB51*, thereby generating a transcriptional knock-out as revealed by RT-PCR (Fig. 3.8). The line is therefore referred to as *hig1-1*. Overexpression lines were generated by introducing the complete coding sequence of *HIG1/MYB51* into pGWB2 for ectopic overexpression under control of the *CaMV* 35S promoter. Three independent lines with a stable overexpression up to the T₃ generation were chosen for biochemical analysis.

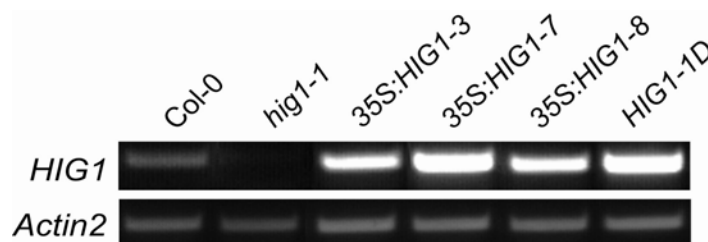


Figure 3.8: RT-PCR analysis of samples taken from wild-type (Col-0), knock-out (*hig1-1*), three independent overexpression lines (*35S:HIG1-1,3,7*) and the activation-tagging mutant (*HIG1-1D*).

The glucosinolate profile of rosette leaves showed a significantly increased I3M content not only in the original activation-tagged line *HIG1-1D*, but also in the three lines with ectopic overexpression of *HIG1/MYB51* (Fig. 3.9). This indicates that the overexpression is sufficient to generate a high indolic glucosinolate chemotype, irrespective of the genomic environment. The increase in I3M was up to 9-fold higher in the mutant lines compared to the wild-type background. In contrast, the *hig1-1* knock-out mutant accumulated only half the amount of I3M compared to wild-type plants. Apart from the increased I3M content in the overexpressors, the content of two minor indolic glucosinolates was also affected. Both 4MOI3M and 1MOI3M were significantly increased in at least three overexpression lines (*35S:HIG1-7*, *35S:HIG1-8*, *HIG1-1D*). Interestingly, the upregulation of indolic glucosinolates was accompanied by a down regulation of the major aliphatic glucosinolate 4MSOB. Nevertheless, the total amount of measured glucosinolates (indolic and aliphatic) in the *HIG1/MYB51* overexpression lines was about twice the amount in wild-type samples. The total glucosinolate concentration in *hig1-1* was reduced by half when

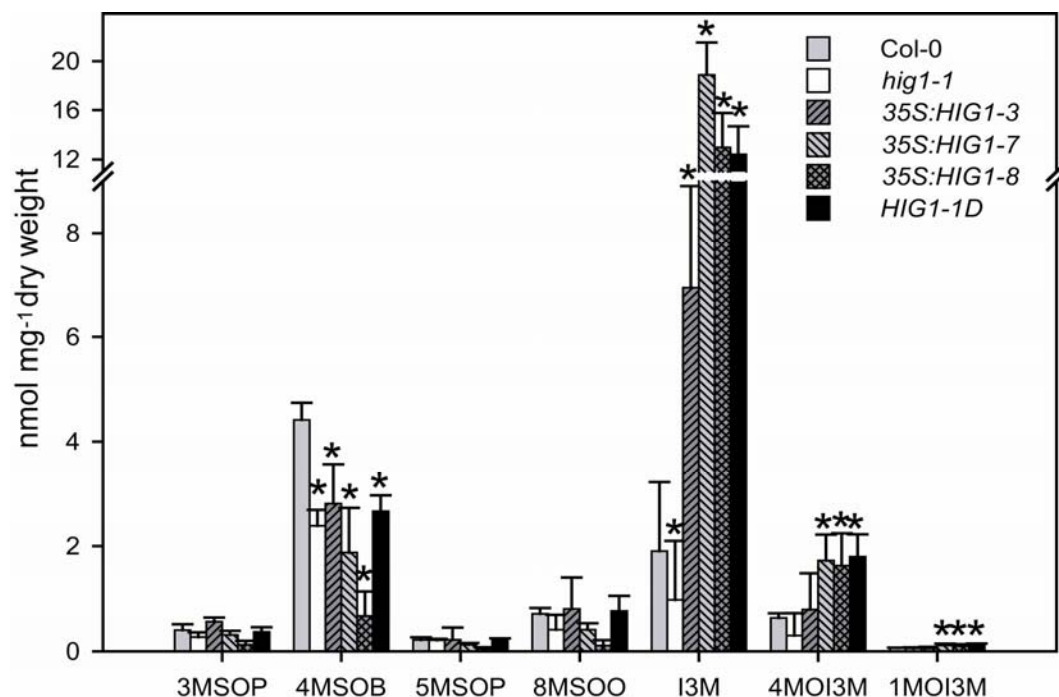


Figure 3.9: Glucosinolate (GS) content of wild-type and transgenic lines extracted from freeze dried rosette leaves of 5-week old plants grown under short day conditions (vegetative growth phase). 3MSOP, 3-methylsulfinylpropyl-GS; 4MSOB, 4-methylsulfinylbutyl-GS; 5MSOP, 5-methylsulfinylpentyl-GS; 8MSOO, 8-methylsulfinyloctyl-GS; I3M, indol-3-yl-methyl-GS; 4MOI3M, 4-methoxyindol-3-ylmethyl-GS and 1MOI3M, 1-methoxyindol-3-ylmethyl-GS. Asterisks denote significant difference in comparison to wild-type (mean \pm SD; n=3; Student's t-test; $P < 0.05$).

compared to the Col-0 wild-type background. Surprisingly, 4MSOB was also reduced in the knock-out mutant. However, the ratio of aliphatic to indolic glucosinolates changed only slightly in *hig1-1* (ratio of aliphatic/indolic glucosinolates (a/i): 2.5) with respect to the observed wild-type ratio (a/i: 2.2). In contrast, the homeostasis between aliphatic and indolic glucosinolates appeared to be altered in the lines overexpressing *HIG1/MYB51*. Here, the high content of indolic glucosinolates decreased the ratio to 0.5 and less. Taken together, overexpression of *HIG1/MYB51* influenced the accumulation of both indolic and aliphatic glucosinolates.

3.6 *HIG1/MYB51* overexpression does not alter the growth phenotype

The tight link of the indolic glucosinolates and IAA pathway often results in an altered IAA accumulation upon alteration of indolic glucosinolate biosynthesis (section 1.2). Unlike previously described glucosinolate mutants, no characteristic auxin phenotype was observed in *HIG1-1D* or *hig1-1*. Both lines were indistinguishable from wild-type plants throughout the life cycle under the tested growth conditions. Analysis of the endogenous IAA level revealed a slight increase in *HIG1-1D* compared to the wild-type level, whereas the IAA concentration in the *hig1-1* knock out was reduced, compared to wild-type plants (Fig. 3.10). However, these changes in the IAA level were minor compared to the effect of overexpressing the close homologue *ATR1/MYB34*. Some lines with ectopic overexpression of *ATR1/MYB34* under control of the *CaMV* 35S promoter showed drastically elevated IAA concentrations (one line is shown in Fig. 3.10) reflected in a high auxin growth phenotype with stunted plants and malformed flowers (Gigolashvili et al., 2007).

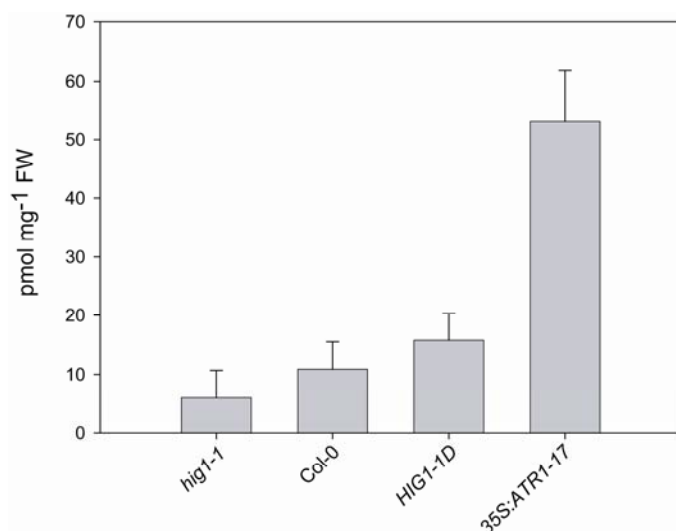


Figure 3.10: Free IAA content in rosette leaves of the indicated lines (mean \pm SD; n=3). The overexpressor of *ATR1/MYB34* (35S:ATR1-17) was described by Gigolashvili et al., 2007. Plants were grown under short day conditions.

A key enzyme in the auxin-glucosinolate homeostasis appears to be anthranilate synthase (section 1.2), which is also activated upon ethylene induced auxin biosynthesis (Stepanova et al., 2005) and influenced by *ATR1/MYB34* (Bender and Fink, 1998; Celenza et al., 2005). To test, whether the slight increase in IAA in the *HIG1-1D* mutant was mirrored by altered anthranilate synthase regulation, the

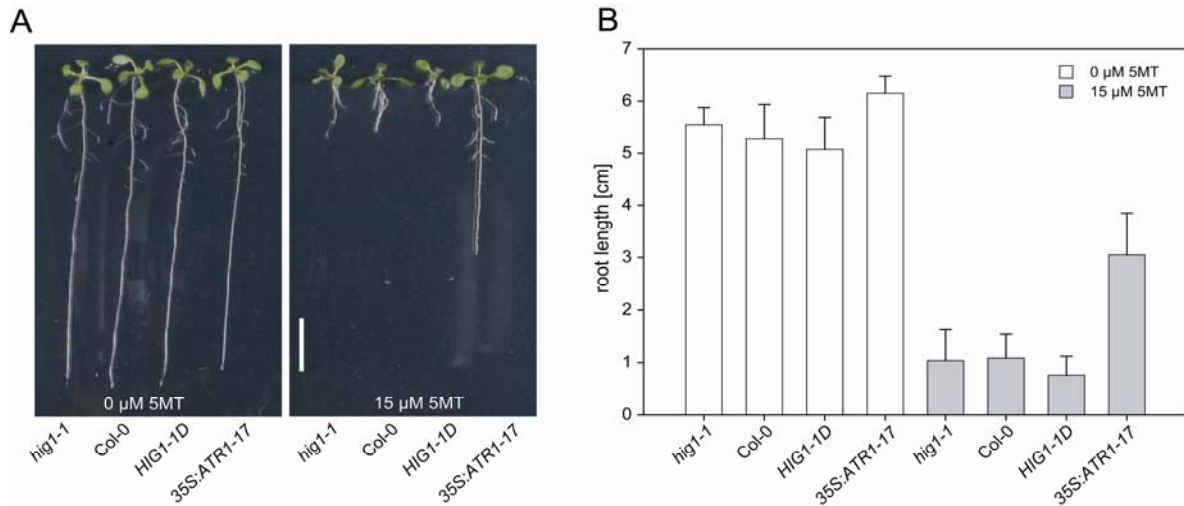


Figure 3.11: Growth phenotype on media containing 5-methyl tryptophan (5MT) of wild-type (Col-0), *hig1-1* knock-out, *HIG1-1D* and an *ATR1/MYB34* overexpression line (*35S:ATR1-17*; Gigolashvili et al., 2007). The seedlings were grown for 10 days on germination medium containing 0 μM and 15 μM 5MT. (A) representative picture of 10-day old seedlings, the white scale bar indicates 1 cm; (B) mean root length of 10-day old seedlings (mean \pm SD; n=10).

response to the toxic tryptophan analogue, 5-methyl tryptophan (5MT) was investigated. Constitutive activation of anthranilate synthase by *ATR1/MYB34* overexpression overcomes the negative feedback regulation by 5MT and ensures a sufficient tryptophan synthesis, reflected by an increased resistance to 5MT (Bender and Fink, 1998). Conversely, *HIG1-1D* did not show an altered 5MT tolerance compared to wild-type plants when grown on 5MT supplemented media. Wild-type, *hig1-1* and *HIG1-1D* seedlings all displayed the same reduced root growth on media containing 15 μM 5MT (Fig. 3.11). However, the transgenic line *35S:ATR1-17*, overexpressing *ATR1/MYB34*, showed a significantly better root growth on 5MT containing medium, reflecting an altered regulation of anthranilate synthase. Unlike *ATR1/MYB34*, *HIG1/MYB51* did not seem to affect the feedback inhibition of anthranilate synthase and had only little influence on the IAA concentration.

3.7 *HIG1/MYB51* overexpression activates indolic glucosinolate pathway genes

Overexpression of *HIG1/MYB51* resulted in an accumulation of indolic glucosinolates and a decrease of 4MSOB. Consequently, the question arises, whether *HIG1/MYB51* controls the expression of glucosinolate pathway genes. The same lines used for the biochemical characterisation were therefore used for expression studies by RT-PCR. The transcript levels of genes involved in the tryptophan synthesis, as well as those downstream of tryptophan participating in the formation of I3M, were analysed. In

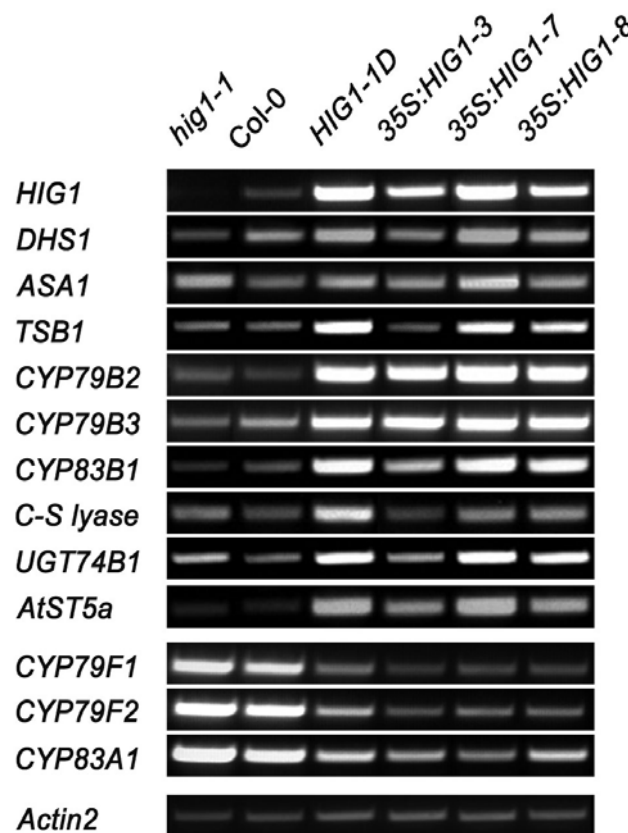


Figure 3.12: RT-PCR analysis of glucosinolate pathway genes. DHS1, DAHP synthase 1; ASA1, anthranilate synthase alpha 1; TSB1, tryptophan synthase beta 1; CYP, cytochrome P450 monooxygenase; UGT, S-glucosyltransferase; AtST, *A. thaliana* sulfotransferase.

addition, expression analyses of genes coding for key enzymes in the aliphatic glucosinolate biosynthesis were performed (pathway is given in Fig. 1.1). Studying the *HIG1/MYB51* overexpression lines, the most striking upregulation in gene expression were observed for *CYP79B2/B3* and *CYP83B1*, the enzymes responsible for the first steps in indolic glucosinolate biosynthesis (Fig. 3.12). However, the genes coding for enzymes further downstream the biosynthesis pathway were also upregulated, like *UGT74B1* and *AtST5a*. This reflects the increased accumulation of

I3M in these lines. In addition, the structural genes further upstream in the pathway were also slightly affected, with a moderate increase in *DHS1* and *TSB1* transcription in the *HIG1/MYB51* overexpressors compared to the wild-type and *hig1-1* mutant. Transcription of *ASA1* appeared unchanged, which reflects the observed sensitivity to 5MT. In contrast, transcription of *CYP79F1/F2* and *CYP79A1*, encoding the key enzymes of aliphatic glucosinolate biosynthesis, were downregulated in *HIG1-1D* and the other overexpression lines, in accordance with the decreased accumulation of the main aliphatic glucosinolates 4MSOB observed in these transgenic lines.

However, transcript profiling in transgenic lines with constitutive overexpression of *HIG1/MYB51* might reflect secondary adaptations to the constitutive overexpression, rather than a direct response. Therefore, an alternative approach was used to investigate the complete transcript pattern in response to *HIG1/MYB51* activation, which also aimed at finding further putative target genes. The complete coding sequence of *HIG1/MYB51* was introduced into the ethanol inducible expression system described by Caddick et al. (1998). More than 20 independent transgenic lines, carrying the ethanol inducible *MYB51/HIG*, were generated in the *hig1-1* background. One homozygous T₃ line, displaying high *HIG1/MYB51* transcription after ethanol induction and a 3:1 segregation ratio in the T₂, indicative of a single insert, was chosen for microarray analysis. Rosette leaves were taken for RNA extraction 24 hours after ethanol induction (plants were irrigated with 0.1% (v/v) ethanol) and compared to samples taken at the zero time point. Synthesised complementary RNA (cRNA) of both samples was labelled with Cy5 and Cy3, resulting in four fluorescently labelled cRNA pools (0h-Cy5, 0h-Cy3, 24h-Cy5, 24h-Cy3). Two Agilent 22K chips were hybridised with cRNA of both time points but differently labelled (Chip 1: 0h-Cy5, 24h-Cy3; Chip 2: 0h-Cy3, 24h-Cy5), using the dye swap between the two chips as an internal control. The raw data was processed with the provided Agilent Feature Extraction Software v.7.1 and transcripts, which met the following criteria: significant increase/decrease (p -value <0.05), signal well above background and greater than twofold change in both hybridisations; were considered significantly altered after ethanol induction of *HIG1/MYB51*. In total, 893 transcripts fulfilled these criteria, 429 being upregulated and 464 being downregulated after 24 hours *HIG1/MYB51* induction. For further analysis of the genes with altered expression, the MapMan software v.2.0.0 was used (Thimm et al., 2004), which allows assigning the transcripts to functional classes and a graphical

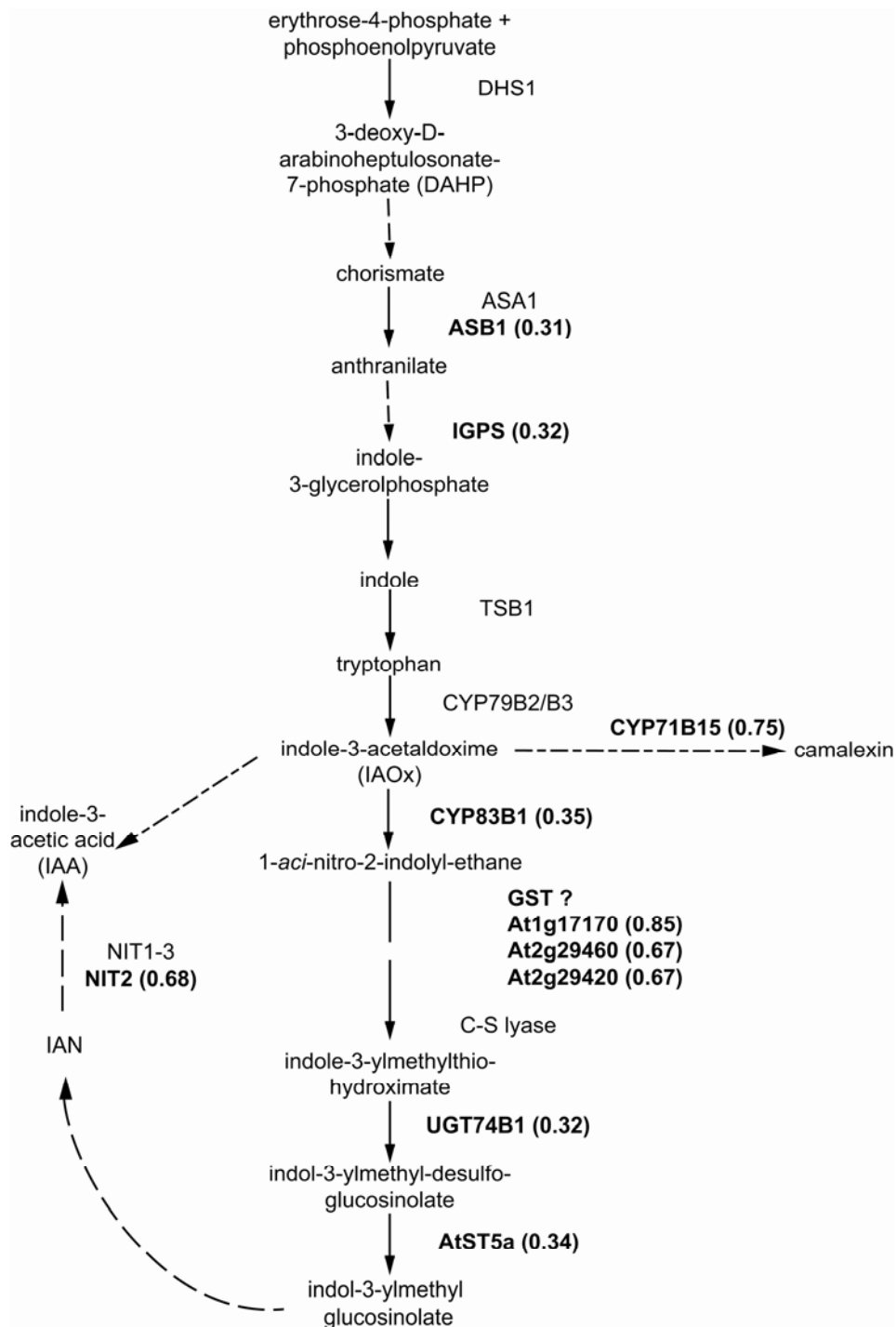


Figure 3.13: Scheme of the indolic glucosinolate biosynthesis with the branches to auxin and camalexin. The genes that are upregulated after 24 hours *MYB51/HIG1* induction are indicated in bold with the respective \log_{10} ratio given in parenthesis. DHS1, DAHP synthase 1; ASA1, anthranilate synthase alpha 1; ASB1, anthranilate synthase beta 1; IGPS, indole-3-glycerolphosphate synthase; TSB1, tryptophan synthase beta 1; CYP, cytochrome P450 monooxygenase, GST, glutathione-S-transferase, UGT, S-glycosyltransferase; AtST, *A. thaliana* sulfotransferase; NIT, nitrilase; IAN, indole-3-acetonitrile.

display of various pathways. Since the RT-PCR analyses indicated a regulation of the indolic glucosinolate biosynthesis genes by *HIG1/MYB51*, it was interesting to see whether these genes are also affected by a transient induction of *HIG1/MYB51*. Furthermore, the effect on other described biosynthesis pathways was investigated using the MapMan software. However, none of the incorporated pathways appeared to be affected at the level of multiple genes, besides the indolic glucosinolate biosynthesis pathway and its branches. The genes upregulated by *HIG1/MYB51* induction in the glucosinolate pathway and their expression ratio (\log_{10}) are represented in Figure 3.13. As seen from the constitutive *HIG1/MYB51* overexpression lines, the genes coding for enzymes downstream IAOx were upregulated (*CYP83B1*, *UGT74B1*, *AtST5a*) with the exception of C-S lyase. Moreover, there was an activation of *ASB1* and *IGPS*, both acting upstream of tryptophan biosynthesis. Interestingly, only *ASB1* was activated but not *ASA1*, encoding the feedback regulated subunit of anthranilate synthase. Apart from genes involved in the synthesis of tryptophan and indolic glucosinolates, also the branching pathway of camalexin biosynthesis appeared to be induced, since *CYP71B15* transcription was highly upregulated. Furthermore, *NITRILASE2* (*NIT2*) was activated in plants subjected to ethanol induced *HIG1/MYB51* expression, which codes for the enzyme catalyzing the conversion of indol-3-acetonitrile (IAN) to IAA. In addition, several GSTs were upregulated. It has been speculated whether GSTs are involved in glucosinolate biosynthesis (Halkier and Gershenzon, 2006), but no GST could be directly assigned to that pathway so far. The GSTs upregulated by *HIG1/MYB51* induction might therefore be candidates, three of them being under the top 25 induced genes (Tab. 3.1; Fig. 3.13). Taken together, the upregulation of indolic glucosinolate pathway genes, observed in constitutive *HIG1/MYB51* overexpression lines could be confirmed after transient induction of *HIG1/MYB51*. Besides a putative upregulation of the pathways related to indolic glucosinolate biosynthesis, no further biosynthesis pathways could be identified as targets of *HIG1/MYB51* regulation. Looking at the strongest induced genes after *HIG1/MYB51* induction, one can find members of large enzyme families, like GSTs, cytochrome P450 monooxygenases (CYPs) and UDP-glucosyl transferases (Tab. 3.1). Furthermore, biotic stress response genes were induced, like *avirulence induced gene 1* (*AIG1*) and a putative disease resistance protein. Interestingly, *MYB4*, a repressor of phenylpropanoid biosynthesis (Jin et al., 2000; Hemm et al., 2001) was also upregulated.

Table 3.1: List of the 25 most strongly upregulated genes by MYB51/HIG1 induction.

AGI code	description	functional group	log ratio
At1g18570	MYB51/HIG1	RNA.regulation of transcription.MYB domain transcription factor family	1.61
At3g14900	expressed protein	not assigned.unknown	1.37
At3g28510	AAA-type ATPase	protein.degradation.AAA type	1.21
At3g17790	acid phosphatase type 5 (ACP5)	misc.acid and other phosphatases	1.10
At3g44990	xyloglucan:xyloglucosyl transferase, putative	cell wall.modification	1.04
At3g11340	UDP-glucuronosyl/UDP-glucosyl transferase family protein	misc.UDP glucosyl and glucoronyl transferases	1.00
At5g49480	sodium-inducible calcium-binding protein (ACP1)	signalling.calcium	0.92
At2g05380	glycine-rich protein (GRP3S)	not assigned.no ontology.glycine rich proteins	0.91
At1g14880	expressed protein	not assigned.no ontology	0.91
At1g17170	glutathione S-transferase, putative	misc.glutathione S transferases	0.85
At4g25630	fibrillarlin 2 (FIB2)	RNA.processing	0.80
At3g13310	DnaJ protein, putative	stress.abiotic.heat	0.79
At1g33960	avirulence induced gene (AIG1)	stress.biotic	0.77
At5g05250	expressed protein	not assigned.unknown	0.77
At4g38620	MYB4	RNA.regulation of transcription.MYB domain transcription factor family	0.76
At1g01520	myb family transcription factor	RNA.regulation of transcription.MYB-related transcription factor family	0.76
At3g26830	cytochrome P450 71B15	misc.cytochrome P450	0.75
At5g09440	phosphate-responsive protein	signalling.in sugar and nutrient physiology	0.74
At4g01870	tolB protein-related	not assigned.no ontology	0.72
At4g34131	UDP-glucuronosyl/UDP-glucosyl transferase family protein	misc.UDP glucosyl and glucoronyl transferases	0.71
At2g32960	tyrosine specific protein phosphatase family protein	protein.posttranslational modification	0.70
At3g44300	nitrilase 2 (NIT2)	misc.nitrilases	0.68
At2g04450	MutT/nudix family protein	not assigned.no ontology	0.67
At1g57630	disease resistance protein (TIR class), putative	stress.biotic	0.67
At2g29460	glutathione S-transferase, putative	misc.glutathione S transferases	0.67
At2g29420	glutathione S-transferase, putative	misc.glutathione S transferases	0.67

Table 3.2: Functional classification of genes with significantly changed expression after *MYB51/HIG1* induction. The analysis was based on the Wilcoxon Rank Sum Test (Benjamini-Hochberg corrected), included in the MapMan software.

functional class	# deregulated genes	direction of deregulation	p-value (Benjamini-Hochberg corrected)
protein	164	↑	1,61E-13
protein.synthesis	108	↑	<0,00E-20
protein.synthesis.misc ribososomal protein	102	↑	<0,00E-20
hormone metabolism	50	↓	1,22E-03
hormone metabolism.auxin.induced-regulated-responsive-activated	14	↓	5,20E-02
hormone metabolism.ethylene.signal transduction	10	↓	6,85E-02
misc.glutathione S transferases	9	↑	1,88E-03
stress.abiotic.heat	20	↑	1,86E-02
DNA.synthesis/chromatin structure	15	↑	2,73E-02

In addition to the examination of single genes, the MapMan software allows to investigate the alteration of complete functional classes (Tab. 3.2). A significant upregulation of genes involved in protein biosynthesis was observed, but also genes for DNA and chromatin modelling were activated. This suggests an increased demand for the transcriptional and translational machinery after ethanol induction, with so many genes being up- and downregulated. Apart from protein synthesis, two further functional classes were induced, GSTs and heat induced genes, mainly heat shock proteins. Both could be a general stress response of the plant, due to the experimental set up. However, the upregulation of GSTs could also be a direct response to *HIG1/MYB51* induction. Apart from functional classes that are significantly induced, there was also one class being downregulated. In total, transcription of 50 genes involved in hormone metabolism was changed, with the majority being downregulated. More specifically, a significant impact on auxin-responsive genes (e.g. *IAA2*, *IAA3*, *IAA6*, *IAA19*) and genes involved in ethylene signalling was observed.

3.8 **HIG1/MYB51 activates promoters of indolic glucosinolate pathway genes**

Analyses of the transcriptional profiles in constitutive and induced *HIG1/MYB51* overexpression lines suggest an induction of indolic glucosinolate pathway genes by HIG1/MYB51. To test the ability of HIG1/MYB51 as a transcriptional activator, a transient expression system in cultured *A. thaliana* cells was employed. The system takes advantage of a hypervirulent *A. tumefaciens* strain yielding high transformation rates (van de Fits et al., 2000). Transformation is achieved by simply mixing the plant cells with the agrobacteria carrying the desired constructs. Effector constructs express the transcriptional regulator under control of a constitutive promoter, the reporter constructs are generated by introducing the putative target promoter in front of an intron-tagged *uidA* ORF. The system was validated previously with described transcription factor/promoter interactions of the phenylpropanoid pathway (Berger et al., 2007).

Here, the potential of HIG1/MYB51 to activate the promoters of seven different indolic glucosinolate pathway genes was tested. Therefore, the overexpression construct of HIG1/MYB51 in pGWB2 (see section 3.5) was used as an effector construct. The reporter constructs were generated by cloning the promoters of three genes upstream tryptophan synthesis (*DHS1*, *ASA1*, *TSB1*) and those of four genes downstream tryptophan synthesis (*CYP79B2*, *CYP79B3*, *CYP83B1*, *AtSt5a*) into pGWB3i, for promoter driven GUS expression (clones were generated by R. Yatusевич, T. Gigolashvili, B. Kleinhenz, University of Cologne, and are described in Gigolashvili et al., 2007). Transformation of *A. thaliana* cells with the reporter constructs alone revealed a moderate background activity of the *DHS1*, *CYP83B1* and *AtSt5a* promoters, as indicated by the measured GUS activity (Fig.3.14B). This was also seen by the histochemical GUS staining of cells transfected with the *DHS1* and *AtSt5a* reporter constructs (Fig. 3.14A). The promoters of *ASA1*, *TSB1*, *CYP79B2* and *CYP79B3* did not drive GUS expression when transformed into the cell culture alone. Cotransformation with the HIG1/MYB51 effector resulted in a significant induction of all tested promoters, except for the promoter of *ASA1*. The strongest activation was observed for the promoter of *DHS1* and *AtSt5a*, but also the promoters of *TSB1*, *CYP79B2*, *CYP79B3* and *CYP83B1* were significantly induced by HIG1/MYB51. As seen by transcriptional profiling and growth on 5MT, HIG1/MYB51 does not appear to activate *ASA1*. However, HIG1/MYB51 is able to

induce the other tested promoters of the indolic glucosinolate pathway genes, further validating the idea of it being a transcriptional regulator.

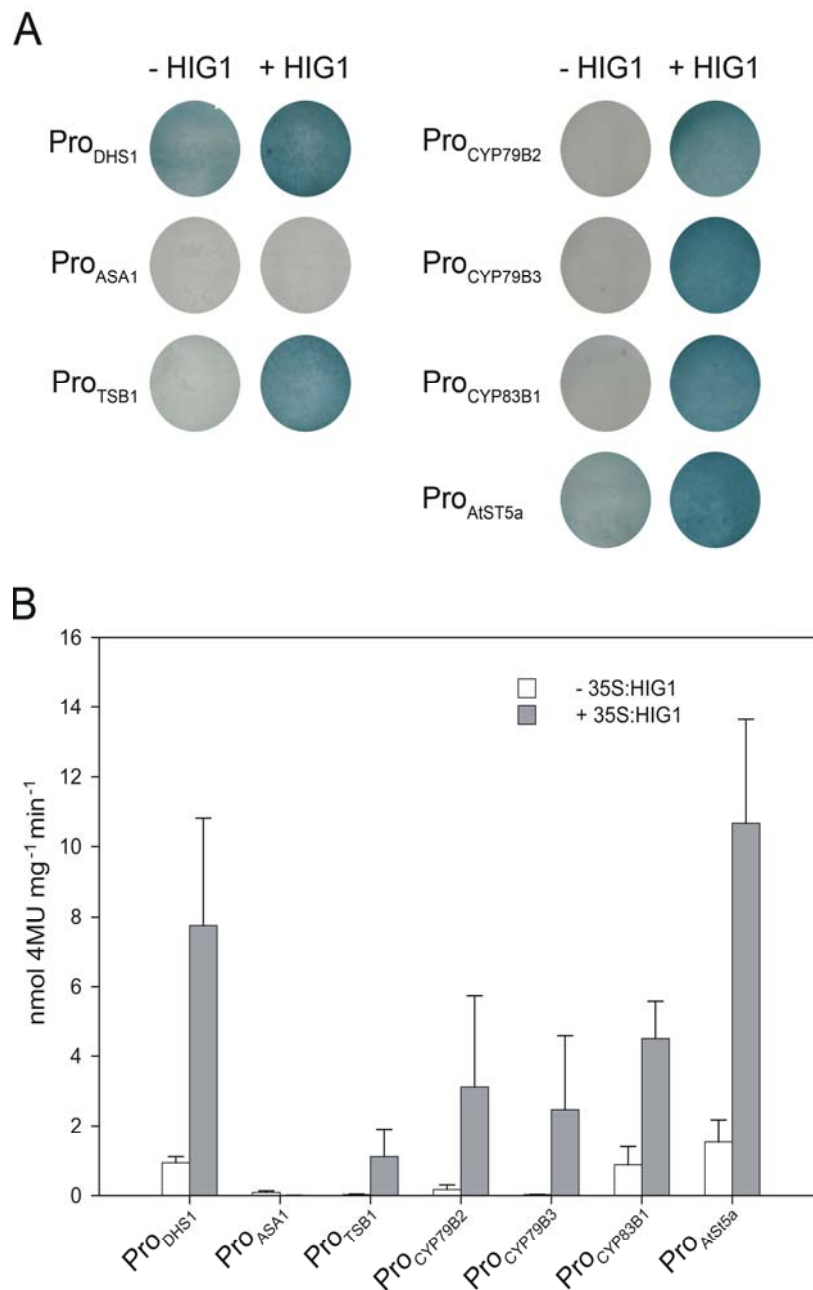


Figure 3.14: GUS activity of reporter constructs in transiently transformed *A. thaliana* cells cotransformed with or without the 35S:HIG1 effector. (A) Histochemical GUS staining of transformed cells; (B) Quantitative measurement of the GUS activity. Values are given as the formation of 4-methylumbelliferone (4MU) per min and mg protein (mean \pm SD; n=4).

3.9 *HIG1/MYB51* expression is mechano-sensitive

The results presented so far, suggest a role of *HIG1/MYB51* as a regulator of glucosinolate biosynthesis. Since glucosinolates are a major component of the plant defence against herbivore attack and are known to be induced by wounding or hormone treatment, the question arises, whether *HIG1/MYB51* is involved in one of these signalling pathways. Therefore, the response of *HIG1/MYB51* to mechanical stimuli and hormone treatment was tested. RT-PCR analysis of punctured rosette leaves showed an induction of *HIG1/MYB51* expression already 15 minutes after wounding (Fig.3.15). *HIG1/MYB51* transcript levels were highest 30 minutes after wounding (Fig.3.15). *HIG1/MYB51* transcript levels were highest 30 minutes after

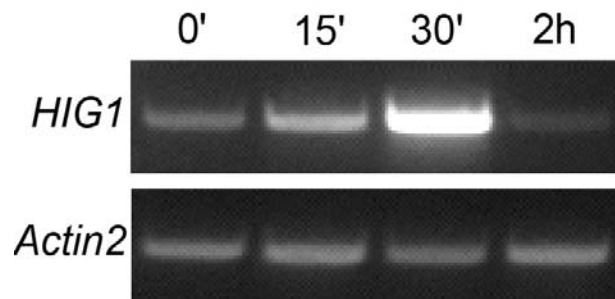


Figure 3.15: RT-PCR analysis of samples taken from punctured rosette leaves 0, 15, 30 and 120 minutes after wounding. 6-week-old wild-type plants were grown under short day conditions and punctured with a whole puncher. Actin2 was used as a control.

wounding and were already back to control level in samples taken after two hours. This strongly indicates a transient induction of *HIG1/MYB51* expression after wounding. In a second attempt for testing the mechano-sensitive induction of *HIG1/MYB51*, the GUS reporter lines (see section 3.4) were employed. It could be

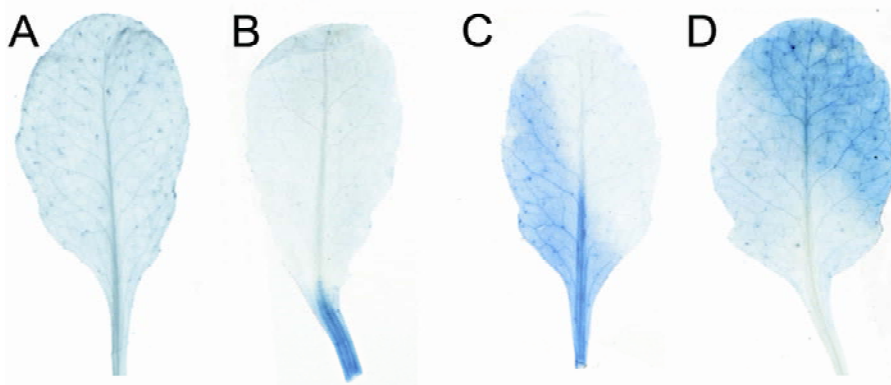


Figure 3.16: Histochemical GUS staining of Pro_{HIG1/MYB51}-GUS rosette leaves. (A) unwounded leaf, detached after staining; (B) leaf with cutting site; (C, D) leaves that were pressed between two fingers.

seen that *HIG1/MYB51* promoter driven GUS expression was more pronounced at sites of cutting than in unwounded tissues (Fig. 3.16B). Also pressing of rosette leaves between two fingers resulted in an activation of the reporter construct (Fig. 3.16C,D).

Since wounding and herbivore attack are often accompanied by the activation of hormone signalling pathways, the responsiveness of *HIG1/MYB51* to one of the major stress signalling hormones was tested. The expression was analysed in response to methyl jasmonate (MeJA), salicylic acid (SA) and the ethylene precursor 1-aminocyclopropane-1-carboxylic acid (ACC). For this purpose, wild-type *Arabidopsis* plants were sprayed with aqueous solutions containing the respective hormones and samples were taken for RT-PCR analysis (Fig. 3.17). An induction of *HIG1/MYB51* could be observed 30 minutes after spraying in all treatments, including the mock treatment. The transcript level decreased two and four hours after spraying, resembling the observed effect after wounding. Consequently, the mechanical stimulus of spraying appears to be sufficient to trigger an upregulation of *HIG1/MYB51*. Since the mechano-sensitivity of *HIG1/MYB51* makes it impossible to study hormone activation by spraying plants, different attempts presented in section 3.10 were used to overcome this problem.

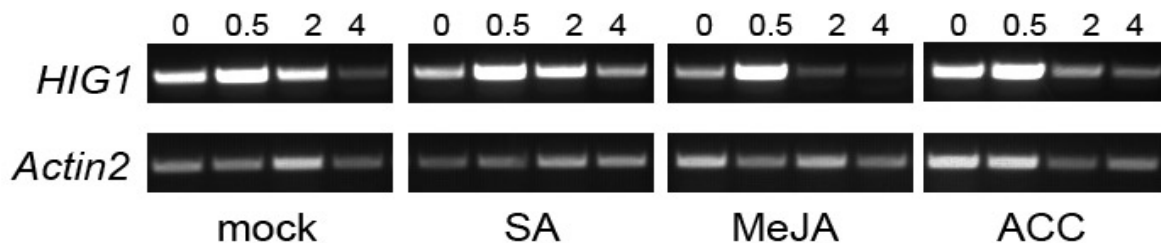


Figure 3.17: RT-PCR analysis of rosette leaves sprayed with no hormone (mock), SA (0.5 mM), MeJA (0.45 mM) or ACC (10 μ M) in 0.1% (v/v) ethanol, 0.01% (v/v) Tween. Samples were taken 0, 0.5, 2 and 4 hours after spraying.

3.10 Ethylene activates the *HIG1/MYB51* promoter in root tips

One attempt to study a possible hormone response of *HIG1/MYB51* was to grow the Pro_{*HIG1/MYB51*}-GUS lines on hormone supplemented media. However, growth and morphology of the seedlings were drastically affected by the chosen hormone concentrations. Conclusions about specific hormone effects were not clear. Growing plants on normal germination media with a later transfer to hormone supplemented

plates was not feasible, because the mechanical stress during transfer would have interfered with the possible hormone response. Therefore, the GUS reporter lines were grown on solid germination media covered with a sterile filter paper, allowing the roots of the seedlings to grow on top. This provided the possibility of a later induction with hormones by applying the respective solution to the filter paper, without damaging the seedlings themselves. For the initial spraying experiments relatively high hormone concentrations of SA and MeJA were used as described in previous studies (SA: 0.5 mM; MeJA: 0.45 mM; Cipollini et al., 2004). However, experiments with seedlings grown in liquid culture showed that these concentrations might be too high when applied directly to the root system. When SA was added to a final concentration of 0.5 mM, the seedlings died within 12 hours. Hence, all hormones were applied at 10 μ M, the same concentration used for the AtGenExpress experiments. Hormone solutions of SA, MeJA and ACC were applied to the roots of 3-week-old Pro_{HIG1/MYB51}-GUS reporter lines and whole plants were fixed and stained for GUS activity 4, 24 and 48 hours after hormone treatment,

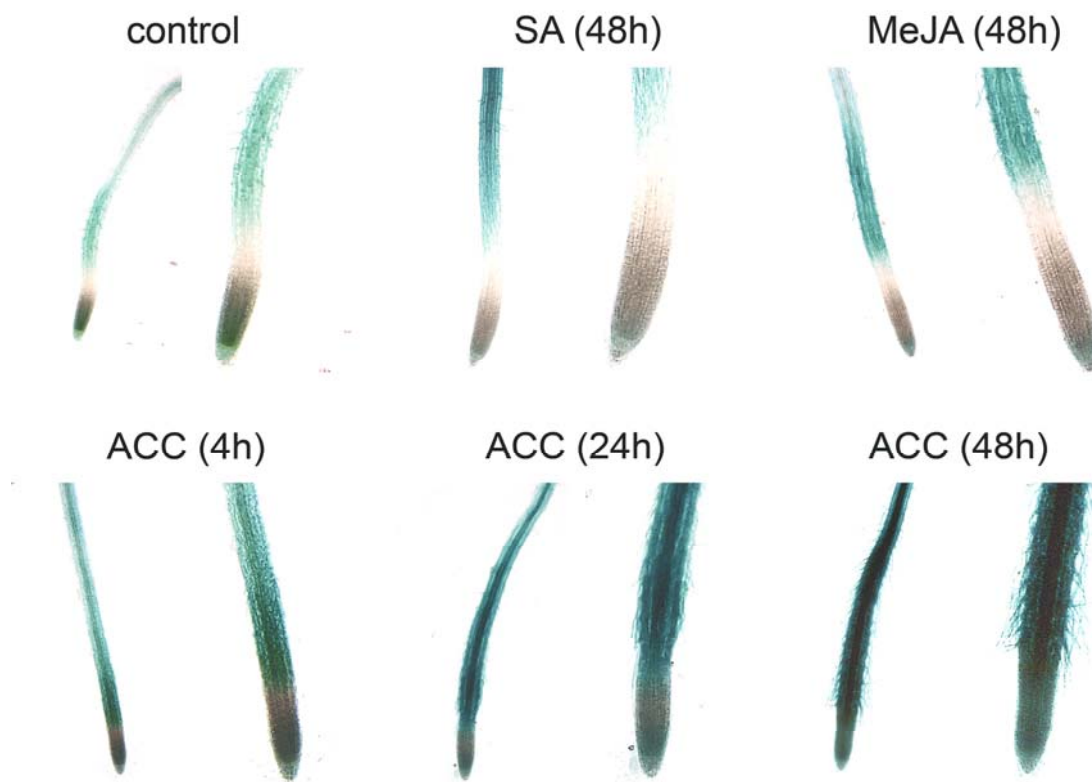


Figure 3.18: Histochemical GUS staining in roots of Pro_{MYB51/HIG1}-GUS lines after hormone treatment. An overview and a close-up of the root tip is displayed. Plants were grown vertically on solid germination medium covered with filter paper. For hormone treatment the filter was soaked with 2 mL of hormone solution (each 10 μ M in 0.01% (v/v) ethanol) and the samples were taken at the indicated time points for GUS staining.

respectively. The GUS staining pattern observed in the rosettes of all tested seedlings was unchanged compared to the control samples with increased staining in expanded leaves as described in section 3.4. Looking at the root system, GUS activity was absent in the meristematic and elongation zone of control samples (Fig. 3.18). Occasionally the root cap displayed light blue GUS staining. However, *HIG1/MYB51* promoter driven GUS expression was detectable in the differentiation zone. The same pattern was observed for plants treated with MeJA and SA, at all tested time points. Application of ACC to the reporter plants led to an altered GUS expression pattern. After 4 hours, strong GUS activity was detectable in the elongation zone. Samples taken 24 and 48 hours after ACC treatment displayed an increased number of elongated root hairs, the described effect of ACC on root growth and morphology. GUS staining in these samples was intense in the complete root tip, also in the meristematic region. However, highest activity was seen in the differentiation zone with strong stained root hairs. Taken together, the tested hormones did not appear to influence *HIG1/MYB51* in the green part of the plants. The only observable effect was seen in root tips, where ACC led to a strong induction of the Pro_{HIG1/MYB51}-GUS reporter. Hence, *HIG1/MYB51* appears to be regulated site specifically by the ethylene precursor ACC.

3.11 Overexpression of *HIG1/MYB51* leads to increased resistance against a generalist herbivore

Glucosinolates, together with myrosinase, present a well characterised defence system against herbivores (section 1.3). Since *HIG1-1D* showed an increased content in total glucosinolates, mainly due to the high I3M concentration, the effect on herbivore consumption was analysed. For this purpose, the feeding preference of the generalist herbivore *Spodoptera exigua* (Lepidoptera) was tested in a dual choice assay (in collaboration with C. Müller, University Würzburg). Fourth-instar larvae of *S. exigua* were kept on artificial diet before being offered two rosette leaves of the same age, but originating from different plant lines (Fig. 3.19A). The larvae were placed in a Petri dish with the two leaves on moistened filter paper and allowed to feed for 8 hours. Afterwards, the consumed leaf weight was calculated according to the consumed leaf area. When offered Col-0 and *hig1-1* leaves at the same time, there was no significant feeding preference (Fig. 3.19B). The same amount of both leaves was consumed by the larvae. However, there was a remarkable difference in

the consumed leaf weight when leaves of *HIG1-1D* were offered. In these cases, there was an increased consumption of the alternative leaf, irrespective whether Col-0 or *hig1-1* was offered as alternative. This clearly indicates that the upregulation of *HIG1/MYB51* along with the accumulation of indolic glucosinolates leads to an increased resistance of *HIG1-1D* plants against the generalist *S. exigua*.

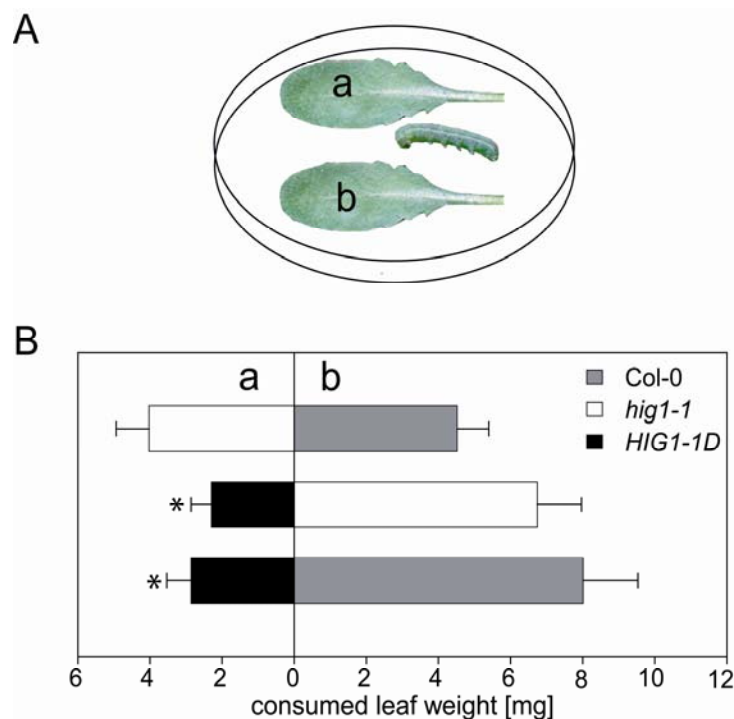


Figure 3.19: Dual choice assay with larvae of *S. exigua*. (A) scheme of the experimental setup with leaf a and b; (B) consumed leaf weight, when larvae were offered leaf a and b (mean \pm SD; n=20). Asterisks denotes significant difference (Student's t test; $p < 0.05$).

3.12 Screening for proteins interacting with *HIG1/MYB51*

It is known from other transcriptional regulators that they often act in concert with other transcription factors. For instance, the interaction between MYB factors and basic helix-loop-helix (bHLH) proteins has been well characterised (Zimmermann et al., 2004a). Furthermore, it is known that transcription factors are often regulated on the protein level by a rapid turnover, mediated by ubiquitin ligases (Moon et al., 2004). Therefore, a yeast-two-hybrid screen in collaboration with J. Uhrig, University of Cologne, was used to search for putative interactors of *HIG1/MYB51*.

Many eukaryotic transcription factors have a separated DNA binding domain (BD) and activation domain (AD) that can function independent of each other. The yeast-two-hybrid assay takes advantage of this functional independence by separating BD and AD of the GAL4 transcription factor (Fig. 3.20). The BD is fused to a "bait" protein, the AD to "prey" proteins. Upon interaction of bait and prey, the BD and AD

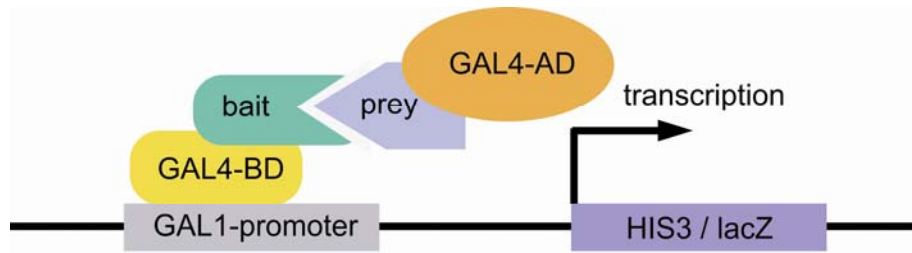


Figure 3.20: Schematic representation of the yeast-two-hybrid assay.

come in close proximity and reconstitute a functional GAL4 transcription factor, which can drive GAL1-promoter controlled reporter gene expression. The system can either be used to analyse the interaction of specific bait and prey proteins, or it is used to screen for putative interacting proteins of a specific bait using a prey library. When working with transcription factors in a yeast-two-hybrid system one deals with the problem that the transcription factor used as bait protein can already contain an AD. Therefore, it can drive reporter gene expression without interacting with the prey fusion protein. As a consequence, proteins used as bait have to be tested for their ability to autoactivate the reporter gene prior to screening. It is known for R2R3 MYB factors that the AD usually resides in the carboxy terminal region. On the other hand, the R2R3 MYB domain, responsible for DNA binding and protein-protein interaction is located in the amino terminus. Consequently, a HIG1/MYB51 bait construct containing the amino terminal R2R3 MYB domain was constructed for the yeast-two-hybrid screen (Fig. 3.21). In addition, three further constructs were used to narrow down the region of the actual activation domain. Construct B also contained the MYB domain and further extended to the amino acid stretch typical for subgroup 12 MYB factors. The third construct (C) was about 260 amino acids in length and contained two further cysteine residues, possibly important for the mature protein conformation. Finally, construct D was generated to express the full-length HIG1/MYB51 protein. All four constructs were cloned into the Gateway compatible yeast expression vector pCD2-attR (Trp¹⁺) for translational fusion with the GAL4 BD. Together with the empty prey plasmid pACT (Leu²⁺), the bait clones were then transformed into the AH109 yeast strain, which contains the *Gal1:His3* reporter construct. As a positive control for bait/prey interaction and activation of the *Gal1:His3* reporter, the known interacting proteins SNF1 and SNF4 were used (Celenza and Carlson, 1989). The negative control consisted of an empty bait and empty prey vector. The cotransformed yeast cells were plated on -Trp/-Leu media to test for positive double transformands containing both plasmids, and on -Trp/-Leu/-His/+3AT to select for clones with

Construct A

```

1 MVRTPCCKAE LGLKKGAWTP EEDQKLLSYL NRHGEGGWRT LPEKAGLKRC
51 GKSCRLRWAN YLRPDIKRGE FTEDEERSII SLHALHGKWK SAIARGLPGR
101 TDNEIKNYWN THIKKRLIKK GI

```

Construct B

```

1 MVRTPCCKAE LGLKKGAWTP EEDQKLLSYL NRHGEGGWRT LPEKAGLKRC
51 GKSCRLRWAN YLRPDIKRGE FTEDEERSII SLHALHGKWK SAIARGLPGR
101 TDNEIKNYWN THIKKRLIKK GIDPVTHKGI TSGTDKSENK PEKQNVNLTG
151 SDHDLNDNKA KKNNKNFGLS SASFLNKVAN RFGK

```

Construct C

```

1 MVRTPCCKAE LGLKKGAWTP EEDQKLLSYL NRHGEGGWRT LPEKAGLKRC
51 GKSCRLRWAN YLRPDIKRGE FTEDEERSII SLHALHGKWK SAIARGLPGR
101 TDNEIKNYWN THIKKRLIKK GIDPVTHKGI TSGTDKSENK PEKQNVNLTG
151 SDHDLNDNKA KKNNKNFGLS SASFLNKVAN RFGKRINQSV LSEIIGSGGP
201 LASTSHTTNT TTTSVSVDSE SVKSTSSSFA PTSNLLCHGT VATTPVSSNF
251 DVDGNVNLTC S

```

Construct D

```

1 MVRTPCCKAE LGLKKGAWTP EEDQKLLSYL NRHGEGGWRT LPEKAGLKRC
51 GKSCRLRWAN YLRPDIKRGE FTEDEERSII SLHALHGKWK SAIARGLPGR
101 TDNEIKNYWN THIKKRLIKK GIDPVTHKGI TSGTDKSENK PEKQNVNLTG
151 SDHDLNDNKA KKNNKNFGLS SASFLNKVAN RFGKRINQSV LSEIIGSGGP
201 LASTSHTTNT TTTSVSVDSE SVKSTSSSFA PTSNLLCHGT VATTPVSSNF
251 DVDGNVNLTC SSSTFSDSSV NNPLMYCDNF VGNNNVDDED TIGFSTFLND
301 EDFMMLEESC VENTAFMKEL TRFLHEDEND VVDVTPVYER QDLFDEIDNY
351 FG

```

Figure 3.21: HIG1/MYB51 bait constructs generated for the yeast-two-hybrid assay. The R2 MYB domain is indicated in blue, the R3 domain in green. The residues highlighted in red form the tryptophan cluster. The sequence highlighted in orange is the motif specific for MYB factors of subgroup 12.

Gal1:His3 reporter gene expression. Growth on -Trp/-Leu medium was observed for all contranformation assays (Tab. 3.3), indicating that none of the constructs is toxic for yeast and efficient transformation is possible. Furthermore, yeast cells transformed with both SNF1 and SNF4 as bait and prey were also growing on -Trp/-Leu/-His/+3AT medium. The interaction of both proteins leads to reconstitution of the GAL4 BD and AD and a subsequent activation of the *Gal1:His3* reporter, thus allowing growth on histidine-free medium. Additionally, transformation with the full-length HIG1/MYB51 as bait (construct D) resulted in growth on -His medium. This clearly proved that the full length protein contains an activation domain in the carboxy terminus, which can drive reporter gene expression without the need for interaction with a prey fusion protein. Since none of the other constructs was autoactivating, the activation domain resides within the hundred amino acids of the carboxy terminal region of the HIG1/MYB51 protein.

Table 3.3: Testing of bait constructs for autoactivation

bait	prey	growth on -Trp/-Leu	growth on -Trp/-Leu/-His/+3AT
empty vector	empty vector	+	-
SNF1	SNF4	+	+
construct A	empty vector	++	-
construct B	empty vector	++	-
construct C	empty vector	++	-
construct D	empty vector	+	+

Even though the focus of the yeast-two-hybrid screen was to search for interactors of the regulatory MYB domain, all three non-autoactivating constructs were used for a first mating with the prey libraries (Fig. 3.22). In total, 510 putative candidates were obtained after this mating, whereas most clones interacted with construct A (216; construct B: 166 clones, construct C: 128 clones). Initial sequencing of several candidates after colony PCR revealed a large number of false positives, mainly ribosomal proteins. To reduce the number of false positives, the PCR products were retransformed into the prey vector via gap repair in yeast and the resulting colonies were used for a second mating. This second mating was performed with construct A only, to screen for specific interactors of the MYB domain. After this selection step, the number of putative candidates was strongly reduced (99 in total; 61 originally interacting with construct A; 38 with construct B, respectively) and these remaining candidates were sequenced. Interestingly, none of the clones originally interacting with construct C showed interaction with construct A in the second mating. This suggests that the carboxy terminal extension of construct C prevents binding of prey proteins to the MYB domain, an effect previously observed for other MYB factors (J. Uhrig, personal communication). Sequencing of the remaining clones revealed that some candidates were present several times whilst others were found only once, resulting in 47 individual candidates (Tab. 3.4). The sequence found most often, was that of At4g19700, which is assigned as E3 ubiquitin ligases and might play a role in protein turnover. Other proteins involved in protein degradation were also found, suggesting a regulation of HIG1/MYB51 on the posttranscriptional level. Apart from the candidates with a predicted function, most of the candidates had no assigned function (Table 3.4). Since it was not feasible within this study to analyse many candidates in detail, the most promising candidates were chosen for further investigation.

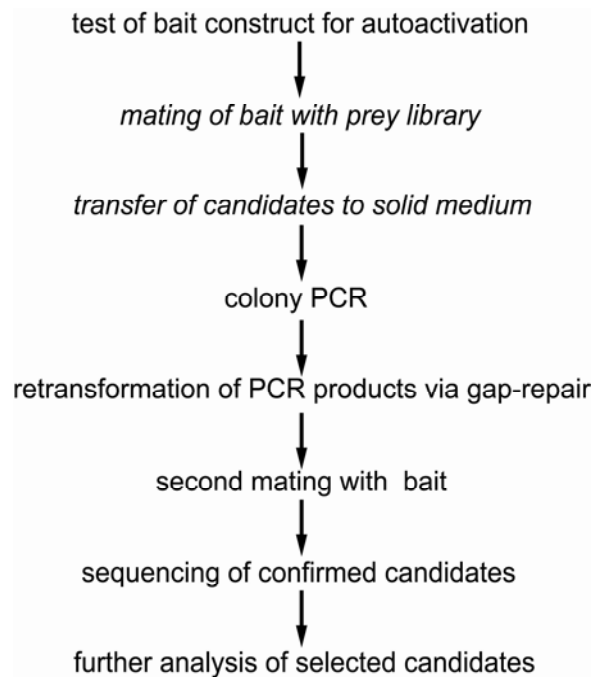


Figure 3.22: Work flow of the yeast-two-hybrid screen. The steps indicated in italics were performed by the AG Uhrig, University of Cologne and are described by Soellick and Uhrig (2001).

The interaction of MYB factors with bHLH proteins has been shown in several cases (Baudry et al., 2004). Therefore, the interacting ATR2/bHLH05 was considered a promising candidate, especially since the dominant allele of *ATR2/bHLH05*, *atr2D*, appeared to be implicated in the regulation of tryptophan biosynthesis (Smolen et al., 2002). Furthermore, it could be shown that *atr2D* and the dominant overexpressor of ATR1/MYB34 (*atr1D*) have additive effects with respect to *ASA1* activation or 5MT resistance. However, an interaction between both proteins could not be observed in a yeast-two-hybrid system, neither with the wild-type, nor the mutated form of ATR2/bHLH05 (Smolen et al., 2002). For that reason, it was all the more interesting that HIG1/MYB51, a close homologue of ATR1/MYB34, appeared to interact with ATR2/bHLH05.

Table 3.4: Confirmed candidates of the yeast-two-hybrid screen after the second mating. The number of clones coding for the same gene is given. The AGI code of candidates coding for genes of unknown function are listed at the end.

AGI code	# clones	description	functional group
At4g19700	17	expressed protein	protein.degradation.ubiquitin.E3.RING
At1g47128	2	cysteine proteinase RD21A	protein.degradation.cysteine protease
At3g24800	2	E3 ubiquitin ligase, PRT1	protein.degradation.ubiquitin.E3.RING
At3g12920	2	expressed protein	protein.degradation.ubiquitin.E3.RING
At5g46760	2	bHLH05, ATR2	RNA.regulation.of.transcription.bHLH.Basic Helix-Loop-Helix family
At5g25480	1	C-5 cytosine-specific DNA methylase family protein	RNA.regulation.of.transcription.DNA methyltransferases
At1g52150	1	homeobox-leucine zipper family protein	RNA.regulation.of.transcription.HB.Homeobox transcription factor family
At4g26930	1	myb family transcription factor (MYB97)	RNA.regulation.of.transcription.MYB domain transcription factor family
At1g08370	2	hydroxyproline-rich glycoprotein family protein	RNA.regulation.of.transcription.putative DNA-binding protein
At3g62100	4	auxin-induced protein homolog auxin-induced protein IAA20	hormone.metabolism.auxin.induced-regulated-responsive-activated
At1g06620	1	2-oxoglutarate-dependent dioxygenase, putative	hormone.metabolism.ethylene.synthesis-degradation
At3g09700	6	unknown protein similar to a region of DNAJ domain-containing protein	stress.abiotic.heat
At1g28210	1	DNAJ heat shock protein, putative	stress.abiotic.heat
At5g17920	1	vitamin-B12-independent methionine synthase	amino acid.metabolism.synthesis.aspartate family.methionine
At5g05170	1	cellulose synthase catalytic subunit	cell.wall.cellulose synthesis
At3g08530	1	clathrin heavy chain, putative	cell.vesicle transport
At5g41770	1	crooked neck protein, putative	cell.cycle
At4g00180	1	axial regulator YABBY3 (YABBY3)	development.unspecified
At5g11980	1	COG complex component-related	minor.CHO metabolism.others
At1g75940	1	glycosyl hydrolase family 1 protein	misc.gluco-, galacto- and mannosidases
At5g33290	1	lexostoin family protein	misc.UDP glucosyl and glucoronyl transferases
At3g57550	1	2-guanylate kinase	nucleotide.metabolism.phosphotransfer and pyrophosphatases.guanylate kinase
At3g53620	1	inorganic pyrophosphatase, putative	nucleotide.metabolism.phosphotransfer and pyrophosphatases.misc
At5g53120	2	spermidine synthase, putative	polyamine.metabolism
At2g24270	1	NADP-dependent glyceraldehyde-3-phosphate dehydrogenase, putative	PS.calvin cycle.GAP
At1g07960	2	thioredoxin family protein	redox.thioredoxin
At1g21270	2	wall-associated kinase 2 (WAK2)	signalling.receptor kinases.wall associated kinase

At5g60340, At5g48545, At5g26190, At5g22640, At4g32190, At2g39795, At1g79280, At4g17330, At5g63200, At5g62090, At5g51200, At5g48610, At5g25757, At4g17240, At3g49570, At3g45900, At3g11690, At3g07780, At3g02910, At1g21170

3.13 HIG1/MYB51 and ATR2/bHLH05 interact in vivo

The results obtained with the yeast-two-hybrid assay showed that HIG1/MYB51 and ATR2/bHLH05 are able to interact in yeast. However, many candidates pulled out by a yeast-two-hybrid screen are false positives, even after several rounds of selection. To test, whether both transcription factors also interact in a plant system, the bimolecular fluorescence assay was used (Walter et al., 2004). The system is based on the separation of the amino and carboxy terminal domain of YFP (“split-YFP”) and their fusion to putative interacting proteins. Upon binding of both fusion proteins, the two YFP domains come in close proximity to reconstitute a functional fluorescent protein. For that reason, the coding sequence of HIG1/MYB51 and ATR2/bHLH05 were cloned into the respective binary vectors (Walter et al., 2004). HIG1/MYB51 was fused to the amino terminus of YFP (pSPYN) and ATR2/bHLH05 was fused to the carboxy terminus (pSPYC). The plasmids were then transformed into

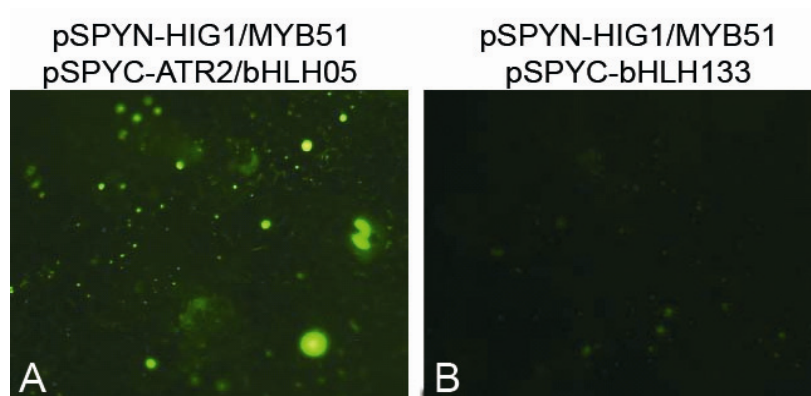


Figure 3.23: Split-YFP assay in agrobacteria infiltrated *N. benthamiana* leaves. (A) the YFP signal indicates the interaction of HIG1/MYB51 and ATR2/bHLH05; (B) bHLH133 did not interact with HIG1/MYB51.

hypervirulent agrobacteria, used for transient expression in tobacco via leaf infiltration. In a second assay, another nuclear localised bHLH factor, bHLH133, used in a different study was also cloned into pSPYC. An interaction with bHLH133 was not observed (Fig. 3.23B) and therefore suits as a nuclear localised negative control rather than an empty vector, which would target the protein to the cytoplasm. On the other hand, the interaction of HIG1/MYB51 and ATR2/bHLH05 could be clearly seen by the nuclear localised YFP signal in leaves infiltrated with the respective constructs (Fig. 3.23A). The plant based *in vivo* expression system thereby confirmed the results obtained by the yeast-two-hybrid assay.

3.14 *ATR2/bHLH05* and *HIG1/MYB51* expression overlap

The interaction of *HIG1/MYB51* and *ATR2/bHLH05* could be shown both in the yeast system and by transient expression in tobacco. However, an interaction of both proteins *in planta* is only possible if both are expressed in the same organs or tissues at the same time. Therefore, the expression pattern of *ATR2/bHLH05* was analysed using the GUS reporter and compared to the results obtained for *HIG1/MYB51* expression. The region upstream *ATR2/bHLH05* (At5g46760) was amplified from genomic DNA (-1325 to -4) and cloned via Gateway into pGWB3 for promoter driven GUS expression. The construct was expressed in *Arabidopsis* through agrobacteria mediated stable transformation. More than 20 independent T₁ plants were used for an initial screening and fifteen lines displaying the same qualitative expression

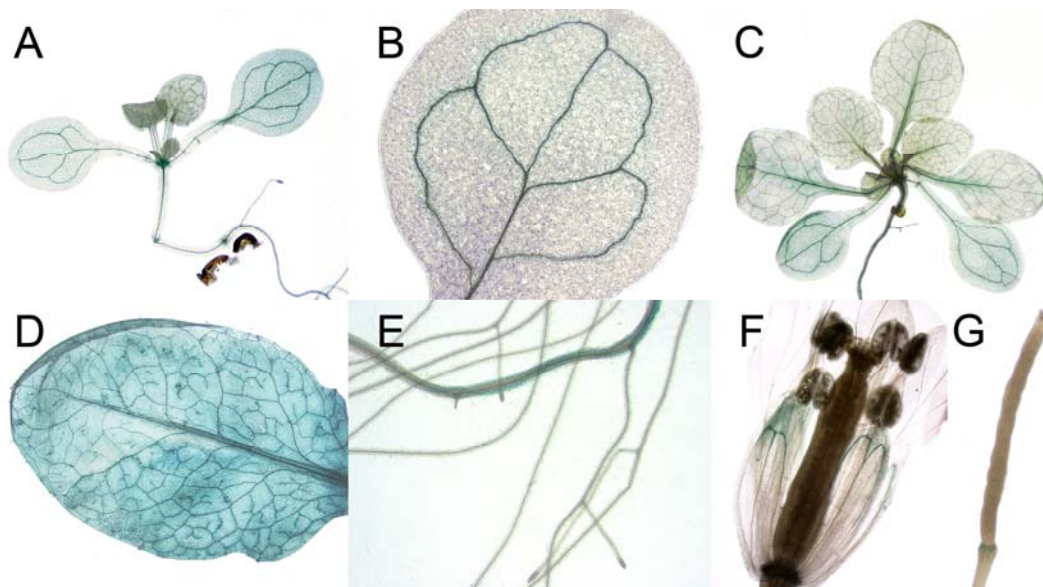


Figure 3.24: Histochemical GUS staining of Pro_{ATR2/bHLH05}-GUS plants. (A) 7-day old seedling; (B) cotyledon; (C) 3-week old plant; (D) mature rosette leaf; (E) main and lateral roots; (F) flower; (G) young silique.

pattern were analysed in more detail in the following generations. Promoter activity was detectable in the cotyledons of 7-day-old seedlings, mainly in the vasculature (Fig. 3.24A,B). Rosette leaves also showed strongest staining in the vasculature (Fig. 3.24C,D), but GUS activity was in general stronger in mature leaves than in young emerging leaves (Fig. 3.24C). Furthermore, GUS reporter expression was detectable in the main and lateral roots, with strongest staining in the cortical cells (Fig. 3.24E). The reproductive organs, namely flowers and siliques, displayed only faint promoter driven GUS activity. Blue staining could be seen in the vasculature of

sepals and in the abscission zone of young siliques (Fig. 3.24F,G). Taken together, the promoter of *ATR2/bHLH05* showed strongest activity in the vegetative organs. Faint and locally restricted GUS staining could be observed in flowers and siliques. A similar pattern was found for *HIG1/MYB51* expression (section 3.4). Hence, *ATR2/bHLH05* and *HIG1/MYB51* appear to be coexpressed to a large extent under normal growth conditions. An interaction of the gene products, as seen by protein interaction assays, could therefore be possible *in planta*.

3.15 **ATR2/bHLH05 represses HIG1/MYB51 activation of indolic glucosinolate promoters**

It is known from other transcription factors that the interaction with other factors is an important part of target gene regulation. A well characterised example is TRANSPARENT TESTA2 (TT2)/MYB123 and TT8/bHLH42, which need to interact for the activation of the *DIHYDROFLAVONOL REDUCTASE (DFR)* promoter (Baudry et al., 2004). Therefore, it was interesting to investigate, whether the interaction of HIG1/MYB51 with ATR2/bHLH05 modulates its potential to induce indolic glucosinolate promoters (section 3.8). Furthermore, Smolen et al. (2002) showed in their study that a point mutation in ATR2/bHLH05 (*atr2D*), but not overexpression of the wild-type coding sequence led to the increased transcription of glucosinolate pathway genes. Plants with ectopic overexpression of wild-type *ATR2/bHLH05* had neither an increased *ASA1* transcript level nor increased 5MT tolerance. Hence, the effect of the mutant *atr2D* was also tested in one of the approaches. The point mutation was introduced via PCR into the wild-type CDS at the position described by Smolen et al. (2002; D94N exchange). Both, the mutated and the wild-type CDS were transformed into the overexpression vector pGWB2, to be used as effector constructs in cotransformation assays. The experimental setup reproduces the one described in section 3.8, however only the qualitative histochemical GUS staining of transfected cells is shown. The effect of ATR2/bHLH05 on the promoter activity of *ASA1*, *CYP79B3* and *CYP83B1* was tested as examples of the indolic glucosinolate pathway. Furthermore, the mutated effector *atr2D* was analysed with respect to its regulation of *ASA1* and *CYP83B1*. The histochemical GUS staining of the transfected Arabidopsis cells indicates no background activity for cells transformed with the Pro_{ASA1}-GUS construct, a moderate activity of the Pro_{CYP79B3}-GUS and Pro_{CYP83B1}-GUS construct (Fig. 3.25, column 1).

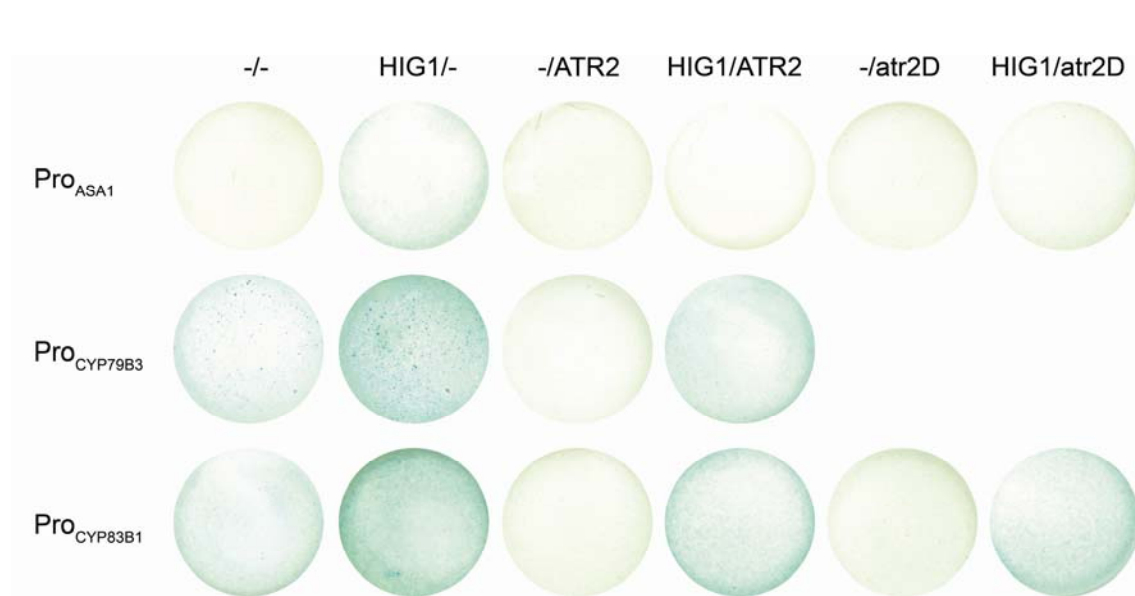


Figure 3.25: Histochemical GUS staining of transfected Arabidopsis cells. Cells were stained for 8 hours 4 days after transfection. The reporter constructs (in pGWB3i) are indicated on the left, the effector constructs (in pGWB2) are indicated on top. The *atr2D* mutant contained the D94N point mutation compared to the *ATR2* wild-type.

Cotransformation with the HIG1/MYB51 effector led to an activation of the two CYP promoters, indicated by the intense blue GUS staining (column 2). The promoter of *ASA1* was indeed not activated, as seen in previous analyses (Fig. 3.14). Interestingly, when *ATR2/bHLH05* was used as effector, there was no detectable GUS staining in any of the three setups (column 3). Even the background activity observed for the *CYP79B3* and *CYP83B1* promoter was not detectable. This suggests a repressive function of *ATR2/bHLH05* on these promoters. The addition of HIG1/MYB51 as a second effector resulted in a low GUS expression driven by the *CYP79B3* and *CYP83B1* promoter (column 4), however below the level when HIG1/MYB51 was used alone. It seems that the repression by *ATR2/bHLH05* can partially be rescued by HIG1/MYB51. However, it is not clear, whether this is mediated by interaction of the two proteins or if it is a dosage dependent regulation. Besides the wild-type *ATR2/bHLH05* protein, the dominant mutant *atr2D* was tested. Even though overexpression of *atr2D* in *planta* results in an upregulation of *ASA1* (Smolen et al., 2002), this effect could not be seen in the cell based system (column 5). There were no observable differences between the wild-type and the mutated effector, indicating a more complex *in planta* situation than mimicked in this cell-based assay. Also the addition of HIG1/MYB51 had no different effect than observed for the wild-type *ATR2/bHLH05* effector. It might be that the phenotype observed in

plants carrying the *atr2D* allele is the result of a more complex interaction with other factors than only with *HIG1/MYB51*. To overcome the limitation of this assay, the stable overexpression of *ATR2/bHLH05* in *HIG1-1D* plants was attempted. However, none of the individual transformants (60 lines tested) showed upregulation of both transcripts at the same time.

4 Discussion

4.1 **HIG1/MYB51 is a positive regulator of indolic glucosinolate biosynthesis**

The properties of glucosinolates as defence compounds along with their role in the biotic stress response have been under investigation for a long time. Glucosinolate biosynthesis is regulated in a developmental manner (Petersen et al., 2002; Brown et al., 2003) but can also be influenced by environmental stimuli, such as pathogen attack or hormone treatment (Brader et al., 2001; Kliebenstein et al., 2002b; Mewis et al., 2005). Even though the elucidation of the biosynthesis pathway has advanced substantially due to the model plant *Arabidopsis thaliana*, little is known about the regulatory machinery controlling this process. So far, only few components that influence glucosinolate accumulation have been described. ATR1/MYB34 was shown to activate both IAA and indolic glucosinolate biosynthesis, playing a role in the homeostasis of both (Celenza et al., 2005). OBP2, a DNA-binding-with-one-finger (DOF) transcription factor, was also described as a component affecting glucosinolate biosynthesis (Skirycz et al., 2006). Furthermore, IQD1, a calmodulin-binding nuclear protein, was shown to have a positive effect on glucosinolate accumulation and plant defence against herbivore attack (Levy et al., 2005).

Here, HIG1/MYB51 is presented, as a new component that regulates glucosinolate biosynthesis. The activation-tagging line *HIG1-1D* was isolated from a screen for mutants with an altered secondary metabolite profile (Schneider et al., 2005). The line displayed a dominant high indolic glucosinolate chemotype, caused by an upregulation of the endogenous *HIG1/MYB51* expression through the inserted enhancer element. *HIG1/MYB51* encodes a nuclear localised R2R3-type MYB transcriptional regulator. The relation between *HIG1/MYB51* expression and indolic glucosinolate accumulation could be demonstrated by analysing ectopic overexpression lines and a null mutant. High transcript levels of *HIG1/MYB51* were correlated with an increased concentration of the major indolic glucosinolate I3M, but also the minor compounds 4MOI3M and 1MOI3M accumulated to higher amounts than in the wild-type (Fig. 3.9). Thereby, ectopic overexpression of *HIG1/MYB51* phenocopies the upregulation of the endogenous expression pattern in the *HIG1-1D* mutant. In contrast, a T-DNA knock-out line of *HIG1/MYB51* (*hig1-1*) contained

significantly less glucosinolates than the wild-type, further confirming the gene-to-trait relation. *HIG1/MYB51* therefore represents a new important regulator of indolic glucosinolate biosynthesis.

Along with the high indolic glucosinolate level in the *HIG1/MYB51* overexpression lines, a decreased content of the short-chain aliphatic glucosinolate 4MSOB was observed. A reason for that might be an interdependence of the two branches, possibly via feedback regulation (Hemm et al., 2003). An alternative explanation was proposed by Grubb and Abel (2006) as “limiting electron model”, where the cytochrome P450 monooxygenases (CYPs) of the different pathways compete for the NADPH pool as electron source. This would explain why upregulation of one glucosinolate branch results in downregulation of the other. However, it is also known that the glucosinolate composition, and not only the total amount, plays a crucial role (Giamoustaris and Mithen, 1995; Rask et al., 2000). Interestingly, the *hig1-1* loss of function mutant accumulates less indolic and aliphatic glucosinolates at the same time, keeping the overall composition close to the wild-type pattern. It might be that under conditions of basal glucosinolates levels, there is a tendency to maintain a specific glucosinolate composition. Strong induction of glucosinolate biosynthesis by overexpression of *HIG1/MYB51* or environmental stimuli could overrule this aspect and the “limiting electron model” would come into play, resulting in upregulation of only one glucosinolate branch and the alteration of the overall composition.

Besides the effect of *HIG1/MYB51* misexpression on the chemotype, an influence on the transcript profile could be shown. First of all, RT-PCR analyses of constitutive *HIG1/MYB51* overexpressors indicated an upregulation of the biosynthesis pathway genes responsible for tryptophan and indolic glucosinolate biosynthesis (Fig. 3.12). An upregulation of *DHS1*, *TSB1* and *CYP79B2/B3*, *CYP83B1*, *UGT74B1* and *AtST5a* could be observed, respectively. The upregulation of the tryptophan pathway is probably due to an increased demand of the precursor tryptophan. Indeed, a common regulation of the tryptophan and indolic glucosinolate pathway could be observed under stress conditions (Gachon et al., 2005) and *HIG1/MYB51* might be a mediator of this regulation. At the same time, the genes coding for the key enzymes of the aliphatic glucosinolate biosynthesis (*CYP79F1/F2*, *CYP83A1*) were downregulated, in accordance with the low 4MSOB level, observed in these lines (Fig. 3.12; Fig. 3.9). Hence, the RT-PCR analysis of selected genes gave a first indication for an important role of *HIG1/MYB51* in transcriptional regulation of at least

some glucosinolate pathway genes. The potential of *HIG1/MYB51* to activate the promoters of several of these genes was tested in a cotransformation assay, taking advantage of the GUS reporter system. Activation by *HIG1/MYB51* was observed for the promoters of *DHS1*, *TSB1*, *CYP79B2/B3*, *CYP83B1* and *AtST5a* (Fig. 3.14). The promoter of *ASA1* appeared to be unaffected by *HIG1/MYB51*. Consequently, *HIG1/MYB51* has the potential to activate at least a subset of the indolic glucosinolate pathway genes *in trans*, supporting the idea of a positive transcriptional regulator.

To further investigate the influence of *HIG1/MYB51* on the total transcriptional profile *in planta*, ethanol inducible *HIG1/MYB51* lines in the *hig1-1* knock-out background were created and used for microarray analysis. However, only one set of experiments was conducted, rendering data difficult to interpret due to a lack of replicates. Nevertheless, analysis of the total transcript allowed the observation of certain tendencies. As seen in constitutive overexpression lines, an upregulation of indolic glucosinolate pathway genes was also observed 24 hours after *HIG1/MYB51* induction (Fig. 3.13). Genes upstream (*ASB1*, *IGPS*) and downstream (*CYP83B1*, *UGT74B1*, *AtST5a*) of tryptophan in the biosynthesis pathway were induced, confirming the RT-PCR analyses.

Besides the observed effect on indolic glucosinolate pathway genes, the transcript levels of *CYP71B15* and *NITRILASE2* (*NIT2*) were upregulated 24 hours after *HIG1/MYB51* induction. *CYP71B15* is the rate limiting enzyme in camalexin biosynthesis, a branching pathway of indolic glucosinolate biosynthesis that also uses IAOx as precursor (Fig. 4.1; Glawischnig et al., 2004; Schuhegger et al., 2006). *NIT2* is able to catalyze the synthesis of IAA from indole-3-acetonitrile (IAN), which in turn is a product of I3M decomposition by myrosinases. *NIT2* transcription is only slightly elevated in constitutive *HIG1/MYB51* overexpression lines (Gigolashvili et al., 2007), unlike the strong activation observed after transient *HIG1/MYB51* induction (Tab. 3.1). Despite the observed upregulation of *NIT2*, a high endogenous IAA level in the induced plants appeared unlikely. Many auxin-responsive genes were downregulated (Tab. 3.2), including *IAA6* and *IAA19* that are upregulated in high-auxin mutants (Zhao et al., 2002), and a member of the *GH3*-like protein family (At4g03400; \log_{10} -ratio=-1.0). Modified *GH3* promoter elements were used to generate the *DR5* reporter, commonly used to monitor endogenous auxin levels

(Ulmasov et al., 1997). Therefore, the question remains, why the IAA synthesis gene *NIT2* was upregulated, even though a low endogenous IAA level seemed likely.

One explanation might be the competition of the different biosynthesis branches for the common precursors (Fig. 4.1). Even though the formation of a metabolon (i.e. multienzyme complex) has not been proven for glucosinolate biosynthesis, there are indications suggesting its existence (reviewed by Jorgensen et al., 2005; Nafisi et al., 2006). If the activity of such a metabolon is increased, the precursor tryptophan or the intermediate IAOx might be less available for branching pathways. The upregulation of *NIT2* and *CYP71B15*, involved in IAA and camalexin biosynthesis, respectively, might therefore be a response to the tryptophan and IAOx shortage,

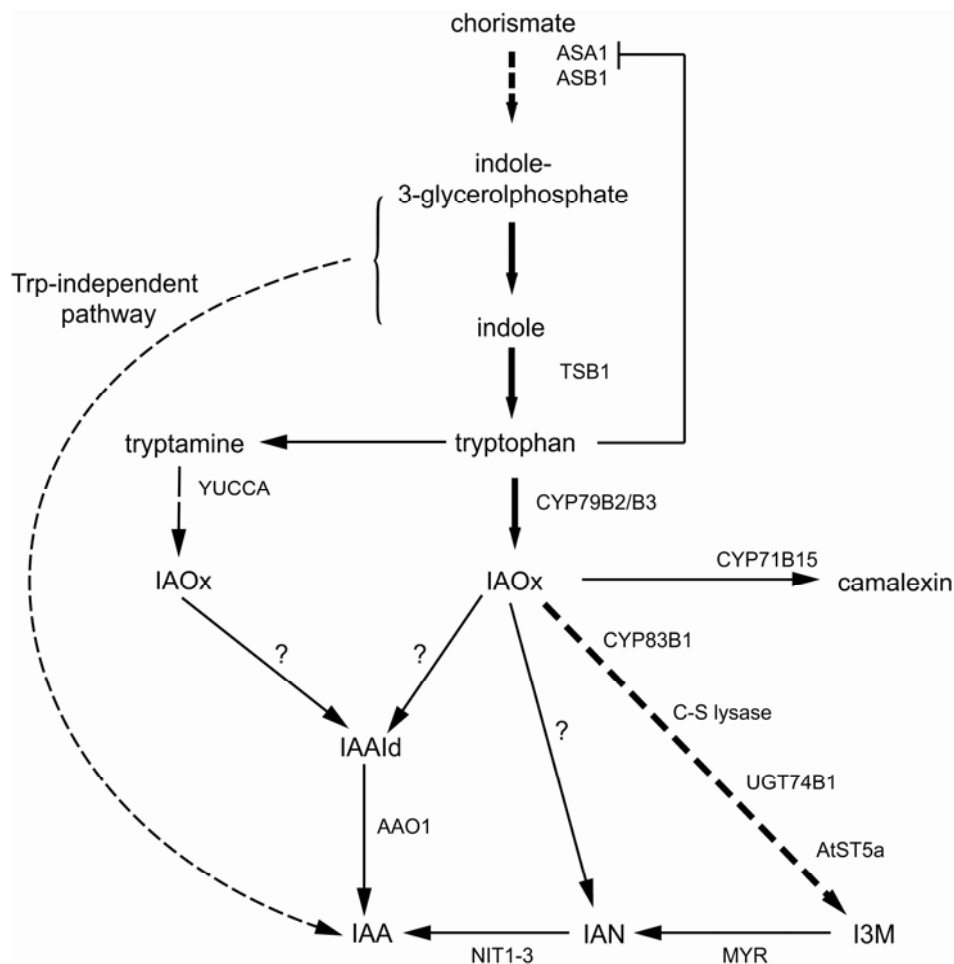


Figure 4.1: Simplified model of the IAA synthesis pathways in *A. thaliana* (modified after Zhao et al., 2002; Woodward and Bartel, 2005; Pollmann et al., 2006). Questionmarks indicate pathways with unknown enzymes. ASA1, anthranilate synthase alpha 1; ASB1, anthranilate synthase beta 1; TSB1, tryptophan synthase beta 1; CYP, cytochrome P450 monooxygenase; UGT, S-glycosyltransferase; AtST, *A. thaliana* sulfotransferase; NIT, nitrilase; MYR, myrosinase; AAO1, indole-3-acetaldehyde oxidase, YUCCA, flavin monooxygenase-like protein; IAOx, indole-3-acetaldoxime; I3M, indole-3-ylmethyl glucosinolate; IAAld, indole-3-acetaldehyde; IAA, indole-3-acetic acid; IAN, indole-3-acetonitrile.

rather than a direct induction by *HIG1/MYB51*. Interestingly, *NIT2* is known to be induced upon pathogen attack and is thought to play only a minor role in *de novo* IAA biosynthesis under normal conditions (Pollmann et al., 2006). This further suggests that *NIT2* might be activated under conditions of high I3M biosynthesis, when the normal IAA synthesis pathways are impaired due to a precursor shortage. Analyses of the transcription pattern of earlier time points after *HIG1/MYB51* induction could reveal at which point *NIT2* is induced. In addition, quantification of the camalexin content in response to *HIG1/MYB51* upregulation could answer the question, whether *HIG1/MYB51* is an activator of this pathway, or if the observed upregulation of *CYP71B15* is a secondary response to a limitation of the precursor IAOx.

4.2 *HIG1/MYB51* is expressed at sites of indolic glucosinolate accumulation

Since *HIG1/MYB51* appeared to be a transcriptional regulator of glucosinolate biosynthesis, one would expect a coexpression with the putative target genes. The expression pattern of several pathway genes and the regulatory component IQD1 and OBP2 have been described. Expression of IQD1 was observed in vegetative organs of non flowering plants (Levy et al., 2005). However, activity of the reporter construct diminished in the rosette during transition to the reproductive growth phase, when highest activity was observed in inflorescences and flower buds. Also OBP2 expression was shown to co-localise with vascular tissue in above and below-ground organs (Skirycz et al., 2006). The promoter of *CYP79B2* drove *GUS* reporter expression mainly in roots and cotyledons, but also in the vasculature of young and mature rosette leaves (Mikkelsen et al., 2000). Moreover, expression of *UGT74B1* was found mainly in vascular tissues, both in roots and leaves, a weak expression was observed in flowers (Grubb et al., 2004). Promoter activity of *HIG1/MYB51* was also found in vascular tissues of roots and the rosette, but extended further to the surrounding mesophyll of mature rosette leaves (Fig. 3.7). Consequently, there is a partial overlap in the expression of *HIG1/MYB51* and putative target genes.

Besides the expression pattern of biosynthesis genes, the distribution and concentration of glucosinolates in various organs has been described for *A. thaliana* (ecotype Col-0) during ontogenesis (Petersen et al., 2002; Brown et al., 2003). Highest glucosinolate concentrations are found in siliques and seeds, mainly due to the accumulation of aliphatic glucosinolates. Even though indolic glucosinolates are

present in basically all organs, they appear most prominent in roots and mature rosettes. Hence, *HIG1/MYB51* expression co-localises with sites of indolic glucosinolate biosynthesis and accumulation.

4.3 *HIG1/MYB51* plays a role in biotic stress response

Production of secondary metabolites, such as glucosinolates, to increase plant resistance against environmental stress is a question of cost and benefit. Highest concentrations of defence compounds are usually found in the reproductive organs and seeds. On the other hand, vegetative organs contain fewer amounts of secondary metabolites, rendering them more vulnerable. To reduce the risk of severe damage, plants have evolved systems to perceive stress stimuli and react appropriately, by a transient activation of defence machineries. Apart from the basal level of glucosinolates present in unstressed plants, the biosynthesis can be drastically induced by wounding, hormone application, pathogen or herbivore attack (Brader et al., 2001; Kliebenstein et al., 2002a; Bednarek et al., 2005; Mewis et al., 2005). The stress related induction of several pathway genes was demonstrated, and also *IQD1*, *OBP2* and *ATR1/MYB34* were shown to respond to wounding (Levy et al., 2005; Skirycz et al., 2006). A basal expression of *HIG1/MYB51* was found in vegetative organs, at sites of indolic glucosinolate accumulation. However, transcription of *HIG1/MYB51* was rapidly induced by mechanical stimuli, such as wounding, touch or spraying (Fig. 3.15-3.17). In addition, the induction of *HIG1/MYB51* by wounding or pathogen attack has been reported in previous microarray studies (Chen et al., 2002; Cheong et al., 2002; Thilmony et al., 2006). Despite a strong upregulation of *HIG1/MYB51* shortly after stress application, the transcript level returned back to the basal level within hours. Therefore, *HIG1/MYB51* appears to be responsive to mechanical stimuli in a transient manner and it is tempting to speculate about a regulatory role of *HIG1/MYB51* in mediating the increased indolic glucosinolate biosynthesis in response to biotic stress conditions. Additional evidence about an implication of *HIG1/MYB51* in an early stress response comes from microarray experiments analysing the response to treatment with the protein synthesis inhibitor cycloheximide (Genevestigator database; www.genevestigator.ethz.ch). Samples treated with cycloheximide showed a drastically increased accumulation of *HIG1/MYB51* transcripts in comparison to control conditions. This shows that the transcriptional machinery, necessary for

HIG1/MYB51 transcription, is independent of *de novo* protein biosynthesis and only requires the modification of existing transcription factors. Such a phenomenon has been reported for many genes involved in early steps of signalling pathways and those genes have been designated as “early responsive genes” (Herschman, 1991; Abel et al., 1995). Also *HIG1/MYB51* might therefore be part of an early signal perception.

To further investigate the potential of *HIG1/MYB51* as part of the defence system, the resistance of the overexpression line *HIG1-1D* against a generalist herbivore was tested. In a dual choice assay, the high indolic glucosinolate leaves of *HIG1-1D* clearly appeared to be more resistant against the generalist herbivore *S. exigua* (Fig.3.19). Further evidence supporting the idea of *HIG1/MYB51* as a regulator of herbivore resistance was provided by QTL mapping in a Col x Ler population (Kliebenstein et al., 2002a). A QTL conferring increased resistance to the generalist herbivore *Trichoplusia ni* was mapped to chromosome 1, in the region between 14-28 cM. This region contains the At1g18570 locus, coding for *HIG1/MYB51*, indicating that *HIG1/MYB51* might play a general role in the defence against generalist herbivores (Fig. 4.2).

4.4 *HIG1/MYB51* has a role distinct from its close homologue *ATR1/MYB34*

Until recently, *ATR1/MYB34* was regarded as a master regulator with respect to indolic glucosinolate biosynthesis and IAA homeostasis (Grubb and Abel, 2006). Here, *HIG1/MYB51* is presented as an additional positive regulator of indolic glucosinolate biosynthesis, distinct of *ATR1/MYB34*. A dominant mutation of *ATR1/MYB34* was first described with respect to an altered tryptophan regulation (Bender and Fink, 1998), identified in a screen for 5MT resistant mutants. The increased resistance to the tryptophan analogue results from a constitutive activation of *ASA1* in the mutant line overexpressing *ATR1/MYB34*. On the other hand, *HIG1/MYB51* overexpression lines are as sensitive to 5MT as wild-type Arabidopsis plants (Fig. 3.11). An activation of *ASA1* was not observed in constitutive *HIG1/MYB51* overexpressors or a transient activation assay in Arabidopsis cell cultures (Fig. 3.14). This shows that even though *ATR1/MYB34* and *HIG1/MYB51* both activate tryptophan and indolic glucosinolate biosynthesis, there are differences regarding the influence on *ASA1* transcription. A further variation between

ATR1/MYB34 and *HIG1/MYB51* consists in the respective influence on the endogenous IAA level. On the one hand, strong *ATR1/MYB34* overexpression lines have a significantly higher IAA level compared to wild-type plants (Fig. 3.10), accompanied by a severe high-auxin growth phenotype (Gigolashvili et al., 2007). On the other hand, constitutive upregulation of *HIG1/MYB51* has only moderate influence on the IAA level (Fig. 3.10) and neither the dominant *HIG1-1D* nor the *hig1-1* knock-out line shows any informative growth phenotype. Furthermore, the transient induction of *HIG1/MYB51* expression in the *hig1-1* background is accompanied by the downregulation of numerous auxin-responsive genes. Whereas *ATR1/MYB34* appears to play a predominant role in the homeostasis of IAA and indolic glucosinolates, *HIG1/MYB51* seems to specifically activate the latter only. This is further supported by the upregulation of genes acting downstream CYP83B1, i.e. UGT74B1 and AtST5a, by *HIG1/MYB51* (Fig. 3.12-14), which was not observed for *ATR1/MYB34* (Gigolashvili et al., 2007).

An additional indication for the different roles of *HIG1/MYB51* and *ATR1/MYB34* is their distinct expression pattern. The expression of *HIG1/MYB51* correlates with sites of indolic glucosinolate accumulation, rather than with sites of IAA synthesis. In contrast, the expression pattern of *ATR1/MYB34* shows spatial and temporal differences compared to *HIG1/MYB51* expression. Plants containing an *ATR1/MYB34-GUS* reporter construct display no GUS expression in mature rosette leaves. However, *ATR1/MYB34* expression can be observed in the meristematic tissues of growing inflorescences and generative organs (Gigolashvili et al., 2007; microarray data analysed with www.geneinvestigator.ethz.ch). Therefore, *ATR1/MYB34* expression appears to be absent from major sites of indolic glucosinolate accumulation. Furthermore, *ATR1/MYB34* and *HIG1/MYB51* respond differently to biotic stress conditions. *ATR1/MYB34* is inducible by MeJA treatment and herbivore attack, but only hours after stress treatment (Smolen and Bender, 2002; Skirycz et al., 2006). In contrast, *HIG1/MYB51* is rapidly induced by wounding or other mechanical stimuli (Fig. 3.15-17) and seems to be involved in an early stress response. Even though *ATR1/MYB34* and *HIG1/MYB51* share common target genes, they differ with respect to their influence on IAA biosynthesis and *ASA1* regulation, but also regarding their expression pattern and response to environmental stimuli.

4.5 Is *HIG1/MYB51* differentially regulated in roots?

Interestingly, biotic stress hormones such as MeJA, SA or the ethylene precursor ACC appeared to have little influence on *HIG1/MYB51* expression in the aerial part of the plant (section 3.9-9.10), as reported for *IQD1* (Levy et al., 2005). However, a differential regulation of *HIG1/MYB51* seems to exist in the roots. Under control conditions, *HIG1/MYB51* expression seems to be absent from the meristem but is present in the differentiation zone. Treatment with the ethylene precursor ACC results in a strong activation of the *HIG1/MYB51* promoter in the root meristem (Fig. 3.18). Interestingly, the root tip is known to actively synthesise IAA, with highest synthesis rates in the meristem (Ljung et al., 2005). This is coherent with expression of *ASA1*, *ASB1*, *CYP79B2* and *CYP79B3* in the meristematic region (Stepanova et al., 2005; Ljung et al., 2005). Furthermore, the IAA synthesis in this tissue is inducible by ethylene treatment as monitored by the *DR5* reporter and accompanied by a site specific upregulation of *ASA1* and *ASB1* (Stepanova et al., 2005). Therefore, the question arises, whether *HIG1/MYB51* is involved in the ethylene-induced auxin biosynthesis in the root tips. A moderate activation of *ASB1* was observed upon *HIG1/MYB51* induction in rosette leaves, whereas *ASA1* was unaffected (Fig. 3.13). Unfortunately, most studies about the regulation of IAA biosynthesis concentrated on the aerial parts of the plant and not on the root system. Furthermore, little is known about the differential regulation of *ASA1* and *ASB1*, coding for the second subunit of anthranilate synthase. *HIG1/MYB51* might be involved in the site specific regulation of IAA and/or indolic glucosinolate biosynthesis upon ethylene induction in the root meristem. However, further studies are needed to elucidate the differential regulation of auxin biosynthesis in aerial parts and the root system, also with respect to IAA and indolic glucosinolate homeostasis.

4.6 Is *HIG1/MYB51* part of a complex regulatory network?

Analysis of the regulation of phenylpropanoid biosynthesis has revealed a complex regulation of the pathway genes, where multiple transcription factors come into play (Winkel-Shirley, 2002). A similar scenario might exist for the regulation of glucosinolate biosynthesis. A reason for that hypothesis is the close link of indolic glucosinolate and IAA biosynthesis (section 1.2). Furthermore, glucosinolates play a role in basal plant resistance but are also induced upon pathogen or herbivore attack. An increased IAA synthesis at the same time seems undesirable for the plant.

Consequently, a tight regulation of glucosinolate biosynthesis can be expected. First components of such a network have been presented (Smolen et al., 2002; Celenza et al., 2005; Levy et al., 2005; Skirycz et al., 2006). However, further evidence is suggesting a more complex situation.

The yeast-two-hybrid screen presented in this study revealed a protein-protein interaction of HIG1/MYB51 with the bHLH transcription factor ATR2/bHLH05. This interaction could be confirmed *in vivo* using the “split-yfp” approach. In addition, cotransformation assays in *Arabidopsis* cell cultures suggest a repression of HIG1/MYB51 action by ATR2/bHLH05. Therefore, HIG1/MYB51 and ATR2/bHLH05 present the first described transcriptional regulators of indolic glucosinolate biosynthesis that interact with one another and thereby influence each other. However, this interaction needs to be further characterised *in planta*, with respect to the putative target genes and the glucosinolate profile. The generation of a double overexpression line was not successful, possibly due to the use of the CaMV 35S promoter or not enough lines tested. It could also be that HIG1/MYB51 and ATR2/bHLH05 not only interact but regulate each other. Different approaches will therefore be needed. First indications could come from the analysis of *ATR2/bHLH05* knock-out or knock-down plants, with respect to *HIG1/MYB51* expression and activation of indolic glucosinolate pathway genes. A further possibility would be the transient overexpression of each gene in the reporter GUS lines of the respective other gene to elucidate a possible transcriptional regulation.

Besides the observed interaction of HIG1/MYB51 and ATR2/bHLH05, several proteins involved in protein degradation were found within the yeast-two-hybrid screen. It is known from other transcriptional regulators that the specific protein turnover plays an important regulatory role (reviewed by Sullivan et al., 2003; Devoto and Turner, 2005). Indeed, the clone identified most often (17-times) was that of a putative E3-ubiquitin ligase (At4g19700), which is known to interact with other MYB transcription factors in yeast, namely MYB4, MYB6, MYB0 and MYB75 (Zimmermann, 2003). Therefore, it is tempting to speculate, whether this E3-ubiquitin ligase plays a role in targeting specific MYB transcriptional regulators for degradation via the proteasome. However, an interaction of the E3 ligase with any of the MYB factors *in planta* still needs to be investigated.

Not only *in vitro* screenings, but also *in silico* studies offer the possibility to find putative interacting genes. Looking at genes that are co-regulated with *HIG1/MYB51*

under pathogen-stress conditions, by means of the GeneAngler tool (Toufighi et al., 2005), a link to the expression of *MYB122*, the closest homologue of *MYB51/HIG1*, can be observed. Ectopic overexpression of *MYB122* in the wild-type background led to an increased transcript level of several genes involved in indolic glucosinolate biosynthesis and increased I3M levels (Gigolashvili et al., 2007). However, this induction was not observed when *MYB122* was overexpressed in the *hig1-1* background. It seems that the positive regulatory role of *MYB122* is dependent on functional *HIG1/MYB51*. *MYB122* might act downstream *HIG1/MYB51*, or the two factors interact with each other. To further investigate this question, the yeast-two-hybrid system was employed to assess a possible interaction of these two MYB factors. The amino terminal MYB domain of *HIG1/MYB51* was used as bait (Fig. 3.21, construct A), the full length *MYB122* as prey. The two constructs were tested by J. Uhrig, University of Cologne, and indeed a positive interaction of *HIG1/MYB51* and *MYB122* could be observed in the yeast system. So far, an interaction of two MYB factors was not reported for plant MYB transcription factors.

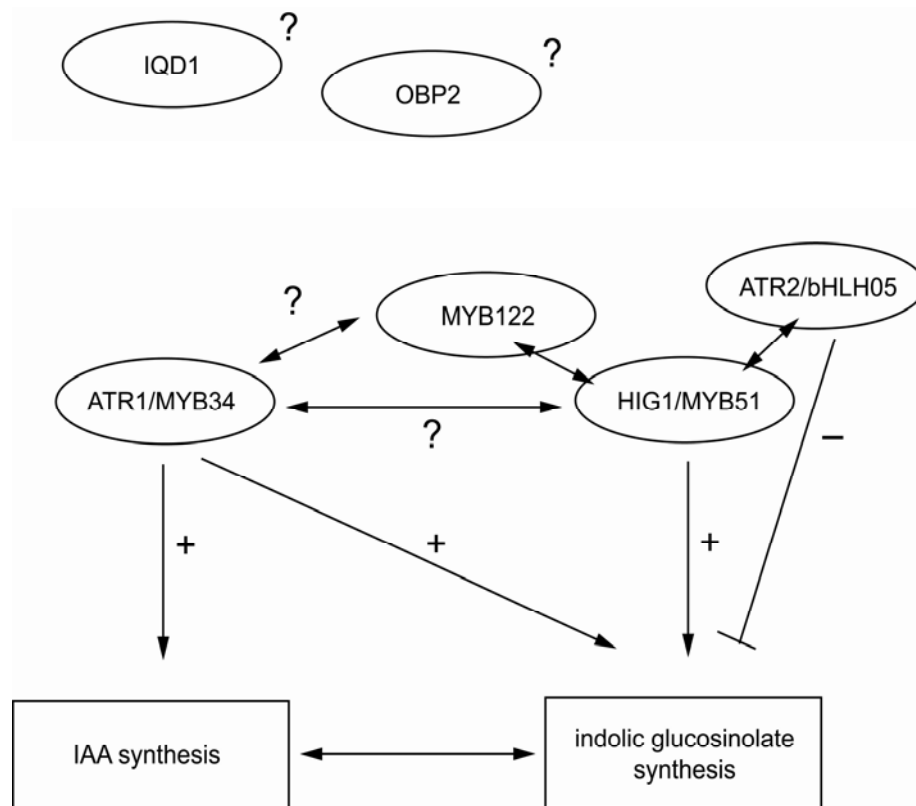


Figure 4.3: Model of the regulatory network controlling indolic glucosinolate accumulation. Known interactions are indicated. Question marks show where further studies are necessary to define an interaction or to place known regulators in the network.

This finding therefore presents a new and interesting possibility for the formation of transcriptional regulator complexes (Fig. 4.3).

In addition to the observed interactions at the protein level, *HIG1/MYB51* is certainly regulated on the transcriptional level (as discussed in sections 4.1 and 4.3). Ongoing studies gave first indications about a transcriptional control of MYB factors belonging to subgroup 12 by other members of the same subgroup. As a consequence, future work should focus on studying the interaction of the transcriptional regulators that control glucosinolate biosynthesis on the transcriptional and protein level (Fig. 4.3).

Summarizing, *HIG1/MYB51* is a positive regulator of indolic glucosinolate biosynthesis that activates pathway genes *in trans* and is expressed at sites of glucosinolate synthesis and accumulation. Furthermore, *HIG1/MYB51* expression is rapidly inducible by biotic stress and a high *HIG1/MYB51* transcript level, accompanied by an increased accumulation of indolic glucosinolates, confers increased resistance against generalist herbivores. Therefore, *HIG1/MYB51* seems to be part of an early biotic stress response in *A. thaliana*. The interaction with the transcriptional regulators *ATR2/bHLH05* and *MYB122* suggest a complex regulatory network controlling indolic glucosinolate biosynthesis and future studies should aim at elucidating the specific role of the individual components of this network.

5 References

- Abel, S., Nguyen, M.D., and Theologis, A.** (1995). The Ps-*Iaa4/5*-Like Family of Early Auxin-Inducible Messenger-Rnas in *Arabidopsis-Thaliana*. *J. Mol. Biol.* **251**, 533-549.
- Agrawal, A.A.** (2000). Mechanisms, ecological consequences and agricultural implications of tri-trophic interactions. *Curr. Opin. Plant Biol.* **3**, 329-335.
- Ausubel, F.M., Brent, R., Kingston, R.E., Moore, D.D., Snuth, F.A., Seidman, J.G., and Struhl, K.** (1997). *Current protocols in molecular biology*. (New York: Greene Publishing Associates and Wiley-Intersciences).
- Bailey, P.C., Martin, C., Toledo-Ortiz, G., Quail, P.H., Huq, E., Heim, M.A., Jakoby, M., Werber, M., and Weisshaar, B.** (2003). Update on the basic helix-loop-helix transcription factor gene family in *Arabidopsis thaliana*. *Plant Cell* **15**, 2497-2501.
- Bak, S., and Feyereisen, R.** (2001). The involvement of two P450 enzymes, CYP83B1 and CYP83A1, in auxin homeostasis and glucosinolate biosynthesis. *Plant Physiology* **127**, 108-118.
- Bak, S., Tax, F.E., Feldmann, K.A., Galbraith, D.W., and Feyereisen, R.** (2001). CYP83B1, a cytochrome P450 at the metabolic branch point in auxin and indole glucosinolate biosynthesis in *Arabidopsis*. *Plant Cell* **13**, 101-111.
- Barlier, I., Kowalczyk, M., Marchant, A., Ljung, K., Bhalerao, R., Bennett, M., Sandberg, G., and Bellini, C.** (2000). The SUR2 gene of *Arabidopsis thaliana* encodes the cytochrome P450CYP83B1, a modulator of auxin homeostasis. *Proc. Natl. Acad. Sci. U. S. A.* **97**, 14819-14824.
- Barth, C., and Jander, G.** (2006). *Arabidopsis* myrosinases TGG1 and TGG2 have redundant function in glucosinolate breakdown and insect defense. *Plant J.* **46**, 549-562.
- Baudry, A., Caboche, M., and Lepiniec, L.** (2006). TT8 controls its own expression in a feedback regulation involving TTG1 and homologous MYB and bHLH factors, allowing a strong and cell-specific accumulation of flavonoids in *Arabidopsis thaliana*. *Plant J.* **46**, 768-779.
- Baudry, A., Heim, M.A., Dubreucq, B., Caboche, M., Weisshaar, B., and Lepiniec, L.** (2004). TT2, TT8, and TTG1 synergistically specify the

- expression of BANYULS and proanthocyanidin biosynthesis in *Arabidopsis thaliana*. *Plant J.* **39**, 366-380.
- Bednarek, P., Schneider, B., Svatos, A., Oldham, N.J., and Hahlbrock, K.** (2005). Structural complexity, differential response to infection, and tissue specificity of indolic and phenylpropanoid secondary metabolism in *Arabidopsis* roots. *Plant Physiology* **138**, 1058-1070.
- Bender, J., and Fink, G.R.** (1998). A Myb homologue, ATR1, activates tryptophan gene expression in *Arabidopsis*. *Proc. Natl. Acad. Sci. U. S. A.* **95**, 5655-5660.
- Berger, B., Stracke, R., Yatusевич, R., Weisshaar, B., Flugge, U.-I., and Gigolashvili, T.** (2007). A simplified method for the analysis of transcription factor-promoter interactions that allows high-throughput data generation. *Plant J.* in press.
- Bones, A.M., and Rossiter, J.T.** (2006). The enzymic and chemically induced decomposition of glucosinolates. *Phytochemistry* **67**, 1053-1067.
- Borevitz, J.O., Xia, Y.J., Blount, J., Dixon, R.A., and Lamb, C.** (2000). Activation tagging identifies a conserved MYB regulator of phenylpropanoid biosynthesis. *Plant Cell* **12**, 2383-2393.
- Brader, G., Tas, E., and Palva, E.T.** (2001). Jasmonate-dependent induction of indole glucosinolates in *Arabidopsis* by culture filtrates of the nonspecific pathogen *Erwinia carotovora*. *Plant Physiology* **126**, 849-860.
- Brader, G., Mikkelsen, M.D., Halkier, B.A., and Palva, E.T.** (2006). Altering glucosinolate profiles modulates disease resistance in plants. *Plant J.* **46**, 758-767.
- Broun, P.** (2004). Transcription factors as tools for metabolic engineering in plants. *Curr. Opin. Plant Biol.* **7**, 202-209.
- Brown, P.D., Tokuhisa, J.G., Reichelt, M., and Gershenzon, J.** (2003). Variation of glucosinolate accumulation among different organs and developmental stages of *Arabidopsis thaliana*. *Phytochemistry* **62**, 471-481.
- Caddick, M.X., Greenland, A.J., Jepson, I., Krause, K.P., Qu, N., Riddell, K.V., Salter, M.G., Schuch, W., Sonnewald, U., and Tomsett, A.B.** (1998). An ethanol inducible gene switch for plants used to manipulate carbon metabolism. *Nat. Biotechnol.* **16**, 177-180.

- Celenza, J.L., and Carlson, M.** (1989). Mutational Analysis of the *Saccharomyces Cerevisiae* Snf1 Protein-Kinase and Evidence for Functional Interaction with the Snf4 Protein. *Mol. Cell. Biol.* **9**, 5034-5044.
- Celenza, J.L., Quiel, J.A., Smolen, G.A., Merrikkh, H., Silvestro, A.R., Normanly, J., and Bender, J.** (2005). The Arabidopsis ATR1 Myb transcription factor controls indolic glucosinolate homeostasis. *Plant Physiology* **137**, 253-262.
- Chen, S.X., Glawischnig, E., Jorgensen, K., Naur, P., Jorgensen, B., Olsen, C.E., Hansen, C.H., Rasmussen, H., Pickett, J.A., and Halkier, B.A.** (2003). CYP79F1 and CYP79F2 have distinct functions in the biosynthesis of aliphatic glucosinolates in Arabidopsis. *Plant J.* **33**, 923-937.
- Chen, W.Q., Provart, N.J., Glazebrook, J., Katagiri, F., Chang, H.S., Eulgem, T., Mauch, F., Luan, S., Zou, G.Z., Whitham, S.A., Budworth, P.R., Tao, Y., Xie, Z.Y., Chen, X., Lam, S., Kreps, J.A., Harper, J.F., Si-Ammour, A., Mauch-Mani, B., Heinlein, M., Kobayashi, K., Hohn, T., Dangl, J.L., Wang, X., and Zhu, T.** (2002). Expression profile matrix of Arabidopsis transcription factor genes suggests their putative functions in response to environmental stresses. *Plant Cell* **14**, 559-574.
- Cheong, Y.H., Chang, H.S., Gupta, R., Wang, X., Zhu, T., and Luan, S.** (2002). Transcriptional profiling reveals novel interactions between wounding, pathogen, abiotic stress, and hormonal responses in Arabidopsis. *Plant Physiology* **129**, 661-677.
- Chomczynski, P., and Sacchi, N.** (1987). Single-Step Method of Rna Isolation by Acid Guanidinium Thiocyanate Phenol Chloroform Extraction. *Anal. Biochem.* **162**, 156-159.
- Cipollini, D., Enright, S., Traw, M.B., and Bergelson, J.** (2004). Salicylic acid inhibits jasmonic acid-induced resistance of Arabidopsis thaliana to *Spodoptera exigua*. *Mol. Ecol.* **13**, 1643-1653.
- Cook, S.M., Smart, L.E., Martin, J.L., Murray, D.A., Watts, N.P., and Williams, I.H.** (2006). Exploitation of host plant preferences in pest management strategies for oilseed rape (*Brassica napus*). *Entomol. Exp. Appl.* **119**, 221-229.
- Delarue, M., Prinsen, E., Van Onckelen, H., Caboche, M., and Bellini, C.** (1998). Sur2 mutations of Arabidopsis thaliana define a new locus involved in the control of auxin homeostasis. *Plant J.* **14**, 603-611.

- Devoto, A., and Turner, J.G.** (2005). Jasmonate-regulated Arabidopsis stress signalling network. *Physiol. Plant* **123**, 161-172.
- Endt, D.V., Kijne, J.W., and Memelink, J.** (2002). Transcription factors controlling plant secondary metabolism: what regulates the regulators? *Phytochemistry* **61**, 107-114.
- Feldmann, K.A.** (2001). Cytochrome P450s as genes for crop improvement. *Curr. Opin. Plant Biol.* **4**, 162-167.
- Feller, A., Hernandez, J.M., and Grotewold, E.** (2006). An ACT-like domain participates in the dimerization of several plant basic-helix-loop-helix transcription factors. *J. Biol. Chem.* **281**, 28964-28974.
- Gachon, C.M.M., Langlois-Meurinne, M., Henry, Y., and Saindrenan, P.** (2005). Transcriptional co-regulation of secondary metabolism enzymes in Arabidopsis: functional and evolutionary implications. *Plant Mol. Biol.* **58**, 229-245.
- Giamoustaris, A., and Mithen, R.** (1995). The Effect of Modifying the Glucosinolate Content of Leaves of Oilseed Rape (*Brassica-Napus Ssp Oleifera*) on Its Interaction with Specialist and Generalist Pests. *Ann. Appl. Biol.* **126**, 347-363.
- Gietz, R.D., Schiestl, R.H., Willems, A.R., and Woods, R.A.** (1995). Studies on the Transformation of Intact Yeast-Cells by the Liac/S-DNA/Peg Procedure. *Yeast* **11**, 355-360.
- Gigolashvili, T., Berger, B., Mock, H.-P., Muller, C., Weisshaar, B., and Flugge, U.-I.** (2007). The transcription factor HIG1/MYB51 regulates indolic glucosinolate biosynthesis in Arabidopsis thaliana. *Plant J.* **in press**.
- Glawischnig, E., Hansen, B.G., Olsen, C.E., and Halkier, B.A.** (2004). Camalexin is synthesized from indole-3-acetaldoxime, a key branching point between primary and secondary metabolism in Arabidopsis. *Proc. Natl. Acad. Sci. U. S. A.* **101**, 8245-8250.
- Grubb, C.D., and Abel, S.** (2006). Glucosinolate metabolism and its control. *Trends Plant Sci.* **11**, 89-100.
- Grubb, C.D., Zipp, B.J., Ludwig-Muller, J., Masuno, M.N., Molinski, T.F., and Abel, S.** (2004). Arabidopsis glucosyltransferase UGT74B1 functions in glucosinolate biosynthesis and auxin homeostasis. *Plant J.* **40**, 893-908.
- Halkier, B.A., and Gershenzon, J.** (2006). Biology and biochemistry of glucosinolates. *Annual Review of Plant Biology* **57**, 303-333.

- Hanahan, D.** (1983). Studies on Transformation of Escherichia-Coli with Plasmids. *J. Mol. Biol.* **166**, 557-580.
- Hansen, C.H., Wittstock, U., Olsen, C.E., Hick, A.J., Pickett, J.A., and Halkier, B.A.** (2001). Cytochrome P450CYP79F1 from Arabidopsis catalyzes the conversion of dihomomethionine and trihomomethionine to the corresponding aldoximes in the biosynthesis of aliphatic glucosinolates. *J. Biol. Chem.* **276**, 11078-11085.
- Harper, J.W., Adami, G.R., Wei, N., Keyomarsi, K., and Elledge, S.J.** (1993). The P21 Cdk-Interacting Protein Cip1 Is a Potent Inhibitor of G1 Cyclin-Dependent Kinases. *Cell* **75**, 805-816.
- Hemm, M.R., Herrmann, K.M., and Chapple, C.** (2001). AtMYB4: a transcription factor general in the battle against UV. *Trends Plant Sci.* **6**, 135-136.
- Hemm, M.R., Ruegger, M.O., and Chapple, C.** (2003). The Arabidopsis ref2 mutant is defective in the gene encoding CYP83A1 and shows both phenylpropanoid and glucosinolate phenotypes. *Plant Cell* **15**, 179-194.
- Herschman, H.R.** (1991). Primary Response Genes Induced by Growth-Factors and Tumor Promoters. *Annu. Rev. Biochem.* **60**, 281-319.
- Holst, B., and Williamson, G.** (2004). A critical review of the bioavailability of glucosinolates and related compounds. *Nat. Prod. Rep.* **21**, 425-447.
- Horton, P., Park, K.-J., Obayashi, T., and Nakai, K.** (2006). Protein Subcellular Localization Prediction with WoLF PSORT. In Proceedings of the 4th Annual Asia Pacific Bioinformatics Conference APBC06 (Taipei, Taiwan), pp. 39-48.
- Hull, A.K., Vij, R., and Celenza, J.L.** (2000). Arabidopsis cytochrome P450s that catalyze the first step of tryptophan-dependent indole-3-acetic acid biosynthesis. *Proc. Natl. Acad. Sci. U. S. A.* **97**, 2379-2384.
- Husebye, H., Chadchawan, S., Winge, P., Thangstad, O.P., and Bones, A.M.** (2002). Guard cell- and phloem idioblast-specific expression of thioglucoside glucohydrolase 1 (myrosinase) in Arabidopsis. *Plant Physiology* **128**, 1180-1188.
- Inoue, H., Nojima, H., and Okayama, H.** (1990). High-Efficiency Transformation of Escherichia-Coli with Plasmids. *Gene* **96**, 23-28.
- Ishihara, A., Asada, Y., Takahashi, Y., Yabe, N., Komeda, Y., Nishioka, T., Miyagawa, H., and Wakasa, K.** (2006). Metabolic changes in Arabidopsis

- thaliana expressing the feedback-resistant anthranilate synthase alpha subunit gene OASA1D. *Phytochemistry* **67**, 2349-2362.
- James, P., Halladay, J., and Craig, E.A.** (1996). Genomic libraries and a host strain designed for highly efficient two-hybrid selection in yeast. *Genetics* **144**, 1425-1436.
- Jefferson, R.A., Kavanagh, T.A., and Bevan, M.W.** (1987). Gus Fusions - Beta-Glucuronidase as a Sensitive and Versatile Gene Fusion Marker in Higher-Plants. *Embo Journal* **6**, 3901-3907.
- Jin, H.L., Cominelli, E., Bailey, P., Parr, A., Mehrtens, F., Jones, J., Tonelli, C., Weisshaar, B., and Martin, C.** (2000). Transcriptional repression by AtMYB4 controls production of UV-protecting sunscreens in Arabidopsis. *EMBO Journal* **19**, 6150-6161.
- Johnson, I.T.** (2002). Glucosinolates: Bioavailability and importance to health. *Int. J. Vitam. Nutr. Res.* **72**, 26-31.
- Jorgensen, K., Rasmussen, A.V., Morant, M., Nielsen, A.H., Bjarnholt, N., Zagrobelny, M., Bak, S., and Moller, B.L.** (2005). Metabolon formation and metabolic channeling in the biosynthesis of plant natural products. *Curr. Opin. Plant Biol.* **8**, 280-291.
- Keck, A.-S., and Finley, J.W.** (2004). Cruciferous Vegetables: Cancer Protective Mechanisms of Glucosinolate Hydrolysis Products and Selenium. *Integr Cancer Ther* **3**, 5-12.
- Kim, J.H., and Jander, G.** (2007). *Myzus persicae* (green peach aphid) feeding on Arabidopsis induces the formation of a deterrent indole glucosinolate. *Plant J.* **49**, 1008-1019.
- Klein, M., Reichelt, M., Gershenzon, J., and Papenbrock, J.** (2006). The three desulfoglucosinolate sulfotransferase proteins in Arabidopsis have different substrate specificities and are differentially expressed. *Febs Journal* **273**, 122-136.
- Kliebenstein, D., Pedersen, D., Barker, B., and Mitchell-Olds, T.** (2002a). Comparative analysis of quantitative trait loci controlling glucosinolates, myrosinase and insect resistance in Arabidopsis thaliana. *Genetics* **161**, 325-332.

- Kliebenstein, D.J., Figuth, A., and Mitchell-Olds, T.** (2002b). Genetic architecture of plastic methyl jasmonate responses in *Arabidopsis thaliana*. *Genetics* **161**, 1685-1696.
- Kliebenstein, D.J., Rowe, H.C., and Denby, K.J.** (2005). Secondary metabolites influence *Arabidopsis/Botrytis* interactions: variation in host production and pathogen sensitivity. *Plant J.* **44**, 25-36.
- Koncz, C., and Schell, J.** (1986). The Promoter of TI-DNA Gene 5 Controls the Tissue-Specific Expression of Chimeric Genes Carried by a Novel Type of *Agrobacterium* Binary Vector. *Molecular & General Genetics* **204**, 383-396.
- Levy, M., Wang, Q.M., Kaspi, R., Parrella, M.P., and Abel, S.** (2005). *Arabidopsis* IQD1, a novel calmodulin-binding nuclear protein, stimulates glucosinolate accumulation and plant defense. *Plant J.* **43**, 79-96.
- Ljung, K., Hull, A.K., Celenza, J., Yamada, M., Estelle, M., Nonmanly, J., and Sandberg, G.** (2005). Sites and regulation of auxin biosynthesis in *Arabidopsis* roots. *Plant Cell* **17**, 1090-1104.
- Matthiessen, J.N., and Shackleton, M.A.** (2005). Biofumigation: environmental impacts on the biological activity of diverse pure and plant-derived isothiocyanates. *Pest Manag. Sci.* **61**, 1043-1051.
- Matthiessen, J.N., and Kirkegaard, J.A.** (2006). Biofumigation and enhanced biodegradation: Opportunity and challenge in soilborne pest and disease management. *Crit. Rev. Plant Sci.* **25**, 235-265.
- Mewis, I., Appel, H.M., Hom, A., Raina, R., and Schultz, J.C.** (2005). Major signaling pathways modulate *Arabidopsis* glucosinolate accumulation and response to both phloem-feeding and chewing insects. *Plant Physiology* **138**, 1149-1162.
- Mewis, I., Tokuhisa, J.G., Schultz, J.C., Appel, H.M., Ulrichs, C., and Gershenzon, J.** (2006). Gene expression and glucosinolate accumulation in *Arabidopsis thaliana* in response to generalist and specialist herbivores of different feeding guilds and the role of defense signaling pathways. *Phytochemistry* **67**, 2450-2462.
- Mikkelsen, M.D., Naur, P., and Halkier, B.A.** (2004). *Arabidopsis* mutants in the C-S lyase of glucosinolate biosynthesis establish a critical role for indole-3-acetaldoxime in auxin homeostasis. *Plant J.* **37**, 770-777.

- Mikkelsen, M.D., Hansen, C.H., Wittstock, U., and Halkier, B.A.** (2000). Cytochrome P450CYP79B2 from *Arabidopsis* catalyzes the conversion of tryptophan to indole-3-acetaldoxime, a precursor of indole glucosinolates and indole-3-acetic acid. *J. Biol. Chem.* **275**, 33712-33717.
- Moon, J., Parry, G., and Estelle, M.** (2004). The ubiquitin-proteasome pathway and plant development. *Plant Cell* **16**, 3181-3195.
- Muller, A., and Weiler, E.W.** (2000). Indolic constituents and indole-3-acetic acid biosynthesis in the wild-type and a tryptophan auxotroph mutant of *Arabidopsis thaliana*. *Planta* **211**, 855-863.
- Muller, C., Agerbirk, N., Olsen, C.E., Boeve, J.L., Schaffner, U., and Brakefield, P.M.** (2001). Sequestration of host plant glucosinolates in the defensive hemolymph of the sawfly *Athalia rosae*. *J. Chem. Ecol.* **27**, 2505-2516.
- Nafisi, M., Sønderby, I.E., Hansen, B.G., Geu-Flores, F., Nour-Eldin, H.H., Nørholm, M.H.H., Jensen, N.B., Li, J., and Halkier, B.A.** (2006). Cytochromes P450 in the biosynthesis of glucosinolates and indole alkaloids. *Phytochemistry Reviews* **5**, 331-346.
- Nair, R., and Rost, B.** (2005). Mimicking cellular sorting improves prediction of subcellular localization. *J. Mol. Biol.* **348**, 85-100.
- Naur, P., Petersen, B.L., Mikkelsen, M.D., Bak, S., Rasmussen, H., Olsen, C.E., and Halkier, B.A.** (2003). CYP83A1 and CYP83B1, two nonredundant cytochrome P450 enzymes metabolizing oximes in the biosynthesis of glucosinolates in *Arabidopsis*. *Plant Physiology* **133**, 63-72.
- Petersen, B.L., Chen, S.X., Hansen, C.H., Olsen, C.E., and Halkier, B.A.** (2002). Composition and content of glucosinolates in developing *Arabidopsis thaliana*. *Planta* **214**, 562-571.
- Piotrowski, M., Schemenewitz, A., Lopukhina, A., Muller, A., Janowitz, T., Weiler, E.W., and Oecking, C.** (2004). Desulfoglucosinolate sulfotransferases from *Arabidopsis thaliana* catalyze the final step in the biosynthesis of the glucosinolate core structure. *J. Biol. Chem.* **279**, 50717-50725.
- Pledge-Tracy, A., Sobolewski, M.D., and Davidson, N.E.** (2007). Sulforaphane induces cell type-specific apoptosis in human breast cancer cell lines. *Mol. Cancer Ther.* **6**, 1013-1021.
- Pollmann, S., Muller, A., and Weiler, E.W.** (2006). Many roads lead to "auxin": of nitrilases, synthases, and amidases. *Plant Biology* **8**, 326-333.

- Rask, L., Andreasson, E., Ekbom, B., Eriksson, S., Pontoppidan, B., and Meijer, J.** (2000). Myrosinase: gene family evolution and herbivore defense in Brassicaceae. *Plant Mol. Biol.* **42**, 93-113.
- Ratzka, A., Vogel, H., Kliebenstein, D.J., Mitchell-Olds, T., and Kroymann, J.** (2002). Disarming the mustard oil bomb. *Proc. Natl. Acad. Sci. U. S. A.* **99**, 11223-11228.
- Reichelt, M., Brown, P.D., Schneider, B., Oldham, N.J., Stauber, E., Tokuhisa, J., Kliebenstein, D.J., Mitchell-Olds, T., and Gershenzon, J.** (2002). Benzoic acid glucosinolate esters and other glucosinolates from *Arabidopsis thaliana*. *Phytochemistry* **59**, 663-671.
- Reintanz, B., Lehnen, M., Reichelt, M., Gershenzon, J., Kowalczyk, M., Sandberg, G., Godde, M., Uhl, R., and Palme, K.** (2001). Bus, a bushy *Arabidopsis* CYP79F1 knockout mutant with abolished synthesis of short-chain aliphatic glucosinolates. *Plant Cell* **13**, 351-367.
- Rosso, M.G., Li, Y., Strizhov, N., Reiss, B., Dekker, K., and Weisshaar, B.** (2003). An *Arabidopsis thaliana* T-DNA mutagenized population (GABI-Kat) for flanking sequence tag-based reverse genetics. *Plant Mol. Biol.* **53**, 247-259.
- Schellmann, S., Hulskamp, M., and Uhrig, J.** (2007). Epidermal pattern formation in the root and shoot of *Arabidopsis*. *Biochem. Soc. Trans.* **35**, 146-148.
- Schmitz, G., and Theres, K.** (2005). Shoot and inflorescence branching. *Curr. Opin. Plant Biol.* **8**, 506-511.
- Schneider, A., Kirch, T., Gigolashvili, T., Mock, H.P., Sonnewald, U., Simon, R., Flugge, U.I., and Werr, W.** (2005). A transposon-based activation-tagging population in *Arabidopsis thaliana* (TAMARA) and its application in the identification of dominant developmental and metabolic mutations. *FEBS Lett.* **579**, 4622-4628.
- Schuhegger, R., Nafisi, M., Mansourova, M., Petersen, B.L., Olsen, C.E., Svatos, A., Halkier, B.A., and Glawischnig, E.** (2006). CYP71B15 (PAD3) catalyzes the final step in camalexin biosynthesis. *Plant Physiology* **141**, 1248-1254.
- Sheen, J.** (2001). Signal transduction in maize and *Arabidopsis* mesophyll protoplasts. *Plant Physiology* **127**, 1466-1475.
- Skirycz, A., Reichelt, M., Burow, M., Birkemeyer, C., Rolcik, J., Kopka, J., Zanon, M.I., Gershenzon, J., Strnad, M., Szopa, J., Mueller-Roeber, B., and Witt, I.** (2006). DOF transcription factor AtDof1.1 (OBP2) is part of a regulatory

- network controlling glucosinolate biosynthesis in Arabidopsis. *Plant J.* **47**, 10-24.
- Smolen, G., and Bender, J.** (2002). Arabidopsis cytochrome p450 cyp83B1 mutations activate the tryptophan biosynthetic pathway. *Genetics* **160**, 323-332.
- Smolen, G.A., Pawlowski, L., Wilensky, S.E., and Bender, J.** (2002). Dominant Alleles of the basic helix-loop-helix transcription factor ATR2 activate stress-responsive genes in Arabidopsis. *Genetics* **161**, 1235-1246.
- Soellick, T.-R., and Uhrig, J.** (2001). Development of an optimized interaction-mating protocol for large-scale yeast two-hybrid analyses. *Genome Biology* **2**, research0052.0051 - research0052.0057.
- Stepanova, A.N., Hoyt, J.M., Hamilton, A.A., and Alonso, J.M.** (2005). A link between ethylene and auxin uncovered by the characterization of two root-specific ethylene-insensitive mutants in Arabidopsis. *Plant Cell* **17**, 2230-2242.
- Sterling, J.D., Atmodjo, M.A., Inwood, S.E., Kolli, V.S.K., Quigley, H.F., Hahn, M.G., and Mohnen, D.** (2006). Functional identification of an Arabidopsis pectin biosynthetic homogalacturonan galacturonosyltransferase. *Proc. Natl. Acad. Sci. U. S. A.* **103**, 5236-5241.
- Stracke, R., Werber, M., and Weisshaar, B.** (2001). The R2R3-MYB gene family in Arabidopsis thaliana. *Curr. Opin. Plant Biol.* **4**, 447-456.
- Sullivan, J.A., Shirasu, K., and Deng, X.W.** (2003). The diverse roles of ubiquitin and the 26S proteasome in the life of plants. *Nat. Rev. Genet.* **4**, 948-958.
- Surh, Y.J.** (2003). Cancer chemoprevention with dietary phytochemicals. *Nature Reviews Cancer* **3**, 768-780.
- Tantikanjana, T., Mikkelsen, M.D., Hussain, M., Halkier, B.A., and Sundaresan, V.** (2004). Functional analysis of the tandem-duplicated P450 genes SPS/BUS/CYP79F1 and CYP79F2 in glucosinolate biosynthesis and plant development by Ds transposition-generated double mutants. *Plant Physiology* **135**, 840-848.
- Thilmony, R., Underwood, W., and He, S.Y.** (2006). Genome-wide transcriptional analysis of the Arabidopsis thaliana interaction with the plant pathogen *Pseudomonas syringae* pv. tomato DC3000 and the human pathogen *Escherichia coli* O157 : H7. *Plant J.* **46**, 34-53.

- Thimm, O., Blasing, O., Gibon, Y., Nagel, A., Meyer, S., Kruger, P., Selbig, J., Muller, L.A., Rhee, S.Y., and Stitt, M.** (2004). MAPMAN: a user-driven tool to display genomics data sets onto diagrams of metabolic pathways and other biological processes. *Plant J.* **37**, 914-939.
- Tierens, K., Thomma, B.P.H., Brouwer, M., Schmidt, J., Kistner, K., Porzel, A., Mauch-Mani, B., Cammue, B.P.A., and Broekaert, W.F.** (2001). Study of the role of antimicrobial glucosinolate-derived isothiocyanates in resistance of arabidopsis to microbial pathogens. *Plant Physiology* **125**, 1688-1699.
- Toufighi, K., Brady, S.M., Austin, R., Ly, E., and Provart, N.J.** (2005). The Botany Array Resource: e-Northern, Expression Angling, and Promoter analyses. *Plant J.* **43**, 153-163.
- Tripathi, M.K., and Mishra, A.S.** (2007). Glucosinolates in animal nutrition: A review. *Anim. Feed Sci. Technol.* **132**, 1-27.
- Ulmasov, T., Murfett, J., Hagen, G., and Guilfoyle, T.J.** (1997). Aux/IAA proteins repress expression of reporter genes containing natural and highly active synthetic auxin response elements. *Plant Cell* **9**, 1963-1971.
- Ulmer, B.J., and Dossall, L.M.** (2006). Glucosinolate profile and oviposition behavior in relation to the susceptibilities of Brassicaceae to the cabbage seedpod weevil. *Entomol. Exp. Appl.* **121**, 203-213.
- van der Fits, L., Deakin, E.A., Hoge, J.H.C., and Memelink, J.** (2000). The ternary transformation system: constitutive virG on a compatible plasmid dramatically increases Agrobacterium-mediated plant transformation. *Plant Mol. Biol.* **43**, 495-502.
- Voinnet, O., Rivas, S., Mestre, P., and Baulcombe, D.** (2003). An enhanced transient expression system in plants based on suppression of gene silencing by the p19 protein of tomato bushy stunt virus. *Plant J.* **33**, 949-956.
- Walter, M., Chaban, C., Schutze, K., Batistic, O., Weckermann, K., Nake, C., Blazevic, D., Grefen, C., Schumacher, K., Oecking, C., Harter, K., and Kudla, J.** (2004). Visualization of protein interactions in living plant cells using bimolecular fluorescence complementation. *Plant J.* **40**, 428-438.
- Weigel, D., Ahn, J.H., Blazquez, M.A., Borevitz, J.O., Christensen, S.K., Fankhauser, C., Ferrandiz, C., Kardailsky, I., Malancharuvil, E.J., Neff, M.M., Nguyen, J.T., Sato, S., Wang, Z.Y., Xia, Y.J., Dixon, R.A., Harrison,**

- M.J., Lamb, C.J., Yanofsky, M.F., and Chory, J.** (2000). Activation tagging in Arabidopsis. *Plant Physiology* **122**, 1003-1013.
- Winkel-Shirley, B.** (2002). Biosynthesis of flavonoids and effects of stress. *Curr. Opin. Plant Biol.* **5**, 218-223.
- Wittstock, U., and Halkier, B.A.** (2002). Glucosinolate research in the Arabidopsis era. *Trends Plant Sci.* **7**, 263-270.
- Wittstock, U., Agerbirk, N., Stauber, E.J., Olsen, C.E., Hippler, M., Mitchell-Olds, T., Gershenson, J., and Vogel, H.** (2004). Successful herbivore attack due to metabolic diversion of a plant chemical defense. *Proc. Natl. Acad. Sci. U. S. A.* **101**, 4859-4864.
- Woodward, A.W., and Bartel, B.** (2005). Auxin: Regulation, action, and interaction. *Annals of Botany* **95**, 707-735.
- Zhang, Z.Y., Ober, J.A., and Kliebenstein, D.J.** (2006). The gene controlling the quantitative trait locus EPITHIOSPECIFIER MODIFIER1 alters glucosinolate hydrolysis and insect resistance in Arabidopsis. *Plant Cell* **18**, 1524-1536.
- Zhao, Y.D., Hull, A.K., Gupta, N.R., Goss, K.A., Alonso, J., Ecker, J.R., Normanly, J., Chory, J., and Celenza, J.L.** (2002). Trp-dependent auxin biosynthesis in Arabidopsis: involvement of cytochrome P450s CYP79B2 and CYP79B3. *Genes Dev.* **16**, 3100-3112.
- Zimmermann, I.** (2003). Systematische Untersuchungen von Proteininteraktionen der MYB und bHLH Transkriptionsfaktoren aus Arabidopsis thaliana. In Max-Planck-Institute for Plant Breeding Research (Cologne: University of Cologne).
- Zimmermann, I.M., Heim, M.A., Weisshaar, B., and Uhrig, J.F.** (2004a). Comprehensive identification of Arabidopsis thaliana MYB transcription factors interacting with R/B-like BHLH proteins. *Plant J.* **40**, 22-34.
- Zimmermann, P., Hirsch-Hoffmann, M., Hennig, L., and Grissem, W.** (2004b). GENEVESTIGATOR. Arabidopsis microarray database and analysis toolbox. *Plant Physiology* **136**, 2621-2632.

Appendix

Table S1: Primers used for RT-PCR analyses

Primer name	AGI code	Genename	Sequence 5' to 3'	Tm	Cycle #
At1g18570 Fw	At1g18570	HIG1/MYB51	GTGTTGCAAAGCTGAACTAGGGTT	61	30
At1g18570 Rv	At1g18570	HIG1/MYB51	TTGTTAACGGAGGAATCAGAGAAC	59,3	30
Actin Ig F	At3g18780	Actin2	TAACCTCTCCCGCTATGTATGTTCGC	62,7	23
Actin Ig R	At3g18780	Actin2	CCACTGAGCACAAATGTTACCGTAC	62,7	23
DHS1 Fw	At4g39980	DHS1	TGGGTCTGCGATCCAATGC	59,5	26
DHS1 Rv	At4g39980	DHS1	CTCTTCTGAGCCGTTCTGC	62,5	26
At5g05730 for	At5g05730	ASA1	GCAACGATGTTGGAAGGTT	55,3	28
At5g05730 rev	At5g05730	ASA1	GCTTTGTTCTGGCACTCACA	57,3	28
At5g54810 for	At5g54810	TSB1	CACGCTGTGATTGGTAAAGAAA	56,5	26
At5g54810 rev	At5g54810	TSB1	GCTTCTCGAGGTAAGCTAGTGC	62,1	26
At4g39950 for	At4g39950	CYP79B2	GAATCAAGTGCATTATGGACA	56,5	30
At4g39950 rev	At4g39950	CYP79B2	ACTGAACGAGATAAACCGGAGA	58,4	30
At2g22330 for	At2g22330	CYP79B3	TTAGGCTTTACGTTTTCGTTTT	54,7	28
At2g22330 rev	At2g22330	CYP79B3	GCTAAGTGGATCAGACCAAACC	60,3	28
At4g31500 for	At4g31500	CYP83B1	CCATCAAATTCACCTCACGAAAA	54,7	28
At4g31500 rev	At4g31500	CYP83B1	CCAGTCATGACGTCCATCTTTA	58,4	28
C-S Lyase FW	At2g20610	C-S lyase	GTTGATTTGGTGTGTGATAGGCTC	63,5	24
C-S Lyase RV	At2g20610	C-S lyase	TTTCTGTCTGTCTTCTTGGCAT	64,1	24
At1g24100 F	At1g24100	UGT74B1	ATCCTGAGCATGGCAGAGTT	58,4	26
At1g24100 R	At1g24100	UGT74B1	GATCACTCCACTGAGGCACA	60,5	26
AtST5a Fw	At1g74100	AtST5a	ATGTCTCCTCGAAGGTCTTTTTCA	61,8	26
AtST5a Rv	At1g74100	AtST5a	CACAATCGAATCGGGTAATAACC	61,1	26
At1g16410 for	At1g16410	CYP79F1	TCACCCAAAGTGCTCATTATGTC	58,4	28
At1g16410 rev	At1g16410	CYP79F1	CAGAGAAAGAAACAAGGCGGTT	56,5	28
At1g16400 for	At1g16400	CYP79F2	GAAAAGCTCTGAAGGAGTTGGA	58,4	32
At1g16400 rev	At1g16400	CYP79F2	CGGGCAATGGATAGTCTAAAAA	56,5	32
At4g13770 for	At4g13770	CYP83A1	AGAACAACCTTTCGCTTCTGAG	58,4	28
At4g13770 rev	At4g13770	CYP83A1	GACTTGTGCATAGCAAGACCAG	60,3	28

Table S2: Primers used for Gateway® cloning

1. Generation of CDS entry clones

Primer name	AGI code	Genename	Sequence 5' to 3'
GW-At1g18570 Fv	At1g18570	HIG1/MYB51	CACCATGGTGCGGACACCGTGTTGCAA
GW-At1g18570 Rv	At1g18570	HIG1/MYB51	TCCAAAATAGTTATCAATTTTCGTC
GW-MYB122 Fw	At1g74080	MYB122	CACCATGGTACGGACGCGGTGTTGTA
GW-MYB122 Rv	At1g74080	MYB122	TCCAAAATAATTGTCAATCCCTTCACAG
GW-bHLH5-fw	At5g46760	ATR2/bHLH05	CACCATGAACGGCACAACATCATCAATC
GW-bHLH5-rv	At5g46760	ATR2/bHLH05	ATAGTTTTCTCCGACTTTTCGTCATCAAAG

2. Generation of promoter entry clones

Primer name	AGI code	Genename	Sequence 5' to 3'
GW-pAt1g18570 Fw	At1g18570	HIG1/MYB51	CACCTTGATGTAAACCAAGCTGGTTAGC
GW-pAt1g18570 Rv	At1g18570	HIG1/MYB51	TTCTTCGTCTTCAGTGAATCTCCTC
prombHLH05 F1	At5g46760	ATR2/bHLH05	CACCTGGAAGCAGACAGACG
prombHLH05 R1	At5g46760	ATR2/bHLH05	AACATACGCCGGTTGAAAAG
GW-pDsh1 Fw	At4g39980	DHS1	CACC GGTGGCTATAATTTGCGAAAAC
GW-pDsh1 Rv	At4g39980	DHS1	CCTAGCTTCTCCGGCGAACAC
GW-pASA1 Fw	At5g05730	ASA1	CACCGTGAATCATATCATTACACCGCA
GW-pASA1 Rv	At5g05730	ASA1	ATTCTACGAGATGTGGCATATTTATAAA
GW-pTSB1 Fw	At5g54810	TSB1	CAACATCCTTTGACTTTCCCCCATAC
GW-pTSB1 Rv	At5g54810	TSB1	GGAGCGAGACGATGGCA
GW-pCYP79B2 Fw	At4g39950	CYP79B2	CACCATTTTAAATTTTCGATCATGCG
GW-pCYP79B2 Rv	At4g39950	CYP79B2	GAGGAGATACAAGGTGCTAAAGGA
GW-pCYP79B3 Fv	At2g22330	CYP79B3	CACCGCTCCATCAAAGAGTTTTTACA T
GW-pCYP79B3 Rv	At2g22330	CYP79B3	GAGGAGATACATGTTGGTAAAGG
GW-pCYP83B1 Fw	At4g31500	CYP83B1	CACCGAGGAAGATTTGACAGAAAAC
GW-pCYP83B1 Rv	At4g31500	CYP83B1	ACCGGCTATAATCAATAAGAGATCC
GW-pAtST5a Fw	At1g74100	AtST5a	CACCGCAACTTTGTTTATCTCTCTGGGTTG
GW-pAtST5a Rv	At1g74100	AtST5a	GTATTGGGTTAAGATCTCATCTGGT

3. Primers used for sequencing

Primer name	plasmids	Sequence 5' to 3'
M13 F	pENTR/Gateway®	GTAAACGACGGCCAG
M13 R	pENTR/Gateway®	CAGGAAACAGCTATGAC
pDONR201/7 fw	pDONR/Gateway®	TCGCGTTAACGCTAGCATGCATCTC
pDONR201/7 rv	pDONR/Gateway®	GTAACATCAGAGATTTTGGAGACAC
uidA rev	pGWB3 binary vector	GATCAGCGTTGGTGGGAAAGC
35S forw	pGWB2 binary vector	GCAAGACCCTTCTCTATATAAG

4. Primers used to amplify the intron of pPCVGNF-Hyg cloned into pGWB3i

Primer name	Sequence 5' to 3'
GUS intron F1	Pho GTAAGTTTCTGCTTCTACCTTTG
GUS intron R1	Pho CTGCACATCAACAAATTTGGTC

Table S3: Primers used for the yeast-two-hybrid screen

Primer name	Purpose	Sequence 5' to 3'
GW-At1g18570 Fw	bait construct A-D	CACCATGGTGCGGACACCGTGTTGCAA
MYB51 363 rev	bait construct A	AATACCTTTCTTGATCAAACG
MYB51 552 rev	bait construct B	CTTTCCGAACCTATTAGCTACTTG
MYB51 783 rev	bait construct C	AGAACACGTCAGATTAACGTTACC
GW-At1g18570 Rv	bait construct D	TCCAAAATAGTTATCAATTTTCGTC
AD 5N	colony PCR of prey clones	GGAGTTTAATACCACACAATGGATGATG
BD 3N	colony PCR of prey clones	GAAAGCAACCTGACCTACAGGAAAGAG
5GAD	sequencing of PCR products	CAAACCCAAAAAAGAGATC
3GAD	sequencing of PCR products	GTTTTTCAGTATCTACGATTC
MK bait 5	sequencing of bait constructs	TAAGTGGGACATCATCATCGG

Table S4: Genes with significant up/downregulation by *HIG1/MYB51* induction

AGI code	description	log ratio
At1g18570	myb family transcription factor	1.61
At3g14900	hypothetical protein	1.37
At3g28510	hypothetical protein	1.21
At3g17790	acid phosphatase type 5	1.10
At3g44990	xyloglucan endotransglycosylase, putative	1.04
At3g11340	glucosyl transferase, putative	1.00
At5g49480	NaCl-inducible Ca ²⁺ -binding protein-like; calmodulin-like	0.92
At2g05380	expressed protein	0.91
At1g14880	unknown protein	0.91
At1g17170	glutathione transferase, putative	0.85
At4g25630	fibrillarin 2 (AtFib2)	0.80
At3g13310	DnaJ protein, putative	0.79
At1g33960	AIG1	0.77
At5g05250	expressed protein	0.77
At4g38620	putative transcription factor (MYB4)	0.76
At1g01520	myb family transcription factor	0.76
At3g26830	cytochrome p450 family	0.75
At5g09440	putative protein	0.74
At4g01870	hypothetical protein	0.72
At4g34131	similar to glucosyltransferase -like protein	0.71
At2g32960	unknown protein	0.70
At3g44300	nitrilase 2	0.68
At2g04450	putative mutT domain protein	0.67
At1g57630	disease resistance protein (TIR class), putative	0.67
At2g29460	glutathione transferase, putative	0.67
At2g29420	glutathione transferase, putative	0.67
At1g26790	Dof zinc finger protein	0.66
At1g07400	heat shock protein, putative	0.66
At4g21930	putative protein	0.66
At3g21150	CONSTANS B-box zinc finger family protein	0.65
At1g55850	cellulose synthase catalytic subunit, putative	0.64
At5g51440	mitochondrial heat shock 22 kd protein-like	0.63
At1g77450	GRAB1-like protein	0.62
At3g24500	ethylene-responsive transcriptional coactivator, putative	0.62
At1g56430	nicotianamine synthase, putative	0.62
At5g61020	putative protein	0.62
At1g13340	hypothetical protein	0.62
At3g09270	glutathione transferase, putative	0.62
At2g38860	expressed protein	0.61
At3g57150	putative protein	0.61
At5g55915	nucleolar protein-like	0.61
At5g11590	transcription factor TINY, putative	0.61
At3g22660	unknown protein	0.6
At3g21890	CONSTANS B-box zinc finger family protein	0.6
At3g56070	peptidylprolyl isomerase	0.59
At2g29490	glutathione transferase, putative	0.59
At4g38100	expressed protein	0.59
At2g44120	60S ribosomal protein L7	0.59
At3g04710	ankyrin-like protein	0.58
At1g02450	unknown protein	0.58
At3g59750	receptor lectin kinase-like protein	0.58

Table S4: continued

AGI code	description	log ratio
At4g13180	short-chain alcohol dehydrogenase like protein	0.58
At5g63790	putative protein	0.57
At4g15550	glucosyltransferase like protein	0.57
At5g03800	putative protein	0.57
At1g61800	glucose-6-phosphate/phosphate-translocator precursor, putative	0.57
At1g69530	expansin (At-EXP1)	0.57
At2g18660	hypothetical protein	0.56
At5g42760	putative protein	0.56
At1g48570	hypothetical protein	0.56
At4g31790	methyltransferase - like protein	0.56
At1g79160	hypothetical protein	0.55
At3g07050	putative GTPase	0.55
At5g40610	dihydroxyacetone 3-phosphate reductase (dhaprd)	0.55
At3g18950	hypothetical protein	0.55
At1g48630	guanine nucleotide-binding protein, putative	0.55
At1g01720	NAC domain protein, putative	0.55
At1g15100	putative RING-H2 zinc finger protein	0.54
At3g09440	heat-shock protein (At-hsc70-3)	0.54
At1g01680	hypothetical protein	0.54
At2g02930	glutathione transferase, putative	0.54
At1g05560	UDP-glucose transferase(UGT1)	0.54
At5g65860	putative protein	0.54
At3g30460	RING zinc finger protein	0.54
At1g52930	expressed protein	0.54
At5g22100	similar to Probable RNA 3-terminal phosphate cyclase-like protein.	0.53
At5g54130	putative protein	0.53
At5g52830	WRKY family transcription factor	0.53
At5g59850	cytoplasmic ribosomal protein S15a - like	0.52
At2g15020	hypothetical protein	0.52
At2g27840	unknown protein	0.52
At5g56030	HEAT SHOCK PROTEIN 81-2 (HSP81-2) (sp P55737)	0.52
At3g47480	putative calcium-binding protein	0.52
At3g12580	heat shock protein 70	0.51
At5g08180	nhp2-like protein	0.51
At4g38210	expansin, putative	0.51
At4g35180	amino acid permease - like protein	0.51
At5g21940	unknown protein	0.51
At3g44750	putative histone deacetylase	0.51
At5g19300	putative protein	0.51
At2g16720	myb DNA-binding protein	0.5
At2g37190	60S ribosomal protein L12	0.5
At1g80750	ribosomal protein L7, putative	0.5
At5g60670	60S ribosomal protein L12 - like	0.5
At1g31660	bystin, putative	0.5
At3g13230	expressed protein	0.5
At1g25260	expressed protein	0.5
At3g57490	40S ribosomal protein S2 (RPS2D)	0.49
At4g12400	stress-induced protein sti1 -like protein	0.49
At5g56080	nicotianamine synthase, putative	0.49
At5g54120	unknown protein	0.49
At3g16780	putative ribosomal protein	0.49

Table S4: continued

AGI code	description	log ratio
At3g15990	putative sulfate transporter	0.48
At3g58660	putative protein	0.48
At4g39670	putative protein	0.48
At1g74310	heat shock protein 101 (HSP101)	0.48
At2g37270	40S ribosomal protein S5	0.48
At2g40700	DEAD/DEAH box RNA helicase protein, putative	0.48
At5g57280	protein carboxyl methylase-like	0.48
At5g22440	60S ribosomal protein L10A	0.48
At1g49600	RNA binding protein 47 (RBP47), putative	0.48
At4g24780	polysaccharide lyase family 1 (pectate lyase)	0.48
At2g20450	60S ribosomal protein L14	0.48
At3g61890	homeobox-leucine zipper protein ATHB-12	0.48
At2g33370	60S ribosomal protein L23	0.48
At5g61770	Peter Pan - like protein	0.48
At5g04950	nicotianamine synthase, putative	0.47
At4g23150	serine/threonine kinase - like protein	0.47
At4g30800	ribosomal protein S11 - like	0.47
At1g02920	glutathione transferase, putative	0.47
At1g18850	expressed protein	0.47
At3g28900	60S ribosomal protein L34, putative	0.47
At3g09350	expressed protein	0.47
At2g28600	putative ATP-dependent RNA helicase	0.47
At1g09180	putative GTP-binding protein, SAR1B	0.47
At1g65030	G-protein beta-subunit (transducin) family	0.47
At2g32220	60S ribosomal protein L27	0.47
At3g27060	ribonucleotide reductase small subunit, putative	0.47
At1g26770	expansin, putative	0.47
At1g48100	polygalacturonase, putative	0.47
At3g60360	putative protein	0.47
At2g20560	putative heat shock protein	0.46
At3g07860	unknown protein	0.46
At1g23280	mak16-like protein-related	0.46
At2g29350	putative tropinone reductase	0.46
At3g19030	expressed protein	0.46
At4g34138	similar to glucosyltransferase -like protein	0.46
At5g09530	surface protein PspC-related	0.46
At1g80130	expressed protein	0.46
At3g18130	protein kinase C-receptor/G-protein, putative	0.46
At1g12960	60S ribosomal protein L27a, putative	0.46
At4g31700	ribosomal protein S6 - like	0.46
At2g34260	G-protein beta-subunit (transducin) family	0.45
At1g75670	expressed protein	0.45
At3g23620	expressed protein	0.45
At2g32060	40S ribosomal protein S12	0.45
At5g04340	putative c2h2 zinc finger transcription factor	0.45
At3g02040	expressed protein	0.45
At3g07110	putative 60S ribosomal protein L13A	0.45
At1g04480	putative putative 60S ribosomal protein L17	0.45
At3g06530	hypothetical protein	0.45
At2g37770	aldo/keto reductase family	0.45
At3g53430	60S RIBOSOMAL PROTEIN L12 -like	0.44

Table S4: continued

AGI code	description	log ratio
At2g27395	putative cysteine proteinase	0.44
At3g54420	glycosyl hydrolase family 19 (class IV chitinase)	0.44
At2g31230	ethylene response factor, putative	0.44
At3g07750	putative 3 exoribonuclease	0.44
At1g29320	hypothetical protein	0.44
At1g63780	putative U3 small nucleolar ribonucleoprotein protein	0.44
At2g27420	cysteine proteinase	0.44
At5g20160	ribosomal protein L7Ae-like	0.44
At4g26780	grpE like protein	0.44
At5g39850	40S ribosomal protein S9-like	0.44
At5g27850	60S ribosomal protein - like	0.44
At1g72680	putative cinnamyl-alcohol dehydrogenase	0.44
At5g10930	serine/threonine protein kinase -like protein	0.43
At1g02460	polygalacturonase, putative	0.43
At4g27380	expressed protein	0.43
At4g10500	2-oxoglutarate-dependent dioxygenase family	0.43
At4g12600	Ribosomal protein L7Ae -like	0.43
At1g78080	AP2 domain protein RAP2.4	0.43
At5g52640	heat-shock protein	0.43
At3g49340	cysteine protease	0.43
At5g10360	40S ribosomal protein S6	0.43
At2g43570	glycosyl hydrolase family 19 (chitinase)	0.43
At3g16810	expressed protein	0.43
At2g45440	putative dihydrodipicolinate synthase	0.43
At3g17170	expressed protein	0.43
At1g26470	expressed protein	0.43
At5g61030	glycine-rich RNA-binding protein	0.43
At5g41040	N-hydroxycinnamoyl/benzoyltransferase-like protein	0.43
At1g61570	expressed protein	0.43
At1g70600	60S ribosomal protein L27A	0.43
At3g22970	unknown protein	0.42
At3g46080	zinc finger -like protein	0.42
At3g05590	putative 60S ribosomal protein L18	0.42
At5g02050	putative protein	0.42
At5g16130	40S ribosomal protein S7-like	0.42
At3g13940	unknown protein	0.42
At5g02450	60S ribosomal protein - like	0.42
At2g37600	60S ribosomal protein L36	0.42
At4g10450	putative ribosomal protein L9, cytosolic	0.42
At1g15250	putative 60s ribosomal protein L37	0.42
At3g01820	putative adenylate kinase	0.42
At2g36630	unknown protein	0.42
At5g25890	putative protein	0.41
At3g58700	ribosomal protein L11 -like	0.41
At5g38720	putative protein	0.41
At5g08620	DEAD/DEAH box RNA helicase, putative	0.41
At5g61170	40S ribosomal protein S19 - like	0.41
At3g62870	60S RIBOSOMAL PROTEIN L7A protein	0.41
At3g16050	putative ethylene-inducible protein	0.41
At5g56950	nucleosome assembly protein	0.41
At3g23830	glycine-rich RNA-binding protein	0.41

Table S4: continued

AGI code	description	log ratio
At4g11890	protein kinase - like protein	0.41
At5g22880	histone H2B like protein (emb CAA69025.1)	0.41
At2g01290	putative ribose 5-phosphate isomerase	0.41
At5g48760	60S ribosomal protein L13a	0.41
At1g78380	glutathione transferase, putative	0.41
At1g03360	hypothetical protein	0.41
At2g46790	expressed protein	0.41
At1g26910	putative 60s ribosomal protein L10	0.41
At1g31630	MADS-box protein	0.41
At3g14990	4-methyl-5(b-hydroxyethyl)-thiazole monophosphate biosyn. protein, putative	0.41
At3g03450	RGA1-like protein	0.41
At5g22650	histone deacetylase-like protein	0.41
At2g27530	60S ribosomal protein L10A	0.41
At4g37370	cytochrome p450 family	0.4
At1g61870	expressed protein	0.4
At5g12110	elongation factor 1B alpha-subunit (emb CAB64729.1)	0.4
At5g40770	prohibitin (gb AAC49691.1)	0.4
At2g17630	putative phosphoserine aminotransferase	0.4
At3g51870	putative carrier protein	0.4
At5g15550	G-protein beta family	0.4
At3g05060	putative SAR DNA-binding protein-1	0.4
At4g16720	ribosomal protein	0.4
At2g39390	60S ribosomal protein L35	0.4
At3g10530	hypothetical protein	0.4
At2g36620	60S ribosomal protein L24	0.4
At5g09590	heat shock protein 70 (Hsc70-5)	0.4
At5g48330	regulator of chromosome condensation (cell cycle regulatory protein) like	0.4
At3g47370	40S ribosomal protein S20-like protein	0.4
At1g33120	ribosomal protein L9, putative	0.4
At3g53460	29 kDa ribonucleoprotein, chloroplast precursor (RNA-binding protein cp29)	0.4
At5g65360	histone H3 (sp P05203)	0.4
At2g47990	unknown protein	0.4
At1g08250	expressed protein	0.4
At2g40360	putative WD-40 repeat protein	0.4
At1g55920	serine acetyltransferase	0.4
At3g49910	60S RIBOSOMAL PROTEIN - like	0.4
At5g23310	iron superoxide dismutase (FSD3)	0.4
At1g15440	hypothetical protein	0.39
At4g02520	glutathione transferase, putative	0.39
At5g08400	putative protein	0.39
At5g20630	germin-like protein	0.39
At2g31160	expressed protein	0.39
At4g03450	hypothetical protein	0.39
At3g60245	Expressed protein	0.39
At5g54840	SGP1 monomeric G-protein (emb CAB54517.1)	0.39
At1g26880	60s ribosomal protein L34	0.39
At3g47420	putative protein	0.39
At5g66540	expressed protein	0.39
At1g22780	putative 40S ribosomal protein S18	0.39
At4g15000	ribosomal protein	0.39
At5g51570	putative protein	0.39

Table S4: continued

AGI code	description	log ratio
At5g25460	putative protein	0.38
At2g33210	mitochondrial chaperonin (HSP60)	0.38
At2g21560	unknown protein	0.38
At4g05410	U3 snoRNP-associated-related	0.38
At2g19730	putative ribosomal protein L28	0.38
At1g61580	ribosomal protein	0.38
At1g58983	40S ribosomal protein S2, putative	0.38
At4g39780	AP2 domain transcription factor RAP2, putative	0.38
At2g26150	putative heat shock transcription factor	0.38
At1g14320	tumor suppressor, putative	0.38
At5g01340	mitochondrial carrier protein family	0.38
At5g58770	dehydrololichyl diphosphate synthase (DEDOL-PP synthase), putative	0.38
At1g57660	60S ribosomal protein L21, putative	0.38
At5g20290	putative protein	0.38
At4g10480	putative alpha NAC	0.38
At5g19750	putative protein	0.38
At3g49010	60S ribosomal protein L13, BBC1 protein	0.38
At1g08360	60S ribosomal protein L10A, putative	0.38
At2g41840	40S ribosomal protein S2 (RPS2C)	0.38
At5g15750	ribosomal protein-like	0.38
At5g04800	40S ribosomal protein S17 -like	0.38
At2g01250	putative ribosomal protein L7	0.38
At1g07070	ribosomal protein, putative	0.38
At1g43910	unknown protein	0.38
At4g16630	DEAD/DEAH box RNA helicase, putative	0.38
At1g57860	60S ribosomal protein L21, putative	0.38
At1g58684	similar to ribosomal protein S2, putative	0.37
At2g34480	60S ribosomal protein L18A	0.37
At4g17390	60S ribosomal protein L15 homolog	0.37
At5g56010	heat shock protein 90	0.37
At4g27490	putative protein	0.37
At1g14050	Expressed protein	0.37
At3g04770	40S ribosomal protein SA (RPSaB)	0.37
At5g64000	3(2),5-bisphosphate nucleotidase (emb CAB05889.1)	0.37
At3g25520	ribosomal protein, putative	0.37
At5g37960	putative protein	0.37
At3g04840	putative 40S ribosomal protein S3A (S phase specific)	0.37
At1g51060	histone H2A, putative	0.37
At1g23100	10kDa chaperonin (CPN10), putative	0.37
At5g14520	pescadillo - like protein	0.37
At5g17760	BCS1 - like protein	0.37
At2g19310	putative small heat shock protein	0.37
At5g09510	ribosomal protein S15-like	0.37
At1g48920	nucleolin, putative	0.37
At3g22910	potential calcium-transporting ATPase 13	0.37
At1g74560	putative SET protein, phosphatase 2A inhibitor	0.37
At2g44860	60S ribosomal protein L30	0.36
At5g52810	putative protein	0.36
At5g03230	putative protein	0.36
At1g33390	RNA helicase, putative	0.36
At4g25730	putative protein	0.36

Table S4: continued

AGI code	description	log ratio
At3g57000	putative protein	0.36
At5g27990	putative protein	0.36
At2g18690	expressed protein	0.36
At3g03920	putative GAR1 protein	0.36
At3g22230	ribosomal protein L27, putative	0.36
At2g42740	60S ribosomal protein L11B	0.36
At5g56710	60S ribosomal protein L31	0.36
At1g54690	histone H2A, putative	0.36
At3g60770	ribosomal protein S13 -like	0.36
At5g52470	fibrillarin 1 AtFib1/SKIP7	0.36
At2g46210	delta-8 sphingolipid desaturase, putative	0.36
At1g27470	hypothetical protein	0.36
At4g36130	putative ribosomal protein L8	0.36
At1g60640	hypothetical protein	0.36
At1g45160	hypothetical protein	0.36
At4g02380	late embryogenesis abundant protein-related	0.36
At1g15425	expressed protein	0.36
At1g34030	ribosomal protein S18, putative	0.36
At5g50200	putative protein	0.36
At4g37090	expressed protein	0.36
At4g31500	cytochrome p450 family	0.35
At3g24520	heat shock transcription factor HSF1, putative	0.35
At3g09200	putative 60S acidic ribosomal protein P0	0.35
At4g37610	putative protein	0.35
At1g66580	60S ribosomal protein L10, putative	0.35
At5g40130	60S RIBOSOMAL PROTEIN L5 -like	0.35
At4g22530	putative protein	0.35
At3g13150	hypothetical protein	0.35
At3g23990	mitochondrial chaperonin hsp60	0.35
At1g08570	putative thioredoxin	0.35
At5g13170	senescence-associated protein (SAG29)	0.35
At4g32290	putative protein	0.35
At1g67430	ribosomal protein, putative	0.35
At5g67510	60S ribosomal protein L26	0.35
At5g08610	DEAD/DEAH box RNA helicase, putative	0.35
At2g21790	putative ribonucleoside-diphosphate reductase large subunit	0.35
At2g19640	putative SET-domain transcriptional regulator	0.35
At1g69200	fructokinase (Frk1), putative	0.35
At3g55010	phosphoribosylformylglycinamide cyclo-ligase precursor	0.34
At3g23000	SNF1 related protein kinase (ATSRPK1)	0.34
At5g59870	histone H2A - like protein	0.34
At1g74100	putative flavonol sulfotransferase	0.34
At4g32720	RRM-containing protein	0.34
At5g60790	ABC transporter family protein	0.34
At2g37640	expansin, putative	0.34
At1g74890	response regulator 7, putative	0.34
At1g22400	UDP-glucose glucosyltransferase, putative	0.34
At5g03690	fructose-bisphosphate aldolase -like protein	0.34
At5g54470	CONSTANS B-box zinc finger family protein	0.34
At5g15950	S-adenosylmethionine decarboxylase (adoMetDC2)	0.34
At3g16080	putative ribosomal protein	0.34

Table S4: continued

AGI code	description	log ratio
At3g25890	AP2 domain transcription factor, putative	0.34
At3g48930	cytosolic ribosomal protein S11	0.34
At5g14050	putative protein	0.34
At1g78190	unknown protein	0.34
At5g16970	quinone oxidoreductase -like protein	0.34
At5g22320	expressed protein	0.34
At3g60440	putative protein	0.34
At1g07930	elongation factor 1-alpha (EF-1-alpha)	0.34
At5g02870	60S ribosomal protein - like	0.34
At2g20690	putative riboflavin synthase alpha chain	0.34
At5g17600	RING-H2 zinc finger protein-like	0.34
At3g20000	membrane import protein, putative	0.33
At1g80270	hypothetical protein	0.33
At1g27050	homeobox RRM-containing protein	0.33
At3g17465	ribosomal protein L3	0.33
At3g16770	AP2 domain protein RAP2.3	0.33
At3g13790	glycosyl hydrolase family 32	0.33
At3g52380	chloroplast RNA-binding protein cp33	0.33
At5g12910	histone H3 -like protein	0.33
At1g18800	expressed protein	0.33
At2g21580	40S ribosomal protein S25	0.33
At2g25000	WRKY family transcription factor	0.33
At5g62440	putative protein	0.33
At5g52380	putative protein	0.33
At3g27180	hypothetical protein	0.33
At1g08580	hypothetical protein	0.33
At2g19670	putative arginine N-methyltransferase	0.33
At2g29760	hypothetical protein	0.33
At4g02230	putative ribosomal protein L19	0.32
At4g13850	glycine-rich RNA-binding protein AtGRP2	0.32
At3g09630	putative 60S ribosomal protein L1	0.32
At3g17610	bZIP family transcription factor	0.32
At1g32900	starch synthase, putative	0.32
At1g24100	UDP-glycosyltransferase family	0.32
At5g61820	putative protein	0.32
At5g27770	60S ribosomal protein L22 - like	0.32
At5g55580	putative protein	0.32
At1g15930	40S ribosomal protein S12, putative	0.32
At2g36530	enolase (2-phospho-D-glycerate hydrolyase)	0.32
At1g10490	unknown protein	0.32
At4g37990	cinnamyl-alcohol dehydrogenase ELI3-2	0.32
At3g52060	putative protein	0.32
At3g10610	putative 40S ribosomal protein S17	0.32
At4g26230	putative ribosomal protein	0.32
At4g34740	amidophosphoribosyltransferase 2 precursor	0.32
At2g04400	putative indole-3-glycerol phosphate synthase	0.32
At4g34200	Phosphoglycerate dehydrogenase - like protein	0.32
At5g28540	luminal binding protein	0.32
At1g07350	transformer serine/arginine-rich ribonucleoprotein, putative	0.32
At5g14040	mitochondrial phosphate translocator	0.32
At4g02930	mitochondrial elongation factor Tu	0.32

Table S4: continued

AGI code	description	log ratio
At2g23380	curly leaf protein (polycomb-group)	0.32
At5g02960	putative protein	0.32
At1g62380	1-aminocyclopropane-1-carboxylate oxidase (ACC oxidase), putative	0.32
At1g25083	F5A9.7	0.31
At5g02500	dnaK-type molecular chaperone hsc70.1	0.31
At4g24230	putative protein	0.31
At1g08410	unknown protein	0.31
At5g24840	methyltransferase-like protein	0.31
At2g04430	putative mutT domain protein	0.31
At1g09080	putative luminal binding protein	0.31
At3g27280	prohibitin, putative	0.31
At2g45030	mitochondrial elongation factor, putative	0.31
At3g02080	putative 40S ribosomal protein S19	0.31
At1g60730	auxin-induced protein, putative	0.31
At1g04360	hypothetical protein	0.31
At4g23570	phosphatase like protein	0.3
At3g51800	putative nuclear DNA-binding protein G2p	0.3
At1g79410	hypothetical protein	0.3
At5g19600	putative protein	0.3
At5g65010	asparagine synthetase (gb AAC72837.1)	0.3
At2g47060	putative protein kinase	-0.3
At4g20260	endomembrane-associated protein	-0.31
At5g01710	putative protein	-0.31
At5g57660	CONSTANS-like B-box zinc finger protein-like	-0.31
At2g01450	putative MAP kinase	-0.31
At1g63800	E2, ubiquitin-conjugating enzyme 5 (UBC5)	-0.31
At1g12710	hypothetical protein	-0.31
At4g37470	putative protein	-0.31
At2g23130	arabinogalactan-protein (AGP17)	-0.31
At3g19970	expressed protein	-0.31
At3g45730	putative protein	-0.31
At5g27520	mitochondrial carrier protein family	-0.31
At2g45170	putative microtubule-associated protein	-0.32
At5g25610	dehydration-induced protein RD22	-0.32
At3g28300	At14a	-0.32
At4g21570	putative protein	-0.32
At1g06540	hypothetical protein	-0.32
At5g42200	putative protein	-0.32
At4g03210	xyloglucan endotransglycosylase, putative	-0.32
At3g53800	putative protein	-0.32
At1g52290	protein kinase, putative	-0.32
At5g45280	pectinacetyltransferase, putative	-0.32
At2g32090	expressed protein	-0.33
At1g35612	hypothetical protein	-0.33
At3g57450	putative protein	-0.33
At1g13210	potential phospholipid-transporting ATPase 11	-0.33
At1g21500	expressed protein	-0.33
At5g04040	expressed protein	-0.33
At2g44840	putative ethylene response element binding protein (EREBP)	-0.33
At3g28290	At14a	-0.33
At1g26920	expressed protein	-0.33

Table S4: continued

AGI code	description	log ratio
At4g23590	tyrosine transaminase like protein	-0.33
At3g57530	calcium-dependent protein kinase	-0.33
At4g30660	stress responsive protein homolog	-0.33
At3g50650	scarecrow-like 7 (SCL7)	-0.33
At5g10750	putative protein	-0.34
At5g40340	PWWP domain protein	-0.34
At4g24380	putative protein	-0.34
At1g53580	glyoxalase II, putative (hydroxyacylglutathione hydrolase)	-0.34
At4g29310	putative protein	-0.34
At3g05490	expressed protein	-0.34
At5g11740	arabinogalactan-protein (AGP15)	-0.34
At2g46140	putative desiccation related protein	-0.34
At1g33970	expressed protein	-0.34
At1g54100	aldehyde dehydrogenase homolog, putative	-0.34
At3g53990	expressed protein	-0.34
At4g13830	DnaJ-like protein	-0.34
At4g08930	putative protein disulfide isomerase	-0.35
At5g57800	lipid transfer protein; glossy1 homolog	-0.35
At1g61670	hypothetical protein	-0.35
At4g29780	expressed protein	-0.35
At1g76600	expressed protein	-0.35
At5g24420	6-phosphogluconolactonase-like protein	-0.35
At2g32800	putative protein kinase	-0.36
At5g23280	unknown protein	-0.36
At4g12730	fasciclin-like arabinogalactan-protein (FLA2)	-0.36
At5g24590	NAC2-like protein	-0.36
At2g39800	delta-1-pyrroline 5-carboxylase synthetase (P5C1)	-0.36
At3g23750	receptor-like kinase, putative	-0.36
At5g08330	putative protein	-0.36
At1g55330	arabinogalactan-protein (AGP21)	-0.36
At1g11380	expressed protein	-0.36
At2g39180	putative protein kinase	-0.36
At4g02350	hypothetical protein	-0.36
At2g45660	MADS-box protein (AGL20)	-0.37
At3g45640	mitogen-activated protein kinase 3	-0.37
At5g50900	putative protein	-0.37
At4g24360	putative protein	-0.37
At1g21120	O-methyltransferase 1, putative	-0.37
At4g08870	putative arginase	-0.37
At4g30280	xyloglucan endotransglycosylase, putative	-0.37
At3g10720	putative pectinesterase	-0.37
At2g20340	putative tyrosine decarboxylase	-0.37
At5g54490	putative protein	-0.37
At3g28200	peroxidase, putative	-0.37
At1g10080	hypothetical protein	-0.37
At4g05150	putative protein	-0.37
At5g23130	unknown protein	-0.37
At3g50800	putative protein	-0.37
At3g54020	putative protein	-0.37
At4g36010	thaumatin-like protein	-0.38
At2g32150	putative hydrolase	-0.38

Table S4: continued

AGI code	description	log ratio
At1g13260	DNA-binding protein (RAV1)	-0.38
At1g03870	fasciclin-like arabinogalactan-protein (FLA9)	-0.38
At1g29440	auxin-induced protein, putative	-0.38
At1g76360	putative protein kinase	-0.38
At1g57680	hypothetical protein	-0.38
At2g42540	cold-regulated protein cor15a precursor	-0.38
At2g18300	expressed protein	-0.39
At2g01850	xyloglucan endotransglycosylase (EXGT-A3)	-0.39
At1g72240	hypothetical protein	-0.39
At2g30360	putative protein kinase	-0.39
At4g17615	calcineurin B-like protein 1	-0.39
At5g61810	peroxisomal Ca-dependent solute carrier - like protein	-0.39
At1g76160	pectinesterase (pectin methylesterase), putative	-0.39
At3g50950	disease resistance protein (CC-NBS-LRR class), putative	-0.39
At3g07470	expressed protein	-0.39
At1g01140	serine threonine kinase, putative	-0.39
At5g43760	beta-ketoacyl-CoA synthase, putative	-0.39
At2g15960	expressed protein	-0.39
At5g37710	calmodulin-binding heat-shock protein	-0.39
At1g20440	hypothetical protein	-0.39
At4g18280	glycine-rich cell wall protein-like	-0.4
At4g14690	Expressed protein	-0.4
At1g73080	leucine-rich repeat transmembrane protein kinase, putative	-0.4
At5g48850	putative protein	-0.4
At1g14330	hypothetical protein	-0.4
At2g23120	expressed protein	-0.4
At1g01240	expressed protein	-0.4
At1g02900	hypothetical protein	-0.4
At1g15550	gibberellin 3 beta-hydroxylase (GA4)	-0.4
At4g33920	putative protein	-0.4
At5g62520	putative protein	-0.4
At1g07000	leucine zipper protein, putative	-0.4
At4g23600	tyrosine transaminase like protein	-0.4
At5g43440	1-aminocyclopropane-1-carboxylate oxidase	-0.4
At2g28305	expressed protein	-0.4
At4g23180	serine/threonine kinase -like protein	-0.4
At1g56660	hypothetical protein	-0.4
At4g15800	Expressed protein	-0.4
At1g06360	fatty acid desaturase family protein	-0.4
At1g69830	putative alpha-amylase	-0.4
At2g36410	expressed protein	-0.4
At3g07460	Expressed protein	-0.4
At3g59310	putative protein	-0.4
At1g52000	myrosinase binding protein, putative	-0.41
At4g25620	unknown protein	-0.41
At1g61260	cotton fiber expressed protein, putative	-0.41
At4g26690	putative protein	-0.41
At2g30500	unknown protein	-0.41
At5g19530	spermine synthase (ACL5)	-0.41
At4g27440	protochlorophyllide reductase precursor	-0.41
At1g68580	unknown protein	-0.41

Table S4: continued

AGI code	description	log ratio
At1g36370	putative hydroxymethyltransferase	-0.41
At4g35110	putative protein	-0.41
At4g34760	putative auxin-regulated protein	-0.41
At2g43290	putative calcium binding protein	-0.41
At1g14280	phytochrome kinase substrate 1, putative	-0.41
At1g09070	expressed protein	-0.42
At1g21130	O-methyltransferase 1, putative	-0.42
At1g60140	trehalose-6-phosphate synthase, putative	-0.42
At4g24530	PsRT17-1 like protein	-0.42
At1g07720	beta-ketoacyl-CoA synthase family	-0.42
At5g52310	low-temperature-induced protein 78 (sp Q06738)	-0.42
At3g02570	putative mannose-6-phosphate isomerase	-0.42
At3g45260	zinc finger protein	-0.42
At2g16660	nodulin-like protein	-0.42
At1g22160	expressed protein	-0.42
At2g29630	putative thiamin biosynthesis protein	-0.42
At5g44130	fasciclin-like arabinogalactan-protein, putative (FLA13)	-0.42
At5g04020	Calmodulin-binding protein	-0.42
At4g36730	G-box-binding factor 1	-0.42
At5g12940	leucine rich repeat protein family	-0.42
At1g17990	12-oxophytodienoate reductase, putative	-0.42
At3g47570	leucine-rich repeat transmembrane protein kinase, putative	-0.42
At2g42760	unknown protein	-0.42
At1g01470	hypothetical protein	-0.42
At4g19530	disease resistance protein (TIR-NBS-LRR class), putative	-0.42
At1g69370	chorismate mutase, putative	-0.42
At2g41100	calmodulin-like protein	-0.43
At3g22740	putative selenocysteine methyltransferase	-0.43
At5g13400	peptide transporter - like protein	-0.43
At5g44360	FAD-linked oxidoreductase family	-0.43
At3g23030	auxin-inducible gene (IAA2)	-0.43
At1g24170	putative glycosyl transferase	-0.43
At2g28120	nodulin-like protein	-0.43
At3g59440	calmodulin-like protein	-0.43
At2g44230	expressed protein	-0.43
At4g02540	CHP-rich zinc finger protein, putative	-0.43
At2g38760	putative annexin	-0.43
At1g58200	unknown protein	-0.43
At1g23390	Kelch repeat containing F-box protein family	-0.43
At4g16950	disease resistance protein, RPP5-like (TIR-NBS-LRR class), putative	-0.43
At4g13340	extensin-like protein	-0.43
At3g16470	putative lectin	-0.43
At3g61260	putative DNA-binding protein	-0.43
At4g30440	nucleotide sugar epimerase-like protein	-0.43
At1g51940	unknown protein	-0.44
At1g05805	bHLH protein	-0.44
At3g29320	glucan phosphorylase, putative	-0.44
At1g51805	receptor protein kinase, putative	-0.44
At3g04910	putative mitogen activated protein kinase kinase	-0.44
At1g33240	DNA-binding factor, putative	-0.44
At1g79700	ovule development protein, putative	-0.44

Table S4: continued

AGI code	description	log ratio
At2g30250	WRKY family transcription factor	-0.44
At5g40380	receptor-like protein kinase	-0.44
At2g25250	unknown protein	-0.44
At2g14080	disease resistance protein (TIR-NBS-LRR class), putative	-0.44
At5g03120	putative protein	-0.44
At2g38310	expressed protein	-0.44
At1g69890	expressed protein	-0.44
At4g20860	FAD-linked oxidoreductase family	-0.44
At4g16860	disease resistance protein (TIR-NBS-LRR class), putative	-0.44
At1g14240	putative nucleoside triphosphatase	-0.44
At3g60290	2-oxoglutarate-dependent dioxygenase family	-0.45
At5g25440	putative protein kinase	-0.45
At5g11070	putative protein	-0.45
At1g27770	calcium-transporting ATPase 1	-0.45
At1g72520	putative lipoxygenase	-0.45
At1g22740	Ras-related GTP-binding protein (Rab7)	-0.45
At1g57590	pectinacetyltransferase, putative	-0.45
At2g42530	cold-regulated protein cor15b precursor	-0.45
At1g18400	helix-loop-helix protein homolog, putative	-0.45
At5g15500	putative protein	-0.45
At1g75380	wound-responsive protein, putative	-0.46
At2g19620	putative SF21 protein {Helianthus annuus}	-0.46
At1g02660	expressed protein	-0.46
At1g73830	putative helix-loop-helix DNA-binding protein	-0.46
At3g62660	putative protein	-0.46
At3g04290	putative GDSL-motif lipase/acylhydrolase	-0.46
At1g24530	G-protein beta family	-0.46
At3g51970	wax synthase-like protein	-0.46
At1g02390	expressed protein	-0.46
At5g47220	ethylene responsive element binding factor 2 (EREBP-2)	-0.46
At2g06050	12-oxophytodienoate reductase (OPR3)(DDE1)	-0.46
At4g35470	putative protein	-0.47
At3g24550	protein kinase, putative	-0.47
At5g42250	alcohol dehydrogenase	-0.47
At5g41750	disease resistance protein (TIR-NBS-LRR class), putative	-0.47
At2g43010	expressed protein	-0.47
At3g51550	receptor-protein kinase-like protein	-0.47
At2g29290	putative tropinone reductase	-0.47
At4g32350	putative protein	-0.47
At4g38690	putative protein	-0.47
At4g34260	hypothetical protein	-0.47
At1g19570	dehydroascorbate reductase, putative	-0.47
At1g28230	purine permease	-0.47
At5g23660	MtN3-like protein	-0.47
At4g11280	ACC synthase (AtACS-6)	-0.47
At3g55940	phosphoinositide specific phospholipase C, putative	-0.47
At4g35480	RING-H2 finger protein RHA3b	-0.47
At1g66150	receptor protein kinase (TMK1), putative	-0.48
At1g75220	integral membrane protein, putative	-0.48
At4g15210	glycosyl hydrolase family 14 (beta-amylase)	-0.48
At5g65470	putative protein	-0.48

Table S4: continued

AGI code	description	log ratio
At5g14120	nodulin-like protein	-0.48
At1g69760	expressed protein	-0.48
At3g13750	glycosyl hydrolase family 35 (beta-galactosidase)	-0.48
At4g03390	leucine-rich repeat transmembrane protein kinase, putative	-0.48
At2g43530	putative trypsin inhibitor	-0.48
At1g20160	subtilisin-like serine protease	-0.48
At5g51190	putative protein	-0.48
At4g01330	putative protein kinase	-0.48
At4g01950	unknown protein	-0.48
At2g31800	putative protein kinase	-0.48
At1g73750	expressed protein	-0.48
At1g74430	myb family transcription factor	-0.49
At4g18970	Expressed protein	-0.49
At3g44860	methyltransferase-related	-0.49
At1g44350	gr1 protein	-0.49
At1g74950	expressed protein	-0.49
At5g07580	transcription factor-like protein	-0.49
At5g58900	l-box binding factor - like protein	-0.49
At5g18130	putative protein	-0.49
At5g05440	putative protein	-0.49
At3g04640	expressed protein	-0.49
At5g01740	putative protein	-0.49
At3g62420	bZIP family transcription factor	-0.49
At5g15350	putative protein	-0.49
At1g27460	calmodulin-binding protein	-0.5
At4g32790	putative protein	-0.5
At3g04210	disease resistance protein (TIR-NBS class), putative	-0.5
At1g52410	myosin-like protein	-0.5
At2g30610	unknown protein	-0.5
At1g29670	lipase/hydrolase, putative	-0.5
At4g34250	fatty acid elongase 1 (FAE1), putative	-0.5
At5g66210	calcium-dependent protein kinase	-0.5
At5g62090	putative protein	-0.51
At3g02070	unknown protein	-0.51
At5g37770	CALMODULIN-RELATED PROTEIN 2, TOUCH-INDUCED (TCH2)	-0.51
At5g44680	putative protein	-0.51
At2g33570	expressed protein	-0.51
At2g27500	glycosyl hydrolase family 17	-0.51
At2g30990	hypothetical protein	-0.51
At4g04840	putative protein	-0.51
At4g32800	transcription factor TINY, putative	-0.51
At2g41430	ERD15 protein	-0.51
At4g22780	Translation factor EF-1 alpha - like protein	-0.52
At1g24070	glucosyltransferase, putative	-0.52
At1g11960	unknown protein	-0.52
At1g53160	transcription factor, putative	-0.52
At4g31000	calmodulin-binding protein	-0.52
At5g50570	putative protein	-0.52
At5g22920	PGPD14 protein	-0.52
At4g28190	expressed protein	-0.52
At2g40435	unknown protein	-0.52

Table S4: continued

AGI code	description	log ratio
At5g06870	polygalacturonase inhibiting protein (PGIP2)	-0.52
At5g05600	2-oxoglutarate-dependent dioxygenase family	-0.53
At4g27280	putative protein	-0.53
At1g12090	pEARLI 1-like protein	-0.53
At1g70090	expressed protein	-0.53
At4g38550	Phospholipase like protein	-0.53
At2g02950	expressed protein	-0.53
At5g66590	putative protein	-0.53
At3g16400	putative lectin	-0.53
At2g38750	putative annexin	-0.53
At1g10020	unknown protein	-0.54
At4g00970	Similar to receptor kinase	-0.54
At1g78100	expressed protein	-0.54
At3g54920	polysaccharide lyase family 1 (pectate lyase)	-0.54
At3g57930	putative protein	-0.54
At3g57120	putative protein	-0.54
At2g03240	unknown protein	-0.54
At5g53500	putative protein	-0.54
At1g29690	expressed protein	-0.55
At2g03260	unknown protein	-0.55
At1g17620	expressed protein	-0.55
At2g34770	fatty acid hydroxylase (FAH1)	-0.55
At5g66580	putative protein	-0.56
At4g02330	hypothetical protein	-0.56
At1g22335	glycine-rich RNA-binding protein, putative	-0.56
At3g44870	methyltransferase-related	-0.56
At1g11210	expressed protein	-0.56
At4g31800	WRKY family transcription factor	-0.56
At5g37540	putative protein	-0.56
At1g35350	unknown protein	-0.56
At1g65450	expressed protein	-0.56
At1g75900	family II extracellular lipase 3 (EXL3)	-0.56
At1g66100	thionin, putative	-0.56
At1g08920	putative sugar transport protein, ERD6	-0.57
At3g58850	putative protein	-0.57
At1g72430	expressed protein	-0.57
At5g64260	phi-1-like protein	-0.57
At2g28630	beta-ketoacyl-CoA synthase family	-0.58
At1g29395	Expressed protein	-0.59
At4g18010	putative protein	-0.59
At1g20510	expressed protein	-0.59
At2g24850	putative tyrosine aminotransferase	-0.59
At4g38400	putative pollen allergen	-0.59
At3g51450	strictosidine synthase-related	-0.59
At1g66160	expressed protein	-0.6
At1g67900	unknown protein	-0.6
At1g11260	glucose transporter	-0.6
At1g36280	adenylosuccinate lyase-like protein	-0.61
At5g56980	putative protein	-0.61
At1g03300	unknown protein	-0.61
At2g01300	predicted by genscan and genefinder	-0.61

Table S4: continued

AGI code	description	log ratio
At5g22380	NAC-domain protein-like	-0.61
At3g55980	putative protein	-0.61
At5g66200	putative protein	-0.61
At5g45750	GTP-binding protein, putative	-0.61
At3g55430	glycosyl hydrolase family 17 (beta-1,3-glucanase)	-0.61
At1g19180	expressed protein	-0.61
At1g52400	glycosyl hydrolase family 1, beta-glucosidase (BG1)	-0.61
At5g24780	vegetative storage protein Vsp1	-0.62
At2g39400	putative phospholipase	-0.62
At1g63750	disease resistance protein (TIR-NBS-LRR class), putative	-0.62
At2g39420	putative phospholipase	-0.62
At2g24600	expressed protein	-0.62
At3g28220	unknown protein	-0.62
At1g80440	expressed protein	-0.63
At4g18440	adenylosuccinate lyase - like protein	-0.63
At2g34510	unknown protein	-0.63
At5g19140	aluminium-induced protein - like	-0.63
At1g53430	receptor-like serine/threonine kinase, putative	-0.63
At2g25460	expressed protein	-0.63
At5g20250	glycosyl hydrolase family 36	-0.64
At1g72180	leucine-rich repeat transmembrane protein kinase, putative	-0.64
At5g01810	serine/threonine protein kinase ATPK10	-0.64
At4g26530	fructose-bisphosphate aldolase - like protein	-0.64
At1g02205	hypothetical protein	-0.64
At4g16780	homeobox-leucine zipper protein HAT4 (HD-Zip protein 4)	-0.64
At2g15090	fatty acid elongase 1 (FAE1), putative	-0.65
At1g17380	expressed protein	-0.65
At1g32170	xyloglucan endotransglycosylase (XTR4), putative	-0.65
At4g25810	xyloglucan endotransglycosylase (XTR-6)	-0.65
At3g28180	expressed protein	-0.65
At2g35930	unknown protein	-0.65
At3g09940	monodehydroascorbate reductase, putative	-0.65
At5g12050	putative serine rich protein	-0.65
At1g04240	putative auxin-induced protein AUX2-11	-0.66
At4g30270	xyloglucan endotransglycosylase (meri5B)	-0.66
At2g22770	putative bHLH transcription factor	-0.66
At1g54010	myosinase-associated protein, putative	-0.67
At5g19190	putative protein	-0.67
At1g63880	disease resistance protein (TIR-NBS-LRR class), putative	-0.67
At3g59080	putative protein	-0.68
At5g58670	phosphoinositide specific phospholipase C	-0.68
At4g35770	senescence-associated protein sen1	-0.68
At4g27100	putative protein	-0.69
At4g27450	putative protein	-0.7
At1g18740	expressed protein	-0.7
At1g02380	hypothetical protein	-0.7
At1g01120	fatty acid elongase 3-ketoacyl-CoA synthase 1 (KCS1)	-0.7
At1g74450	expressed protein	-0.7
At4g17500	ethylene responsive element binding factor 1 (frameshift !)	-0.7
At1g22530	unknown protein	-0.71
At5g45340	cytochrome p450 family	-0.71

Table S4: continued

AGI code	description	log ratio
At2g42980	putative chloroplast nucleoid DNA binding protein	-0.71
At5g52900	expressed protein	-0.71
At3g50060	myb DNA-binding protein (MYB77)	-0.71
At1g70290	trehalose-6-phosphate synthase, putative	-0.72
At3g62630	putative protein	-0.72
At4g17230	scarecrow-like 13 (SCL13)	-0.72
At1g61120	terpene synthase/cyclase family	-0.72
At3g50260	putative protein	-0.73
At5g62165	MADS-box protein	-0.73
At3g15540	early auxin-induced protein, IAA19	-0.73
At5g25240	putative protein	-0.74
At5g47240	mutT domain protein-like	-0.74
At5g54380	receptor-protein kinase-like protein	-0.74
At3g62550	putative protein	-0.74
At2g42580	expressed protein	-0.75
At5g67480	putative protein	-0.75
At5g50950	fumarate hydratase	-0.75
At1g61100	disease resistance protein (TIR class), putative	-0.75
At5g24770	vegetative storage protein Vsp2	-0.75
At1g66180	expressed protein	-0.76
At5g45820	serine threonine protein kinase	-0.77
At3g06500	neutral invertase, putative	-0.77
At3g54810	GATA zinc finger protein	-0.78
At4g37260	myb DNA-binding protein (AtMYB73)	-0.78
At2g18700	putative trehalose-6-phosphate synthase	-0.78
At1g18710	myb-related transcription factor mixta, putative	-0.78
At2g30930	expressed protein	-0.79
At3g55840	nematode resistance protein-like protein	-0.79
At2g35290	hypothetical protein	-0.8
At2g41640	expressed protein	-0.8
At2g39030	expressed protein	-0.8
At1g72150	cytosolic factor, putative	-0.81
At1g17420	lipoxygenase	-0.81
At4g34410	putative protein	-0.81
At1g58270	expressed protein	-0.82
At5g67300	myb family transcription factor	-0.82
At1g72450	expressed protein	-0.82
At5g49360	glycosyl hydrolase family 3	-0.83
At1g70820	phosphoglucomutase, putative	-0.83
At3g26740	light regulated protein, putative	-0.84
At1g68600	expressed protein	-0.84
At3g11480	S-adenosyl-L-methionine:carboxyl methyltransferase family	-0.84
At2g17840	putative senescence-associated protein 12	-0.84
At4g32280	Expressed protein	-0.85
At1g02610	hypothetical protein	-0.87
At3g06070	expressed protein	-0.88
At1g23030	unknown protein	-0.89
At5g51550	putative protein	-0.89
At2g34930	disease resistance protein family	-0.89
At1g57990	unknown protein	-0.89
At1g76650	putative calmodulin	-0.89

Table S4: continued

AGI code	description	log ratio
At2g23290	MYB family transcription factor	-0.91
At4g08950	putative phi-1-like phosphate-induced protein	-0.91
At1g16370	putative transport protein	-0.92
At1g52830	putative IAA6 protein	-0.95
At3g62720	alpha galactosyltransferase-like protein	-0.97
At2g27080	expressed protein	-0.98
At4g03400	putative GH3-like protein	-0.99
At4g37240	putative protein	-1.0
At2g47440	unknown protein	-1.0
At4g08040	strong similarity to 1-aminocyclopropane-1-carboxylic acid synthases	-1.03
At1g50040	hypothetical protein	-1.04
At1g10550	xyloglucan endotransglycosylase, putative	-1.05
At5g25190	ethylene-responsive element - like protein	-1.06
At2g44500	similar to axi 1 protein from <i>Nicotiana tabacum</i>	-1.09
At4g17460	homeobox-leucine zipper protein HAT1 (HD-Zip protein 1)	-1.13
At5g61590	ethylene responsive element binding factor - like	-1.14
At4g16563	similar to chloroplast nucleoid DNA-binding protein-like	-1.2
At2g17230	expressed protein	-1.25
At2g27690	cytochrome p450, putative	-1.34
At3g19680	unknown protein	-1.42
At1g21910	TINY-like protein	-1.44
At5g57560	xyloglucan endotransglycosylase (TCH4)	-1.45
At1g35140	phosphate-induced (phi-1) protein, putative	-1.52
At3g45970	putative protein	-1.62
At1g33760	transcription factor TINY, putative	-1.73

Abbreviations

1MOI3M	1- methoxyindol-3-ylmethyl glucosinolate
4MOI3M	4-methoxyindol-3-ylmethyl glucosinolate
4MSOB	4-methylsulfinylbutyl glucosinolate
8MSOO	8-methylsulfinyloctyl glucosinolate
3MSOP	3-methylsulfinylpropyl glucosinolate
5MSOP	5- methylsulfinylpropyl glucosinolate
5MT	5-methyl tryptophan
4MU	4-methylumbelliferone
35S	35S promoter of the cauliflower mosaic virus
aa	amino acids
AAO1	indole-3-acetaldehyde oxidase
ACC	1-aminocyclopropane-1-carboxylic acid
AD	activation domain
AGI	<i>Arabidopsis</i> Genome Initiative number
<i>A. thaliana</i>	<i>Arabidopsis thaliana</i>
ATR	altered tryptophan regulation
AtST	<i>A. thaliana</i> sulfol transferase
<i>A. tumefaciens</i>	<i>Agrobacterium tumefaciens</i>
Arabidopsis	<i>Arabidopsis thaliana</i>
ASA1	anthranilate synthase alpha 1
ASB1	anthranilate synthase beta 1
BD	binding domain
bHLH	basic helix-loop-helix
bp	base pairs
BSA	bovine serum albumin
BY2	bright yellow 2
°C	centigrade
CaMV	cauliflower mosaic virus
cDNA	complementary DNA
CDS	coding sequence
Chlor ^R	chloramphenicol resistance
cRNA [^]	complementary RNA
cm	centimetre
Col-0	Columbia 0
CYP	cytochrome P450 monooxygenase
DAHP	3-deoxy-D-arabinoheptulosonate-7-phosphate
DHS1	DAHP synthase 1
DNA	desoxyribonucleic acid
dd	double distilled
DEPC	diethylpyrocarbonate
DMF	dimethylformamide
DMSO	dimethyl-sulfoxide
dNTPs	deoxynucleotides
DTT	di-thiotreitol
<i>E. coli</i>	<i>Escherichia coli</i>
EDTA	ethylenediaminetetraacetic acid
Gent ^R	gentamycin
GFP	green fluorescent protein

GS	glucosinolate
GST	glutathione-S-transferase
GUS	β -glucuronidase
HEPES	N-2-Hydroxyethylpiperazin-N'-2-ethansulfonic acid
IAA	indole-3-acetic acid
IAAld	indole-3-acetaldehyde
IAN	indole-3-acetonitrile
IAOx	indole-3-acetaldoxime
IGPS	indole-3-glycerolphosphate synthase
I3M	indole-3-ylmethyl glucosinolate
kDa	kilo Daltons
kg	kilograms
L	litre
LB	Luria-Bertani medium
<i>Ler</i>	Landsberg <i>erecta</i>
M	molar
MeJA	methyl jasmonate
MES	4-morpholinoethan-sulphonic acid
mg	milligram
μ F	micro Faraday
μ g	microgram
μ l	microlitre
min	minute
mL	millilitre
mM	millimolar
mRNA	messenger RNA
MS	Murashige and Skog 10 medium
MUG	4-methylumbelliferyl- β -D-glucuronide
MYR	myrosinase
<i>N. benthamiana</i>	<i>Nicotiana benthamiana</i>
n	number of experiments
ng	nanogram
NIT	nitrilase
Ω	Ohm
ORF	open reading frame
PCR	polymerase chain reaction
PEG	polyethyleneglycol
QTL	quantitative trait loci
Rif ^R	rifampicin
RNA	ribonucleic acid
rpm	revolutions per minute
RT	room temperature
RT-PCR	reverse transcribed PCR
SA	salicylic acid
<i>S. cerevisiae</i>	<i>Saccharomyces cerevisiae</i>
<i>S. exigua</i>	<i>Spodoptera exigua</i>
SD	standard deviation
SD-medium	single drop-out medium
SDS	sodium docecyl sulphate
sec	seconds
ss	single stranded

ST	sulfo transferase
SUR	superroot
TAE	Tris-Acetate/EDTA
T-DNA	Transfer DNA
TE	Tris/EDTA
TGG	β -thioclucoside glycohydrolase (=MYR)
Tris	tris-(hydroxymethyl)-aminomethan
TSB1	tryptophan synthase beta 1
U	units (enzymatic)
UGT	S-glucosyl transferase
v/v	volume/volume
w/v	weight/volume
wt	wild-type
x g	times gravity
X-Gluc	5-bromo-4-chloro-3-indoly- β -D-glucoronid acid
YFP	yellow fluorescent protein
YUCCA	flavin monooxygenase-like protein
#	number

(nucleotides and amino acids are abbreviated according to international conventions)

Abstract

Glucosinolates are amino-acid derived plant secondary metabolites found mainly in Brassicaceae, including the model plant *Arabidopsis thaliana*. Due to their role in plant defence and their cancer-preventive properties in human nutrition, they have gained increasing interest over the last years. This study presents the characterisation of the activation-tagging mutant *HIG1-1D*, which displays a *high indolic glucosinolate* phenotype, caused by an activation of the R2R3-type MYB transcription factor *HIG1/MYB51*. A positive correlation between *HIG1/MYB51* transcription and the accumulation of indolic glucosinolates could be confirmed in gain and loss-of-function mutants. *HIG1/MYB51* expression overlaps with sites of indolic glucosinolate biosynthesis and the expression of biosynthesis genes, which are activated by *HIG1/MYB51 in trans*. Unlike previously characterised mutants affected in indolic glucosinolate biosynthesis, *HIG1-1D* displays only minor effects on auxin biosynthesis. However, a role of *HIG1/MYB51* in the biotic stress response of *A. thaliana* appears likely, due to the mechano-sensitive expression of *HIG1/MYB51* along with an increased resistance of *HIG1-1D* plants against a generalist herbivore. Yeast-two-hybrid screening allowed identifying the interaction of *HIG1/MYB51* with *ATR2/bHLH05*, a putative regulator of tryptophan and indolic glucosinolate biosynthesis. Therefore, *HIG1/MYB51* appears to be part of a complex network controlling indolic glucosinolate biosynthesis.

Kurzzusammenfassung

Glucosinolate sind eine Gruppe pflanzlicher Sekundärmetabolite, die hauptsächlich in den Brassicaceae vorkommen, unter anderem auch in *Arabidopsis thaliana*. Aufgrund ihrer Rolle in der pflanzlichen Pathogenabwehr und ihrer krebsvorbeugenden Eigenschaften haben Glucosinolate in den letzten Jahren an Bedeutung gewonnen. In der vorliegenden Studie wird die activation-tagging Mutante *HIG1-1D* charakterisiert, die aufgrund einer Aktivierung des R2R3-MYB Transkriptionsfaktors *HIG1/MYB51* eine erhöhte Konzentration an Indol-Glucosinolaten aufweist. Durch die Untersuchung von gain- und loss-of-function Mutanten konnte die positive Korrelation zwischen der Expression von *HIG1/MYB51* und der Akkumulation von Indol-Glucosinolaten bestätigt werden. *HIG1/MYB51* wird in Geweben exprimiert, in denen Indol-Glucosinolate und die daran beteiligten Enzyme synthetisiert werden, deren Expression von *HIG1/MYB51* induziert wird.

Im Gegensatz zu bereits charakterisierten Mutanten, bei denen die Indol-Glucosinolate Biosynthese dereguliert ist, scheint die Auxin Biosynthese in *HIG1-1D* nur wenig beeinflusst zu sein. Eine regulatorische Rolle von *HIG1/MYB51* in der biotischen Stressantwort von *A. thaliana* scheint hingegen wahrscheinlich, da *HIG1/MYB51* durch mechanische Reize induziert wird. Darüber hinaus, zeigen *HIG1-1D* Pflanzen eine erhöhte Resistenz gegenüber unspezifischen Herbivoren.

In einem yeast-two-hybrid Ansatz konnte die Interaktion von *HIG1/MYB51* mit dem basic helix-loop-helix Transkriptions Faktor *ATR2/bHLH05* gezeigt werden, welcher eine regulatorische Rolle in der Tryptophan und Glucosinolat Biosynthese hat. Es erscheint daher möglich, dass *HIG1/MYB51* Teil eines regulatorischen Netzwerks ist, das die Biosynthese von Indol-Glucosinolaten kontrolliert.

Ich danke...

in erster Linie Prof. Dr. Flügge, für die nötige Unterstützung und Freiheit bei der Durchführung meiner Doktorarbeit.

Prof. Dr. Hülskamp für die spontane Bereitschaft, das Zweitgutachten zu übernehmen.

Tamara Gigolashvili, dafür dass sie zu jeder Zeit bereit war, mir mit Rat und Tat zur Seite zu stehn. Vielen vielen Dank!

der IMPRS Köln, für die finanzielle Unterstützung.

Hans-Peter Mock, Carolin Müller und den Mitarbeitern der AG Weiler für die biochemischen Analysen, ohne die diese Arbeit nicht möglich gewesen wäre.

Joachim Uhrig und Ilona Zimmermann für die Unterstützung und das Know-How beim Yeast-Two-Hybrid Screening.

den TAs der AG Flügge, die mir während der Doktorarbeit geholfen haben. Danke an Kerstin für die Betreuung der Zellkultur, an Sonja für die Probenaufbereitung und Hybridisierung des Microarrays, und an Barbara für die Unterstützung beim Yeast-Two-Hybrid Screen, den Protoplasten und Promoter-Klonierungen. Vielen Dank!

Markus Gierth für die Analyse der Microarray Daten, das Korrekturlesen meiner Arbeit, und die Unterstützung bei meinem Kampf mit Microsoft-Word.

Rainer Schwacke, der so unendlich viel mehr von Computern versteht als ich.

Ruslan, der so einige Plasmide und die Höhen und Tiefen der Zellkultur mit mir teilte.

den Sekretärinnen Frau Lorbeer und Frau Schwanitz, ohne die ich vor der Bürokratie kapituliert hätte.

den vielen Helfern aus Gärtnerei und Werkstatt, die den Alltag so viel leichter machen.

all denen, die meine Hochs und Tiefs in den letzten Jahren geteilt und ertragen haben, vor allem Tanja, Marcella, Kirsten, Inga und Esther, meinen IMPRS Kollegen und Ralf Petri, und der ganzen AG Flügge, für die tolle Atmosphäre im Labor.

zu guter Letzt meinen Eltern und meiner Schwester, die so manche meiner Launen geduldig ertragen haben, und mich immer bedingungslos unterstützt haben. Danke!

Erklärung

Ich versichere, dass ich die von mir vorgelegte Dissertation selbständig angefertigt habe, die benutzten Quellen und Hilfsmittel vollständig angegeben und die Stellen der Arbeit – einschließlich Tabellen, Karten und Abbildungen –, die anderen Werken im Wortlaut oder dem Sinn nach entnommen sind, in jedem Einzelfall als Entlehnung kenntlich gemacht habe; dass diese Dissertation noch keiner anderen Fakultät oder Universität zur Prüfung vorgelegen hat; dass sie abgesehen von unten angegebenen Teilpublikationen noch nicht veröffentlicht worden ist sowie, dass ich eine solche Veröffentlichung vor Abschluss des Promotionsverfahrens nicht vornehmen werde. Die Bestimmungen dieser Promotionsordnung sind mir bekannt. Die von mir vorgelegte Dissertation ist von Prof. Dr. U.-I. Flugge betreut worden.

Teilpublikation:

Gigolashvili, T., Berger, B., Mock, H.-P., Muller, C., Weisshaar, B., and Flugge, U.-I. (2007). The transcription factor HIG1/MYB51 regulates indolic glucosinolate biosynthesis in *Arabidopsis thaliana*. *Plant J.* **in press**.

Berger, B., Stracke, R., Yatusевич, R., Weisshaar, B., Flugge, U.-I., and Gigolashvili, T. (2007). A simplified method for the analysis of transcription factor-promoter interactions that allows high-throughput data generation. *Plant J.* **in press**.

Gigolashvili, T., Yatusевич, R., Berger, B., Muller, C., and Flugge, U.-I. (2007) The R2R3-MYB transcription factor HAG1/MYB28 is a regulator of methionine-derived glucosinolate biosynthesis in *Arabidopsis thaliana*. *Plant J.* **in press**.

Beiträge in Mitteilungsbänden von Tagungen:

Berger et al. (2004). International Conference on Arabidopsis Research, Berlin

Berger et al. (2004). Deutsche Botaniker-Tagung, Braunschweig

Berger et al. (2005). International EMBL PhD Students Symposium, Heidelberg

Berger et al. (2006). ISPMB Conference, Adelaide, Australia

Lebenslauf

Bettina Berger

Geboren am 30.04.1979 in Heilbronn
Staatsangehörigkeit: deutsch
Familienstand: ledig

Schulbildung

August 1985 – Juli 1989	Johann-Dietz-Grundschule Ellhofen
August 1989 – Juli 1998	Justinus-Kerner-Gymnasium Weinsberg
	Abschluss: Abitur (Notendurchschnitt: 1,3)

Hochschulstudium

Oktober 1998 – August 2000	Grundstudium der Biologie an der Eberhard-Karls-Universität Tübingen Abschluss: Vordiplom (Notendurchschnitt: 1,4)
September 2000 – September 2003	Studium der Biotechnologie an der Ecole Supérieure de Biotechnologie de Strasbourg (ESBS), Frankreich Abschluss: Diplom (Notendurchschnitt: 1,0)
Seit Oktober 2003	Promotionsstudium der Biologie an der Universität zu Köln

Praktika

Februar – Juni 2000	Anstellung als wissenschaftliche Hilfskraft im Institut für spezielle Botanik und Mykologie an der Universität Tübingen
August 2001	Institut für Physiologie und Biotechnologie der Pflanzen an der Universität Hohenheim
November/ Dezember 2002	Institut für Mechanische Verfahrenstechnik an der Universität Karlsruhe
Januar – September 2003	Praktischen Arbeit zur Diplomarbeit am Department of Plant Science, University of Cambridge, Großbritannien

